LUND UNIVERSITY

Isolation of Circulating Tumor Cells with Acoustophoresis

Towards a biomarker assay for prostate cancer

Undvall, Eva

2022

Document Version:
Publisher's PDF, also known as Version of record

Link to publication

Citation for published version (APA):
Undvall, E. (2022). *Isolation of Circulating Tumor Cells with Acoustophoresis: Towards a biomarker assay for prostate cancer*. Department of Biomedical Engineering, Lund university.

Total number of authors:
1

General rights
Unless other specific re-use rights are stated the following general rights apply:
Copyright and moral rights for the publications made accessible in the public portal are retained by the authors and/or other copyright owners and it is a condition of accessing publications that users recognise and abide by the legal requirements associated with these rights.
• Users may download and print one copy of any publication from the public portal for the purpose of private study or research.
• You may not further distribute the material or use it for any profit-making activity or commercial gain
• You may freely distribute the URL identifying the publication in the public portal

Read more about Creative commons licenses: https://creativecommons.org/licenses/

Take down policy
If you believe that this document breaches copyright please contact us providing details, and we will remove access to the work immediately and investigate your claim.

LUND UNIVERSITY

PO Box 117
221 00 Lund
+46 46-222 00 00

Isolation of Circulating Tumor Cells with Acoustophoresis

Towards a biomarker assay for prostate cancer

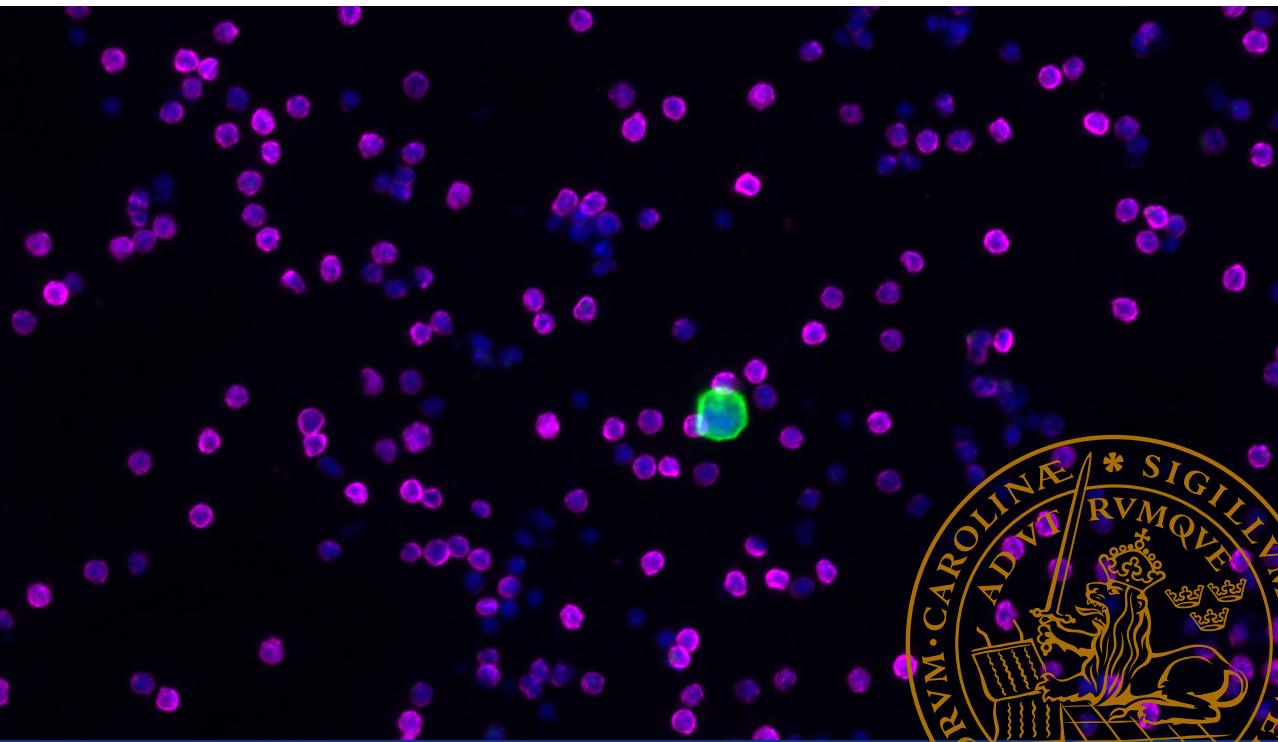

Eva Undvall Anand

Department of Biomedical Engineering
Faculty of Engineering
Lund University

Isolation of Circulating Tumor Cells with Acoustophoresis

Towards a biomarker assay for prostate cancer

Eva Undvall Anand

LUND
UNIVERSITY

DOCTORAL DISSERTATION

by due permission of the Faculty of Engineering, Lund University, Sweden.
To be defended at Segerfalksalen BMC, Klinikgatan 32, Lund. February 11 at 09:00, 2022

Faculty opponent
Professor Jean-Louis Viovy
Institut Curie, Paris, France

Organization LUND UNIVERSITY Department of Biomedical Engineering P.O. Box 118, SE-221 00 Lund, Sweden	**Document name** DOCTORAL DISSERTATION
	Date of issue February 11, 2022
Author Eva Undvall Anand	**Sponsoring organization** Knut and Alice Wallenberg Foundation, VR Swedish Research Council, SSF Swedish Foundation for Strategic Research, Cancerfonden

Title

Isolation of Circulating Tumor Cells with Acoustophoresis - Towards a biomarker assay for prostate cancer

Abstract

Microfluidics has emerged as an essential approach in the development of novel technological platforms to detect and isolate rare circulating tumor cells (CTCs) in the blood of cancer patients. Micro-scaled fluidic systems offer means to precisely control fluid flow. This enables cell separation when combined with techniques for manipulating cells across fluid streams. Various microfluidic methods have been developed, either using passively generated forces or an applied force field methodology to move cells across streamlines. Acoustophoresis uses ultrasonic standing waves to separate cells and particles in microfluidic channels. An acoustic standing wave field generates acoustic forces that acts on cells and particles based on their individual acoustic properties and forms the basis for the cell separation technology explored in this thesis.

In this dissertation, a novel approach for live CTC isolation has been developed. Micron-sized elastomeric particles with negative acoustic contrast were used for negative selection acoustophoresis. The surface of the elastomeric particles was functionalized to bind WBCs through the CD45 antigen, which enabled their transportation to pressure antinodes and facilitated an enrichment of cancer cells at the pressure node. Live cell negative selection acoustophoresis was demonstrated as a proof-of-concept study in paper 1 and was further extended to carry out processing of whole blood by a two-step acoustophoresis method in paper 2.

The sample throughput is an important parameter for microfluidic processing of clinical samples, especially for rare cell applications where a larger volume might be required for the detection of target cells. In paper 3, a fluid inertia phenomenon that may compromise cell separation performance at higher flow velocities was discovered. The inertial effects in an acoustofluidic device at increased sample throughputs and its consequences on particle separations were therefore investigated. Through numerical modelling and experimental validation, the main reason for the impaired acoustophoresis separation, at elevated flow rates, was attributed to the formation of a curved fluid boundary between the sample and sheath flow, both at the inlet of the separation channel as well as at the outlet flow splitter.

Finally, paper 4 outlines the benchmarking of CTC-acoustophoresis to the FDA cleared CELLSEARCH system in a comparative clinical study. Higher numbers of CTCs were detected after acoustophoretic processing of the patient samples as compared to the CELLSEARCH system. Further studies are currently being conducted to establish the full performance characteristics of CTC-acoustophoresis in the laboratory setting.

To conclude, the presented dissertation extends the use of acoustophoresis towards the clinical application of CTC enrichment of live and fixed cells. The aim of establishing an efficient technology that can target the full heterogeneity of the rare tumor cells is essential for the development of novel CTC biomarker assays for metastatic cancer. This dissertation builds towards the goal of an unbiased CTC isolation approach.

Keywords

acoustophoresis, biomarkers, cell separation, circulating tumor cells, elastomeric particles, microfluidics, negative selection, prostate cancer

Classification system and/or index terms (if any)

Supplementary bibliographical information ISRN LUTEDX/TEEM – 1128 – SE Report no. 1/22		**Language** English
ISSN and key title		ISBN 978-91-8039-135-1 (electronic) ISBN 978-91-8039-136-8 (print)
Recipient's notes	**Number of pages** 161	**Price**
	Security classification	

I, the undersigned, being the copyright owner of the abstract of the above-mentioned dissertation, hereby grant to all reference sources permission to publish and disseminate the abstract of the above-mentioned dissertation.

Signature: Eva Undvall Anand Date: 2022-02-11

Isolation of Circulating Tumor Cells with Acoustophoresis

Towards a biomarker assay for prostate cancer

Eva Undvall Anand

Cover photo Eva Undvall Anand

Copyright Eva Undvall Anand

Paper 1 © Elsevier

Paper 2 © American Chemical Society

Paper 3 © by the Authors (Manuscript unpublished)

Paper 4 © by the Authors (Manuscript unpublished)

Faculty of Engineering
Department of Biomedical Engineering

ISBN 978-91-8039-135-1 (electronic)
ISBN 978-91-8039-136-8 (print)
Report-nr. 1/22
ISRN LUTEDX/TEEM – 1128 – SE

Printed by Tryckeriet i E-huset, Lund University
Lund, Sweden 2022

Media-Tryck is a Nordic Swan Ecolabel certified provider of printed material. Read more about our environmental work at www.mediatryck.lu.se

MADE IN SWEDEN

To my family

Table of Contents

Publications

Included in thesis

1 Reducing WBC background in cancer cell separation products by negative acoustic contrast particle immuno-acoustophoresis
Kevin Cushing, **Eva Undvall***, Yvonne Ceder, Hans Lilja, and Thomas Laurell*

Analytica Chimica Acta, 2018, 1000:256-264

2 Two-step acoustophoresis separation of live tumor cells from whole blood
Eva Undvall Anand, Cecilia Magnusson*, Andreas Lenshof, Yvonne Ceder, Hans Lilja and Thomas Laurell*

Analytical Chemistry, 2021, 93(51):17076-17085

3 Inertia effects in acoustofluidic particle separation
***Eva Undvall Anand**, Fabio Garofalo, Giuseppe Procopio, Wei Qiu, Andreas Lenshof, Thomas Laurell and Thierry Baasch*

Submitted manuscript, 2021

4 Outline for the benchmarking of CTC-acoustophoresis to the current state-of-the-art technology
*Cecilia Magnusson, **Eva Undvall Anand**, Andreas Lenshof, Andreas Josefsson, Anders Bjartell, Yvonne Ceder, Thomas Laurell and Hans Lilja*

Preliminary manuscript, 2021

* Shared first authorship

Not included in thesis

I Organoid cultures derived from patients with advanced prostate cancer

Dong Gao, Ian Vela, Andrea Sboner, Phil J. Iaquinta, Wouter R. Karthaus, Anuradha Gopalan, Catherine Dowling, Jackie N. Wajala, ***Eva A. Undvall****, Vivek K. Arora, John Wongvipat, Myriam Kossai, Sinan Ramazanoglu, Luendreo P. Barboza, Wei Di, Zhen Cao, Qi Fan Zhang, Inna Sirota, Leili Ran, Theresa Y. MacDonald, Himisha Beltran, Juan-Miguel Mosquera, Karim A. Touijer, Peter T. Scardino, Vincent P. Laudone, Kristen R. Curtis, Dana E. Rathkopf, Michael J. Morris, Daniel C. Danila, Susan F. Slovin, Stephen B. Solomon, James A. Eastham, Ping Chi, Brett Carver, Mark A. Rubin, Howard I. Scher, Hans Clevers, Charles L. Sawyers, and Yu Chen*

Cell, 2014, 159: 176–18

Authors contributions to publications

Paper 1. Shared contribution of planning and performing the experiments, data collection, result analysis and writing of the manuscript.

Paper 2. Shared contribution of planning the experiments. Synthesized surface-modified and antibody-functionalized elastomeric particles. Shared contribution of separation experiments, in which I performed the secondary negative selection acoustophoresis step. Shared data collection and result analysis. Wrote major part of the manuscript.

Paper 3. Shared contribution of planning the experiments. Major contribution to the experimental work and data collection. Shared contribution to the result analysis and writing of the manuscript.

Paper 4. Participated in planning the study. Minor contributions to experimental work. Performed part of the data evaluation and shared contribution in writing of the manuscript.

Abbreviations

ADT	Androgen deprivation therapy
ARF	Acoustic radiation force
AR	Androgen receptor
ARSI	Androgen receptor signal inhibitor
ARV7	Androgen receptor splice variant 7
BAW	Bulk acoustic wave
BCR	Biochemical recurrence
CD45	Lymphocyte common antigen (Cluster of differentiation 45)
cDNA	Complementary DNA
CGH	Comparative genomic hybridization
CK	Cytokeratin
CNV	Copy number variation
COU	Context of use
CSC	Cancer stem cell
CTC	Circulating tumor cell
DAPI	4', 6-diamidino-2-phenylindole
DEP	Dielectrophoresis
DFF	Dean flow fractionation
DLD	Deterministic lateral displacement
DNA	Deoxyribonucleic acid
DSC	Disuccinimidyl carbonate

DTC	Disseminated tumor cells
EMT	Epithelial-mesenchymal transition
EP	Elastomeric particle
EPCAM	Epithelial cellular adhesion molecule
FACS	Fluorescence-activated cell sorting
FDA	U.S. Food and Drug Administration
FISH	Fluorescence *in situ* hybridization
HF	Hydrofluoric acid
ICC	Immunocytochemistry
IF	Immunofluorescence
IFC	Image flow cytometry
IHC	Immunohistochemistry
KOH	Potassium hydroxide
LBD	Ligand binding domain
MACS	Magnetic-activated cell sorting
mCRPC	Metastatic castration resistant prostate cancer
mRNA	Messenger RNA
NGS	Next generation sequencing
OS	Overall survival
PCa	Prostate cancer
PCR	Polymerase chain reaction
PDMS	Polydimethylsiloxane
PIV	Particle image velocimetry
PSA	Prostate-specific antigen
PSMA	Prostate-specific membrane antigen
PZT	Lead zirconate titrate

qRT-PCR	Real time quantitative reverse transcription PCR
RBC	Red blood cell
RNA	Ribonucleic acid
SNP	Single nucleotide polymorphism
WBC	White blood cell
WGA	Whole genome amplification

Abstract

Microfluidics has emerged as an essential approach in the development of novel technological platforms to detect and isolate rare circulating tumor cells (CTCs) in the blood of cancer patients. Micro-scaled fluidic systems offer means to precisely control fluid flow. This enables cell separation when combined with techniques for manipulating cells across fluid streams. Various microfluidic methods have been developed, either using passively generated forces or an applied force field methodology to move cells across streamlines. Acoustophoresis uses ultrasonic standing waves to separate cells and particles in microfluidic channels. An acoustic standing wave field generates acoustic forces that acts on cells and particles based on their individual acoustic properties and forms the basis for the cell separation technology explored in this thesis.

In this dissertation, a novel approach for live CTC isolation has been developed. Micron-sized elastomeric particles with negative acoustic contrast were used for negative selection acoustophoresis. The surface of the elastomeric particles was functionalized to bind WBCs through the CD45 antigen, which enabled their transportation to pressure antinodes and facilitated an enrichment of cancer cells at the pressure node. Live cell negative selection acoustophoresis was demonstrated as a proof-of-concept study in paper 1 and was further extended to carry out processing of whole blood by a two-step acoustophoresis method in paper 2.

The sample throughput is an important parameter for microfluidic processing of clinical samples, especially for rare cell applications where a larger volume might be required for the detection of target cells. In paper 3, a fluid inertia phenomenon that may compromise cell separation performance at higher flow velocities was discovered. The inertial effects in an acoustofluidic device at increased sample throughputs and its consequences on particle separations were therefore investigated. Through numerical modelling and experimental validation, the main reason for the impaired acoustophoresis separation, at elevated flow rates, was attributed to the formation of a curved fluid boundary between the sample and sheath flow, both at the inlet of the separation channel as well as at the outlet flow splitter.

Finally, paper 4 outlines the benchmarking of CTC-acoustophoresis to the FDA cleared CELLSEARCH system in a comparative clinical study. Higher numbers of CTCs were detected after acoustophoretic processing of the patient samples as compared to the CELLSEARCH system. Further studies are currently being conducted to establish the full performance characteristics of CTC-acoustophoresis in the laboratory setting.

To conclude, the presented dissertation extends the use of acoustophoresis towards the clinical application of CTC enrichment of live and fixed cells. The aim of establishing an efficient technology that can target the full heterogeneity of the rare tumor cells is essential for the development of novel CTC biomarker assays for metastatic cancer. This dissertation builds towards the goal of an unbiased CTC isolation approach.

Prostate cancer

The two most common cancers in men and women are prostate cancer (PCa) and breast cancer, respectively. In Sweden, PCa was the most commonly diagnosed cancer in 2019 and the most common cancer-related cause of death in men with 10,984 new cases and 2,220 deaths [1]. PCa was considered a rather rare type of cancer until at least the middle of the 20th century, with the major reason simply being the formerly shorter lifespan among men. Often, prostate tumors grow slowly and have a long clinical course with a low risk of causing problems or death (*i.e.,* indolent disease). Autopsy studies have shown that a majority of men over seventy years of age have slow-growing local PCa [2, 3]. Although, for some patients the disease progresses much more rapidly through the various clinical states, eventually causing metastatic disease and death. Therefore, there is an urgent need for better tools to early on identify individuals at higher risk to develop aggressive PCa and improve the patient management throughout the various disease stages.

Untreated disease

A few decades ago, PCa was diagnosed first at an advanced stage of the disease, often as metastasized cancer and consequently the patients had a poor prognosis [4]. In the 1990s, a new diagnostic test was introduced, the prostate-specific antigen (PSA) test, which has the capacity to detect even early-stage PCa including the indolent disease. Hence, the PSA test has dramatically increased the incidence of PCa, and it is now possible to identify the disease even before any symptoms occur. As PCa most commonly develops in the outer part of the prostate, the peripheral zone (Figure 1), symptoms (for example related to the bladder) can be a late occurring event [5]. PSA is a proteolytic enzyme (*i.e.,* protease) that is produced by the epithelial cells of the prostate, and it can also be detected at low levels in the blood of healthy men due to normal minimal leakage. In PCa, the levels of PSA in the blood increases as a result of damaged barriers between tissue and blood vessels and it can therefore be used as a diagnostic marker for the disease [6]. The PSA-threshold value to recommend further examination is age dependent and increases

with age. After an elevated PSA test, the diagnostic path continues with digital rectal examination, and a transrectal ultrasound guided biopsy to access tumor material for a prognostic risk classification.

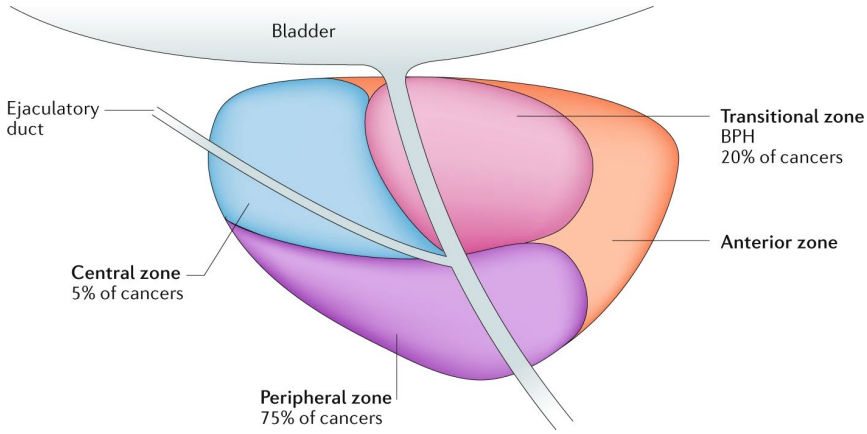

Figure 1. The anatomical zones of the prostate, including the largest peripheral zone, the transitional zone, and the central zone. Reprinted from reference [7] with permission from Springer Nature.

Untreated PCa patients are stratified into four different risk classes (high risk, intermediate risk, low risk, and very low risk) based on the assessed diagnostic factors [8, 9]. The strongest prognostic component is the histological grading of tissue biopsies using the Gleason grading system [10]. It was developed by Donald F. Gleason in 1966 after he identified five different growth patterns of prostate cells in histological sections based on the extent of abnormality (Figure 2). Higher Gleason grades are strongly associated with poor prognosis and PCa aggressiveness [11, 12]. The risk classification also weighs the clinical tumor stage based on the extent of the localized PCa (and any spread to regional lymph nodes or distant sites) and the measured concentration of PSA in blood.

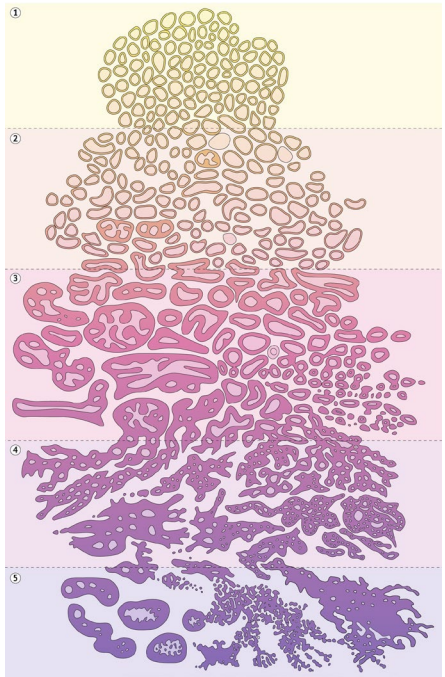

Figure 2. The original Gleason grades 1-5 (top to bottom) from 1966. Reprinted from reference [7] with permission from Springer Nature.

The optimal treatment for the patient is selected based on the risk stratification as described above, but also on age, general health, and personal preference. For low- and very low-risk groups, the recommendation is often active surveillance, where the patient is monitored for changes over time through repeated blood draws and biopsies. Such approach lowers the possibility of overtreatment and thereby avoiding unnecessary side effects [13]. In the case of disease progression or for intermediate- or high-risk tumors, local treatment with radiotherapy in combination with hormonal treatment or radical prostatectomy are offered. Radical prostatectomy is the surgical removal of the prostate tumor together with the prostate gland and the surrounding tissue.

Disease progression

Following active treatment of the primary prostate tumor, the patient is monitored for any rise in PSA value. In approximately 30% of the patients, the disease relapses,

and the patient progress to biochemical recurrent (BCR) disease with rising PSA levels (Figure 3) [14].

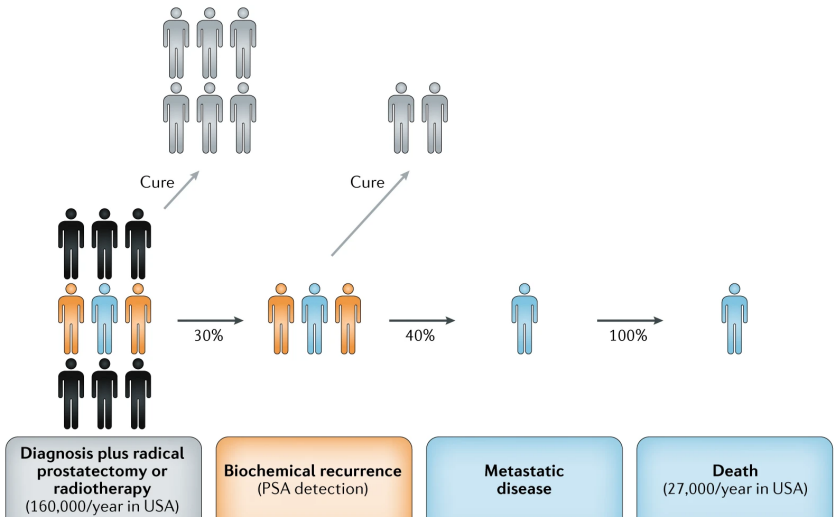

Figure 3. Prostate cancer progression from localized disease to disease recurrence (rising levels of prostate-specific antigen [PSA]), and finally castration resistant metastatic disease. Adapted from [15] with permission from Springer Nature.

Once the patient has been diagnosed with BCR, the most common therapy is androgen deprivation therapy (ADT) in which the secretion of testosterone and dihydrotestosterone hormone is inhibited. Testosterone and dihydrotestosterone are so-called androgens and are the substrates for the essential androgen receptor (AR) (Figure 4). The androgen hormone receptor drives the normal prostatic development and growth but is also central in the progression and maintenance of PCa. Therefore, AR is a main target for PCa treatments [16-18]. AR is highly expressed in most PCa cells, but can be absent in some cases, especially for patients with rare neuroendocrine or small-cell PCa [19, 20].

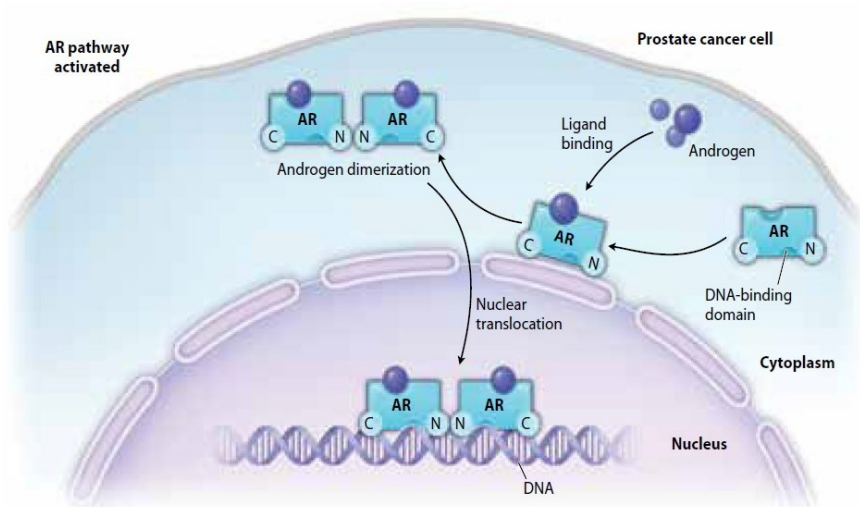

Figure 4. The androgen receptor (AR) pathway. The binding of androgens to the AR initiates nuclear translocation and gene transcription of AR targeted genes. Reprinted from reference [21] with permission from Millennium Medical Publishing.

AR is a transcription cofactor that can bind to specific locations in the DNA and initiate or downregulate the transcription of targeted genes, such as the expression of PSA and TMPRSS2 or the suppression of prostate-specific membrane antigen (PSMA). Activation of the AR occurs when androgens bind to the ligand binding domain (LBD), which introduces a conformational change required for AR dimers and the following translocation into the nucleus (Figure 4). Several variants of the AR have been found resulting from alternative splicing of the transcript pre-mRNA (Figure 5). The truncated variant AR-V7 has gained the most attention due to its nuclear localization and active transcriptional function despite absence of LBD domain and bound substrate [22] and its expression has been shown to increase with advancing PCa stages [23-25]. Additionally, AR-V7 has been associated with resistance to AR targeted treatments and has potential prognostic implications [26-34]. However, further prospective studies are needed to establish its clinical significance.

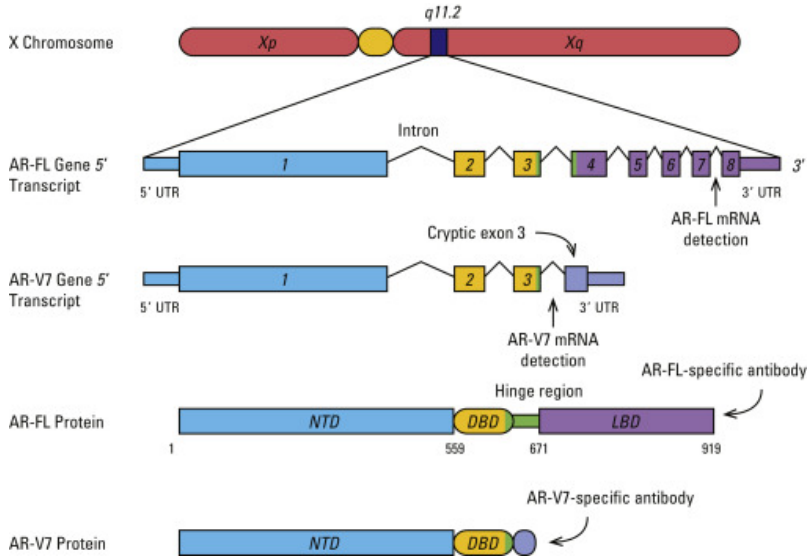

Figure 5. The structure of full-length androgen receptor (AR-FL) gene transcript and translated protein and the truncated variant AR-V7. Reprinted from reference [35].

Approximately 40% of men with BCR will eventually fail ADT and progress to castration resistant metastatic prostate cancer (mCRPC) and eventually succumb to the disease (Figure 3) [14]. The treatment options for mCRPC patients include various antiandrogens, such as AR signaling inhibitors (ARSI), radioactive isotopes, and chemotherapeutic agents.

Biomarkers

Biomarkers are biological characteristics that can be objectively measured and evaluated to assess normal biological processes, pathological processes, or responses to specific treatments [36]. They can be molecular, histological, radiographical, or physiological, and classified based on their clinical utility. The most frequently used biomarkers from a drug development perspective can be divided into four main categories: diagnostic, prognostic, predictive and treatment-response [37], in which the first three categories are pre-treatment biomarkers (baseline) and the last is a post-treatment marker (Figure 6).

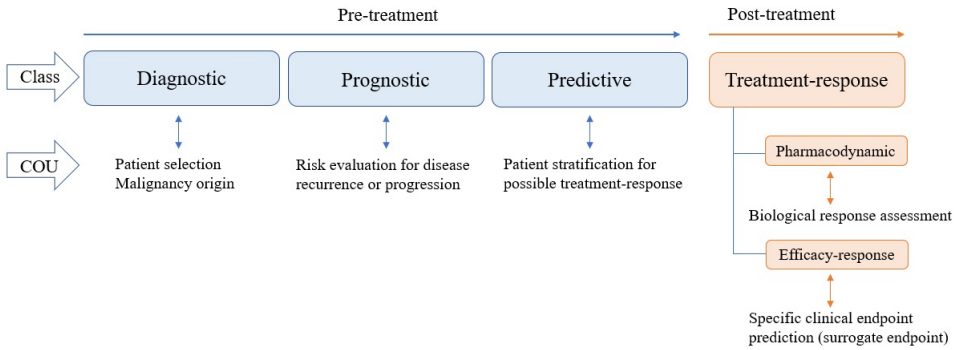

Figure 6. Biomarker classification with predefined context of use (COU).

Diagnostic biomarkers identify presence and potentially origin of malignancy. Prognostic markers evaluate risk for disease recurrence or progression, independent of subsequently selected therapies. The last category of pre-treatment biomarkers, predictive biomarkers, assess the possibility for a favorable response to one or more specific treatments. The challenge with targeted therapies, such as ARSI, is identifying the patients most likely to respond and thus minimize unnecessary side effects in others who will have insufficient therapeutic responses. Here, predictive biomarkers would significantly improve patient management. Additionally, such assessment would be beneficial in the development of new targeted therapies by choosing clinical trial participants accordingly.

Post-treatment biomarkers (treatment response biomarkers) can be classified further into pharmacodynamic and efficacy-response (surrogate endpoint) biomarkers. They dynamically evaluate if a favorable biological response has occurred after a given treatment and can in that way offer an expedited answer to a therapy's efficacy. Thereby, they also inform if a therapy needs to be altered. Efficacy-response biomarkers predict a specific clinical endpoint, such as overall survival (OS), and can therefore be used as intermediate surrogate measures. Such biomarkers can significantly reduce time and cost of clinical trials by revealing the success or failure of a candidate drug at an early stage. The classification of biomarkers into the various categories and subgroups are not definite and there are frequent overlaps between the different groups.

In oncology, biomarkers have a central role in the clinical practice and have contributed to an increased survival and an improved overall morbidity [38]. Although, there are still important limitations and there is an urgent need for further development of clinically relevant biomarkers, both for untreated and metastatic

disease. A critical problem is that most biomarkers are tissue-specific rather than disease-specific and therefore changes are not necessarily representative for a true clinical benefit. As described in the first section, one of the main problems in patient management of PCa is the occasional inability to distinguish between indolent and aggressive disease upon diagnosis. Hence, there is a need for complementary biomarkers to early on be able to identify patients at higher risk to develop aggressive PCa and thereby also avoid unnecessary overtreatments.

In recent years, several new therapeutic agents have been approved for patients with mCRPC after successfully demonstrating an increased OS. However, The United States Food and Drug Administration (FDA) has so far not approved any biomarkers in PCa to support clinicians in selecting the therapy best suited for the individual patient. Further, the traditional measures of treatment response in PCa (PSA and radiographic response) have shown to be of limited use in metastatic disease [39-41]. A post-treatment decline of PSA in mCRPC has shown weak association with OS and is therefore not considered to be a true indicator of a favorable treatment response [42]. Thus, new pre-treatment and post-treatment biomarkers showing clinical benefit in mCRPC patients are urgently needed and would significantly improve both patient management and the success of clinical trials.

The metastatic seed

How can a localized tumor lead to widespread lethal cancer? What are the pathways to secondary tumors and metastatic disease? The details of the metastatic process are to a large extent still unknown, but the escape of malignant cells from the primary site into the bloodstream (Figure 7) is considered an important link to the development of metastasis [43-45]. Tumor cells that are shed into the circulation are called circulating tumor cells (CTCs) and can be of both primary and secondary tumor origin. Only a small subset of these cells can survive the shear stress in the circulatory system, the lack of cell-to-cell adhesion, and escape the immune systems defense to manifest tumor initiation capacities at a distant site [15, 46].

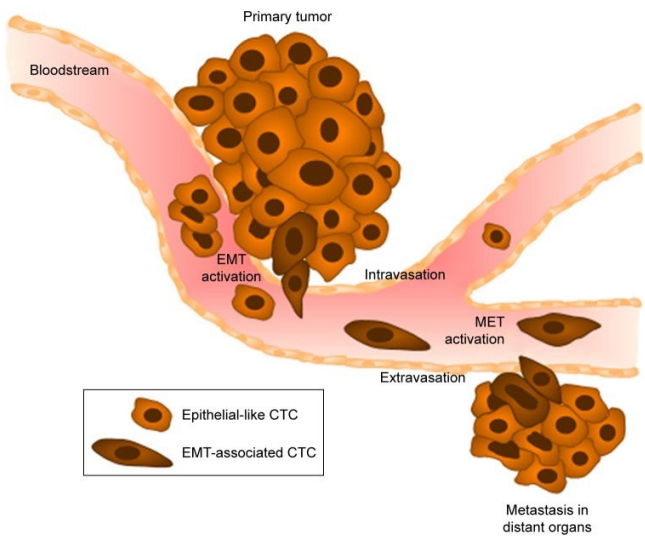

Figure 7. The shedding of circulating tumor cells (CTCs) from the localized tumor into the bloodstream and the manifestation of a secondary tumor at a distant organ. Reprinted from reference [47] with permission from Dove Medical Press.

CTCs have emerged as an important biomarker for the management of metastatic cancer, as the enumeration of CTCs in blood samples from metastatic patients

showed that higher amounts were associated with poor prognosis and low OS in several epithelial cancers [46-48]. CTCs are extremely rare, and the scarcity creates a technical hurdle for their study, as they circulate in the blood together with approximately five billion red blood cells (RBCs) and five to ten million white blood cells (WBCs) per milliliter. Hence, analysis of CTCs requires successful separation from the vast amount of blood cells. Over the last two decades, numerous technological innovations have been introduced for the detection, isolation, and characterization of CTCs.

In this thesis, I will present a novel methodology of sequential acoustophoresis for CTC isolation (paper 1 and 2), subsequently, I will outline the benchmarking of CTC-acoustophoresis technology with the current state-of-the-art in CTC isolation (paper 4) and discuss considerations to be made when scaling up throughput in acoustophoresis (paper 3).

In the following chapters, I will describe the available methods for cell separation targeting CTCs, using both macroscale and microscale approaches, and the potential of CTCs as versatile biomarkers of cancer.

Tumor heterogeneity and liquid biopsies

Malignant tumors consist of cancerous cells which have an abnormal cell growth, cell division, and ability to avoid cell death (apoptosis) due to alterations and instability of their genetic material. Such changes can be DNA mutations in protective tumor-suppressor genes, driving oncogenic mutations, chromosomal and epigenetic changes, that all causes defect cells [48, 49]. Additionally, during the growth of malignant tumors the microenvironment surrounding the cells changes due to a lack of oxygen (hypoxia), space constraints as the tumor grows, and inflammatory and immune responses, which creates an ongoing regional selection pressure for advantageous genotypes and phenotypes [50, 51]. This variation is known as tumor heterogeneity (Figure 8) and can be found between cancer patients with the same type of cancer, *i.e.,* intertumor heterogeneity, and within a single tumor tissue, *i.e.,* intratumor heterogeneity [48].

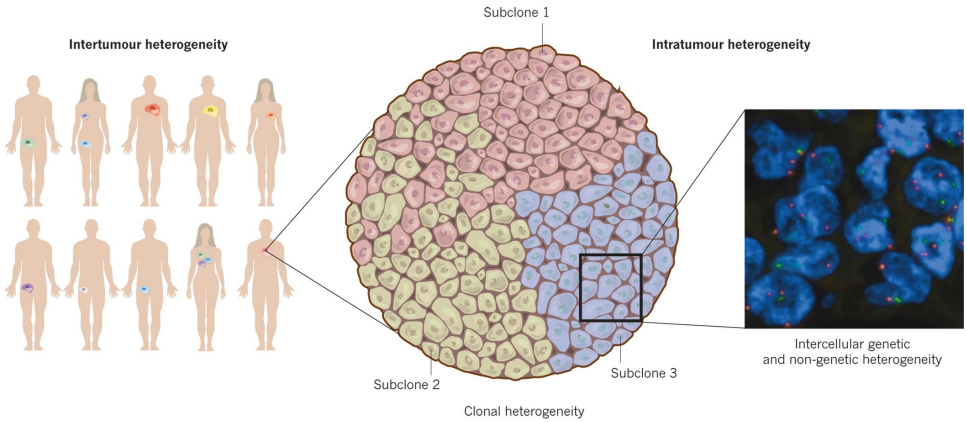

Figure 8. Tumor heterogeneity between patients (inter) and within a tumor tissue (intra). Subclones can be off different genotypes and phenotypes. Reprinted from reference [48] with permission from Springer Nature.

The large tumor heterogeneity can impose a sampling bias to diagnostic biopsies, which causes a major problem for clinicians to guide patient management and select patient-specific treatments, and it highlights a need for alternative procedures [52]. Further, a tissue biopsy is invasive, painful, imposes risks, and is therefore not suitable for frequent sampling. Correspondingly, CTCs demonstrate heterogeneity as they are shed from different parts of both primary and secondary sites and they have been shown to represent different subclones present in a cancer patient [53, 54]. As a blood sample on the other hand is fast, cheap, minimally invasive and can be repeated on a regular basis throughout the patient care, it may serve as a so-called "liquid biopsy" for tumor material. The isolation and profiling of CTCs from a blood sample could likely give a better real-time snap-shot of the current disease status than a tissue biopsy and help in patient stratification [55].

CTC genotypes and phenotypes

A fundamental issue to isolate and analyze a certain cell type is to distinguish what defines that specific group. First, there is no single definition of CTCs and various assays uses different strategies and targets [56], but there are commonly employed cell characteristics which will be explained below.

Carcinoma is the most common type of cancer, where the disease starts in the epithelial cells of the skin or the tissue lining the internal organs. Therefore, CTCs are most often targeted by the expression of different epithelial markers, such as

epithelial cell adhesion molecule (EpCAM), E-cadherin, and different types of cytokeratin (CK). Although, such classification neglects potential CTCs that have undergone a phenotypic transformation from epithelial tumor cells to fibroblastic-type tumor cells in a so-called epithelial-to-mesenchymal transition (EMT) [57, 58]. This transition has shown to increase cellular motility by activation of the cytoskeleton and reduction of intercellular junctions, and enable tumor invasion of the basement membrane and then intravasation into the bloodstream (Figure 9) [59]. For most carcinomas, an EMT transition is thus considered a pre-requisite for tumor infiltration and metastasis formation by allowing a more migratory phenotype and through the expression of mesenchymal genes. Although, most CTCs express both epithelial and mesenchymal markers (*e.g.,* vimentin and E-cadherin) through a highly dynamic process, where the reversed transition, *i.e.,* mesenchymal to epithelial transition (MET), is suggested to be required for the colonization of CTCs at a secondary site [60, 61].

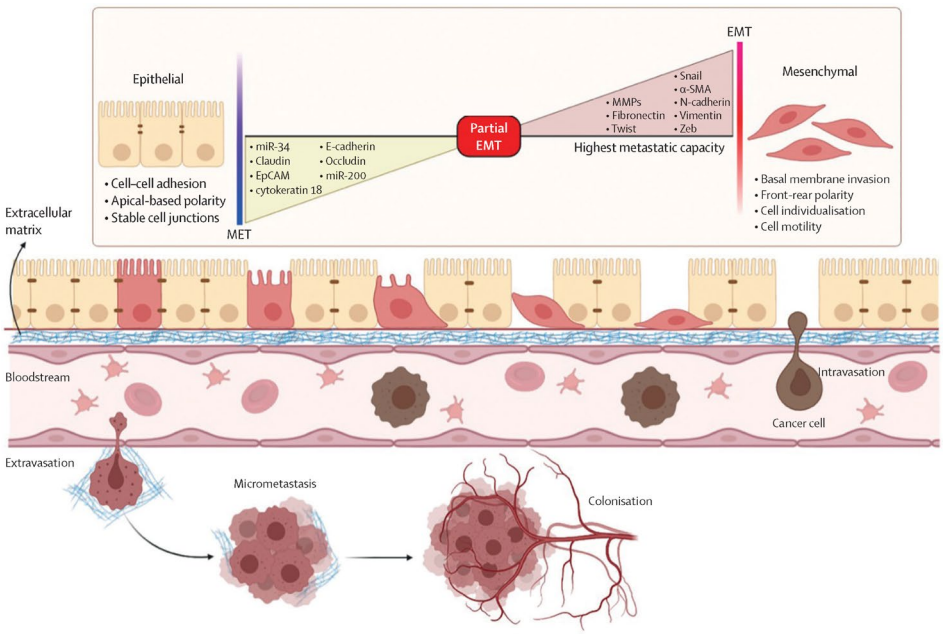

Figure 9. Changes of the phenotype and genotype through epithelial to mesenchymal transition (EMT) of tumor cells facilitates cell motility and invasion of the basement membrane. Reprinted from [62] with permission from Elsevier Inc.

Importantly, CTC phenotype and number are affected by cancer treatment. Studies have found that patients who responded to given chemotherapy had significantly

fewer CTCs and were of a more epithelial-like phenotype, whereas treatment resistant patients had more mesenchymal featured CTCs [63-65]. One of the studies identified a chemoresistant subpopulation of CTCs with both partial EMT and cancer stem cell (CSC) traits. Detection of CTCs with such phenotype could independently predict an unfavorable outcome in metastatic breast cancer patients [65]. CSCs are tumor cells with increased self-renewal and proliferation (stemness) capabilities that have shown resistance to radiation and chemotherapy [66]. Further knowledge regarding the molecular characteristics of CTCs and how the EMT status impact malignant potential and treatment response is needed and could help in patient stratification and risk assessments [67].

An additional class of CTCs that has gained increased attention over the last decade is CTC clusters, which is a rare group of two or more CTCs that are kept together by intercellular adhesion (Figure 10). They are not a result of cellular aggregation within the blood vessels, but instead derived from small detachments of the primary tumor [68]. They have been shown to be exceedingly rare and only represent a few percent of the total CTCs, but with a considerably higher metastatic potential than single CTCs, and its abundance have also been associated with unfavorable outcomes for cancer patients [68, 69]. Hence, it has been suggested that the shedding of CTC clusters represent one of the most important events in the metastatic process, although the details of their formation, survival advantages and metastatic potential are still largely unknown [70]. Existing CTC enrichment methods are mostly aimed for isolation of single CTCs, but novel technologies targeting CTC cluster are being developed [71-73].

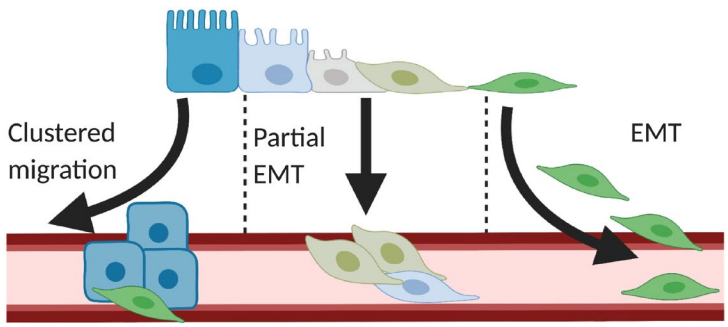

Figure 10. Shedding of CTC clusters and single CTCs of various subtypes. Reprinted from reference [74] with permission from Elsevier.

A last group of distant tumor cells is disseminated tumor cells (DTCs), which are CK positive cells found in the bone marrow of cancer patients. The bone marrow is a major site of metastatic lesion for both breast and PCa and the detection of DTCs at the time of diagnosis have been associated with an increased risk of tumor recurrence [75-77]. Studies have suggested that the bone marrow may act as a reservoir organ for viable but dormant DTCs that could contribute to further spreading to other sites of the bone marrow, as well as to other tissues [56].

Consequently, the CTC identification strategies vary and can comprise of different cellular markers and analyses. An important consideration in the sample preparation process for CTC isolation is if the CTCs are to be analyzed as live cells with intact tumor-initiating potential or if fixed cells are suitable. Fixed cells are treated with a chemical agent (*e.g.,* paraformaldehyde, ethanol, methanol) to permanently preserve the cell in a life like state. The chemical agent (*i.e.,* fixative) cross-links the majority of the cellular proteins and peptides to form an intracellular meshwork and thereby makes the cells resistant to degradation or deformation. The preservation of cells has some technical advantages as it allows a longer sample processing window and thereby facilitate transportation of samples between hospitals and clinical labs. The cells are more tolerant to preanalytical challenges, such as transport conditions, temperature variations *etc.* Fixed cells also allow for direct staining and analysis of intracellular markers, such as hormonal receptors and different intracellular cytokeratins. However, critical advantages of live CTC isolation are the possibilities for unaltered transcriptional and functional studies and *in vitro* culturing of patient-derived malignant cells to aid in the development of personalized cancer care and the detailed understanding of CTC properties and functions. Most of the CTC isolation technologies are designed for fixed cells and not for intact viable CTCs. Hence, there is an unmet clinical need for live CTC capture for downstream analysis and *in vitro* expansion to enable drug testing and predict therapy responses in metastatic cancer.

Following CTC isolation, the cells can be analyzed either as pooled cells or by single-cell analysis. Single-cell profiling is still at an early stage with technical issues that need to be addressed, but it is a promising approach as it may discover the true CTC heterogeneity, which could be hidden by bulk background cells, *i.e.,* contaminating WBCs [78].

Live cell analysis – *In vitro* culturing and biophysical profiling

Currently, available *in vitro* models of PCa are limited and do not reflect the large heterogeneity of the disease. There are approximately 1,000 different cancer cell lines in public sources, but as PCa cells have shown to be very difficult to expand in culture, only seven of them are of PCa origin. Recent advancements in cell culturing have identified successful growth conditions for newly derived patient PCa cells and established novel PCa cell lines [79, 80]. The majority of the cell lines were derived from metastatic tissue, but one had CTC origin, the MSK-PCa5 cell line. The expanded cells were responsive to drug testing *in vitro* and *in vivo,* and they could recapitulate the molecular and phenotypic diversity of the patient's tumors [80]. An *in vitro* expansion of isolated tumor cells could facilitate personalized medical advancements and help to identify essential cellular traits for the initiation of metastatic lesions [80]. These studies have opened a new path for future CTC research.

Live cells can also be assessed for their biophysical phenotypes. Cellular properties like elasticity, deformability, adhesion, motility, and allocation of membrane receptors can be measured, which can reveal changes that have been induced by disease status or microenvironmental or external factors, such as cancer therapies [78]. An essential prerequisite to establish patient-derived CTC cell lines or to perform functional assays is to isolate intact viable cells. Therefore, in addition to not using any fixative treatment prior to isolation, the selected CTC isolation method needs to be gentle and have a short sample processing time to avoid cell alterations and death.

Fixed cell analysis – Imaging technologies

Preservation of tissue biopsies and blood samples with chemical fixatives allows for identification of specific proteins and genes by immunochemistry and cytogenetic techniques. Immunohistochemistry (IHC) uses antibodies for detection of proteins in thin tissue sections with intact cellular and tissue structure. Immunocytochemistry (ICC) studies the individual cells, in which antibodies can localize and quantitate cytoplasmatic and nuclear proteins. Visualization can be done by direct labeling of the antibody with a fluorescent marker or a reactive enzyme (direct detection), or through a labeled secondary antibody targeting the specific primary antibody

(indirect detection) (Figure 11). By using indirect detection, the signals can be amplified, which is useful for low abundance target proteins. A disadvantage is the more cumbersome procedure with a risk of increased background noise.

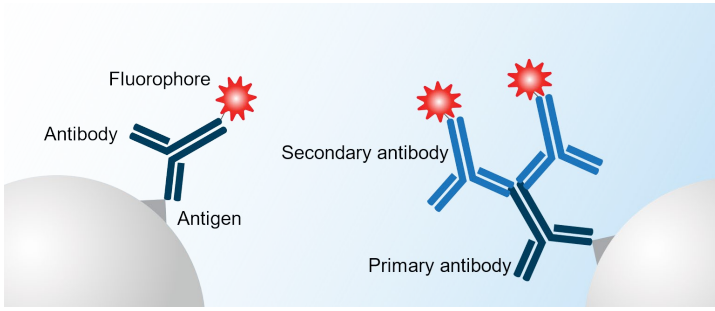

Figure 11. Direct (left) and indirect (right) fluorescent detection of a cellular antigen. Signal amplification can be obtained through multiple secondary antibodies binding to a primary antibody.

Fluorescent *in situ* hybridization (FISH) studies genetic variations and abnormalities by hybridizing fluorescently labeled DNA fragments (probes) onto a glass slide containing appropriately prepared cells or tissue sections. Genetic amplifications, deletions, and rearrangements can then be identified in individual cells by microscopy analysis. Several specific abnormalities are examined in oncology for the purpose of diagnosis or selection of targeted therapy [81]. For example, in PCa the most common alterations are relative gain of the oncogene MYC, amplification of the AR gene (Figure 12), loss of the tumor suppressor gene PTEN, and translocation followed by gene fusion of TMPRSS2 with the oncogene ERG [82-84].

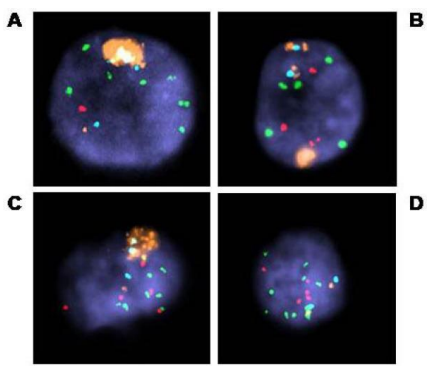

Figure 12. Fluorescent *in situ* hybridization (FISH) staining of patient-derived CTCs showing AR (orange) amplification in some cells (A-C) and high copy gain for MYC (green) in all (A-D). Reprinted from reference [82] with permission from American Association for Cancer Research.

Various cellular epitopes can be targeted simultaneously by using a mixture of antibodies, in which each type is labeled with a different fluorophore. Thereby, a cell can be characterized by the presence or absence of several essential markers to confirm the cells' identity. Additionally, multiple immunolabeling with several fluorophores can investigate the co-localization of proteins, such as diverse hormone receptors [85]. A crucial step for successful staining is to validate the combination of antibodies and markers by confirming their accuracy, separately and together, and check for unspecific binding and cross-reactivity. Further, the fluorochromes need to be carefully selected as they often have broad emission bands which can contribute to spectral overlap and impaired measurements of the individual emission spectra. Thus, the detection system often limits the number of possible epitopes during multicolor imaging.

There are different types of technology platforms for the gene and protein visualization. In addition to two-dimensional brightfield and immunofluorescence (IF) microscopy, confocal microscopy offers a three-dimensional view of cells by digital image processing using so-called z-stacks (Figure 13). Multiple layered images are taken and combined in a composite image with a thicker plane of focus. For precise localization of proteins within a cell, confocal microscopy can be advantageous. Although, the image acquisition is slower compared to standard IF and for an increased image resolution with more details further layers are required.

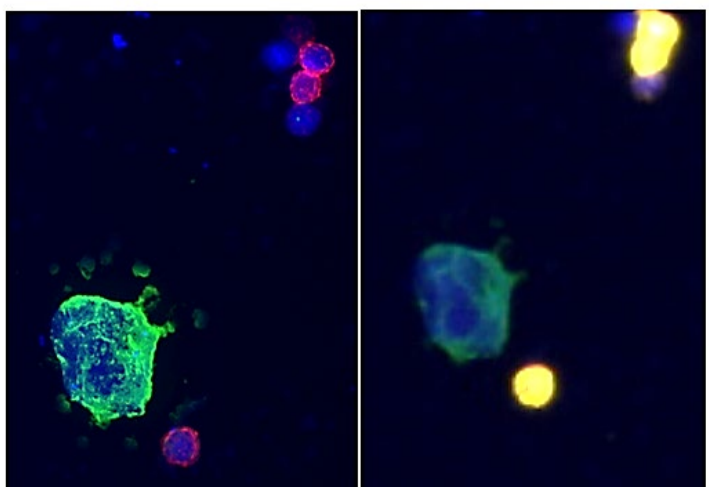

Figure 13. Confocal (left) and immunofluorescent (right) microscopy images of a larger cytokeratin (green) positive cell and smaller CD45 (red) positive WBCs. Nuclear DAPI (blue) staining in all cells. Confocal imaging offers enhanced image resolution at the expense of time.

Automated high-throughput detection systems are suitable for analysis of larger number of cells, such as liquid biopsies containing millions of blood cells. A standard technology for sensitive, high-throughput analysis of single cells in heterogenous samples is flow cytometry. Flow cytometry detects and measures physical and chemical characteristics of cells in a sample fluid, such as cell size, DNA content, cell count, and presence of specific proteins using fluorochrome-labeled antibodies. The sample is injected into a sheath flow in the instrument and through hydrodynamic focusing directed into a narrow stream before a laser interrogation point, where the forward and side scattered light from a single cell and multiple fluorescent emission spectra can be assessed (Figure 14). When the cell passes through the laser beam at the interrogation point, information regarding presence or absence of targeted proteins is obtained from fluorescence pulse-analysis and thus, no details regarding localization or distribution of the proteins are given [86].

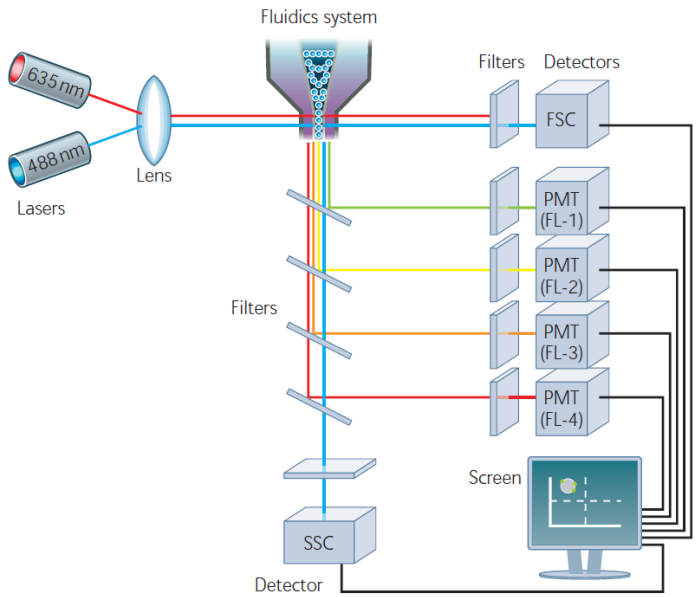

Figure 14. Setup of a typical flow cytometer. Detection of forward (FSC) and side (SSC) scattered light and fluorescent emission spectra by FSC/SSC detectors and photon multiplier tubes (PMTs). Reprinted from [87].

An advanced development of flow cytometry is image flow cytometry (IFC), which integrates the features of flow cytometry with IF microscopy and data processing algorithms [86, 88, 89]. In IFC the multiplexed fluorescent information is acquired through cellular images and can thereby demonstrate cell morphology and

subcellular distribution of proteins (Figure 15). A key drawback for IFC compared to non-imaging flow cytometry is the lower throughput of approximately one order of magnitude. In addition, IFC has problems to generate high-resolution images, which relates to cell motion blur at high velocities. Although, a high-throughput multiparametric imaging flow cytometer that enables blur-free fluorescent detection of cells was recently described [89].

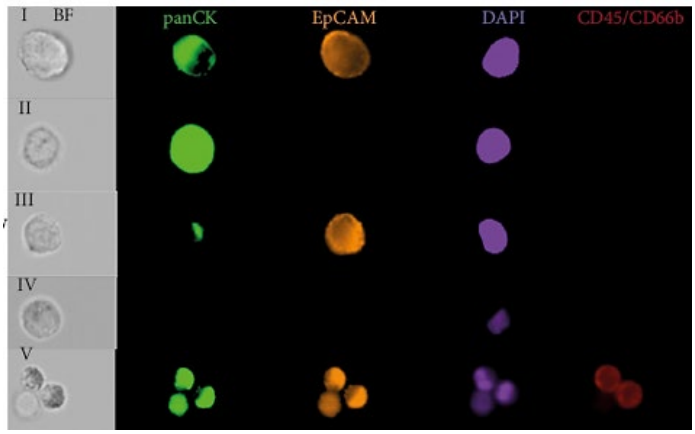

Figure 15. Representative images of cells detected with the ImageStream system from a metastatic prostate cancer patient blood sample after acoustophoretic cell separation (from manuscript 4). The five rows are different cells, and the columns are brightfield images (BF) and the different fluorescent markers (panCK, green; EpCAM, orange; DAPI, purple; CD45, red). The last row shows a CTC cluster consisting of two WBCs and one CTC.

An alternate method to obtain high-resolution images of a multitude of single cells is through automated cell imaging platforms with IHC- or ICC-stained glass slides, which automates image collection and uses algorithms to identify the target cells and record their positions [90]. The method can identify target proteins or genetic aberrations through IF and FISH staining. Nevertheless, even automated platforms will be lengthy and inefficient with a massive number of cells and therefore, it is desired to first distinguish the target cells through an enrichment process.

Single-cell analysis – Molecular profiling

Molecular profiling of a group of pooled cells will result in an average value and could miss specific characteristics that is only present in a single cell or a small

subset of the cells. Consequently, as CTCs are a highly heterogenous population, single-cell analysis is desired and have gained increasing attention in the last decade [54, 91]. The approach poses several technical challenges in cell separation from a complex blood sample, individual sorting of the CTCs, confirming tumor origin, and finally perform analysis on a very limited sample material. A single cell only contains picogram (pg) amounts of DNA and RNA, and therefore an amplification of the genetic material through targeted amplification or whole genome amplification (WGA) combined with exceptionally sensitive analytical methods are required for analysis. The analyses can provide important knowledge about tumor biology, such as how CTCs survive in the bloodstream, transform, migrate, and extravasate at distant tissues, as well as information regarding patient-specific mutation status of primary tumor and developed metastasis.

There are two types of molecular analyses targeting different kind of information, gene expression analysis and mutational analysis. Gene expression analysis investigate the current RNA content of a cell and thereby studies the currently active genes. Mutational analysis explores somatic mutations of the cell's DNA, such as copy number changes, nucleotide base substitution, insertions and deletions of bases, and structural rearrangements. As earlier described, cancer cells have an altered and instable genome, which may acquire additional mutations during the progression of the disease due to the ongoing selection pressure for advantageous genotypes and phenotypes [48].

Gene expression analysis

After lysing isolated live cells and extracting the RNA content, it is necessary to perform complementary DNA (cDNA) synthesis as RNA is more fragile than DNA and easily gets degraded [92]. Once the cDNA has been synthesized through reverse transcription, it needs to be amplified before quantitative real-time polymerase chain reaction (qRT-PCR), microfluidic qRT-PCR, or RNA sequencing can be performed. The qRT-PCR analysis of upregulated or downregulation genes and pathways can target a single gene of interest or be multiplexed with several genes. Numerous studies have explored the expression of genes associated to EMT, metastasis, and driving disease specific hormone receptors, and they demonstrate a vast heterogeneity of CTCs, even among the cells retrieved from the same blood sample [54, 91, 93, 94]. One study showed that CTCs reflected the gene expression patterns in metastatic tissue biopsies for a selection of genes and another study demonstrated CTCs with expression patterns found in both the primary tumor and in the metastasis

[93, 94]. The studies support the use of CTCs as an alternative to tissue biopsies, as mutations of both primary and metastatic sites might be detected.

The major problem with single-cell molecular profiling is the technical noise resulting from the miniscule input of starting material [95]. For a gene with low copy transcript, it is even more problematic. To solve these issues, so-called RNA spike-in transcripts of known sequence and quantity have been developed for calibration purposes, as well as new quantitative statistical software programs [96]. Further, another technical hurdle is the preservation of RNA, both the RNA quality and the current transcriptional status, without introducing alterations during the CTC isolation process. As gene expression can be influenced by cellular and environmental stimuli [78], the selected technology for isolating CTCs should be gentle and fast to avoid changing the transcriptional profile.

Mutational analysis

The DNA molecule is less prone to hydrolysis and degradation compared with RNA due to the absence of a hydroxyl group in the sugar phosphate backbone of the DNA nucleotide. Therefore, DNA can be long-termed stored without degradation, which facilitates analysis [97, 98]. To elucidate genomic changes in single tumor cells, the extracted DNA first need to be amplified using WGA before array comparative genomic hybridization (aCGH) or next-generation sequencing (NGS) can be performed [99-101]. aCGH allows for genome wide screening for copy number variations (CNV) of genes, *i.e.,* net gains and losses of genetic material (Figure 16). The genome of interest and a reference genome (nonmalignant) are different labeled with fluorescent markers before competitively hybridized to an array with spotted DNA fragments. The resulting fluorescent signal intensity is measured, where genetic gains and losses are shown by the absence or surplus of the sample fluorophore. These structural variations of the DNA includes normally occurring variations between healthy individuals (which may be associated to increased disease risks) but also gene amplifications and deletions commonly acquired in tumor cells [102]. Such CNVs are frequently detected in regions containing oncogenes (amplifications) and tumor suppressor genes (deletions) [103].

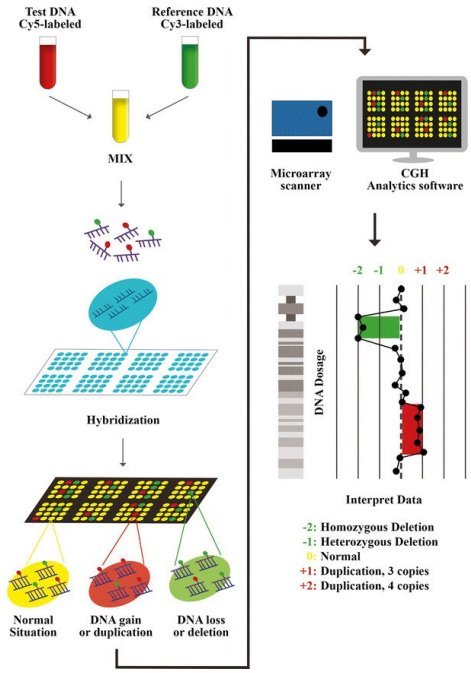

Figure 16. Copy number variations (CNVs) studied by array comparative genomic hybridization (aCGH). Reprinted from reference [104].

NGS can determine the exact order of nucleotides in the entire genome or in selected areas and reveal absolute copy numbers and single nucleotide polymorphism (SNPs) in a single cell [99]. SNPs are mutations of single nucleotides at specific locations in the DNA, which could result in a change of the amino acid sequence of a protein if it is located within a coding region (exon). Millions of SNPs have been detected within the human genome, most are likely harmless but some have been correlated with disease, such as cancer and diabetes [102]. NGS has ultra-high throughput due to massively parallel sequencing of millions of DNA fragments at the same time and it covers each base several times for correct assessment of any DNA alterations [105].

Mutational analysis has confirmed the intrapatient heterogeneity of CTCs and found that mutations in tumor-related genes in the primary and metastatic tissue samples also can be identified in the corresponding CTCs [99, 101, 106]. Some mutations were found only at subclonal levels in the tumor tissues, which highlights the constant regional selection pressure for advantageous genotypes and phenotypes. Additional unique mutations were also detected in the CTCs, which could be influencing the tumor evolution and metastasis [101].

Cell separation approaches

The process of separating CTCs from a peripheral blood sample is a challenging task due to the complexity of blood and the scarcity of the tumor cells. Blood contains a mixture of cell types at vastly different concentrations, blood clot assisting platelets and blood plasma carrying various biomolecules (proteins, antibodies, ions *etc.*) (Figure 17). The most abundant cell type in the blood stream is oxygen transporting red blood cells (RBCs) with an approximate concentration of 10^9 cells/mL whole blood. The white blood cells (WBCs), also called leucocytes, have an approximate concentration of 5×10^6 cells/mL whole blood. WBCs are an essential part of the immune system and can be further categorized as granulocytes (neutrophils, basophils, eosinophils), monocytes/macrophages and lymphocytes (B-cells, T-cells, and NK cells). CTCs have an extremely low concentration in patient blood samples, a cancer patient might have one CTC in a background of millions of blood cells [107] and their detection is often referred to the common phrase "finding the needle in the haystack". Not only are the CTCs rare, but an additional difficulty to their isolation is the large heterogeneity described earlier. To meet the challenge, several technologies have been developed for cell separations and CTC isolation, all with different advantages and drawbacks.

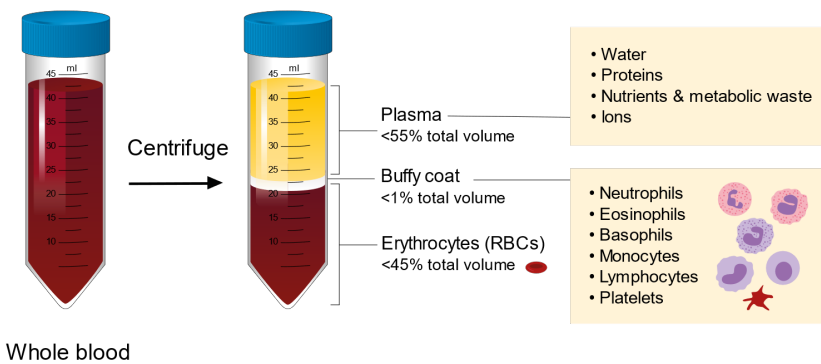

Figure 17. Centrifugation separates a whole blood sample into well-defined component parts of plasma, buffy coat (WBCs and platelets) and RBCs.

Performance terminology

To evaluate the performance of a cell separation assay various measures are determined. In the following section, the commonly referred terms are described.

During testing of CTC isolation technologies, the term *recovery* is used to describe how many of the reference cells that were retrieved in an assay. It should not be mixed up with *separation efficiency*, which report on how well different cell types separate in an assay. Such a measure is often greater than the recovery of the assay as it only analyses the cells that were retrieved in the output sample, and thereby neglects the cells that were lost throughout the process. The *purity* is a measure of the cellular uniformity of the output sample, *i.e.,* the proportion of desired cells in relation to the cellular contamination by unwanted cell types. Purity is consequently heavily influenced by the cell composition of the starting sample. The *enrichment factor* is an assessment to determine the extent of removal of unwanted cells from the original sample. The efficiency of a cell separation assay is described by the *volumetric throughput*, which quantifies the rate of sample processing as volume per time unit. The measure can be ambiguous as it does not reveal sample dilution factors, which will have an obvious impact on the actual sample processing time. An alternative measure is the processed cell number per time unit.

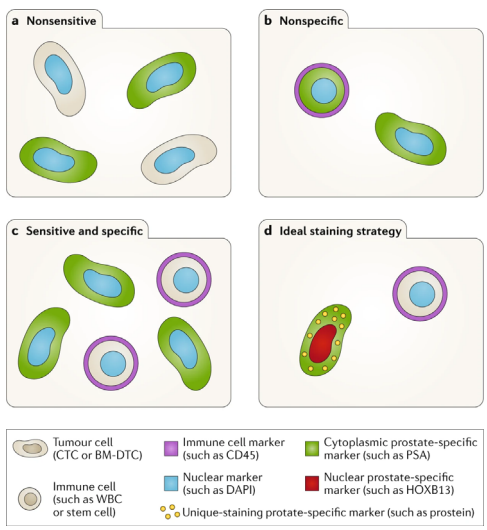

Figure 18. Sensitivity and specificity of immunofluorescent staining of CTCs and WBCs. High sensitivity might result in false positives (nonspecific), whereas high specificity might result in false negatives (nonsensitive). Reprinted from reference [15] with permission from Springer Nature.

The analytical measures *sensitivity* and *specificity* are assessed during the validation process of a technology. The sensitivity demonstrates to what extent the assay identifies true positive cases of the disease, malignant cells *etc.*, whereas the specificity shows how many of the true negative cases that get classified as negative. There is often a trade-off between the two performance measurements, a focus on high sensitivity may result in increased false positives, which lowers the assay's specificity (Figure 18).

Macroscale techniques and current "gold-standard" for CTC isolation

Traditional cell separation techniques are based on physical properties of the cells, such as cell size, density, and cell contents. These techniques can be classified as macroscale methods, where a large number of cells can be separated as a bulk. However, the purity of the separated cell fractions is often quite limited, and a substantial number of cells may be lost during the process. The most common conventional methods for cell separation include centrifugation and filtration, which also can be used as preparatory steps for further cell enrichment.

Centrifugation is a simple and effortless separation method based on the cell density. It is extensively used in clinical laboratories as it can separate a very large number of cells in a fast and inexpensive matter. However, in addition to the problem of low purity, the method also suffers from cell loss, *i.e.,* poor recovery. Therefore, the suitability of centrifugation as the separation method depends on the targeted blood component. To obtain cell-free blood plasma for measurements of clinical chemistry analytes, centrifugation is an excellent choice (Figure 17). Alternatively, a density gradient medium, such as Ficoll-Paque, can be used to separate cells into different layers during the centrifugation process (Figure 19). An intermediate layer will form on top of the density medium and below the blood plasma containing the mononuclear cells (monocytes, lymphocytes, CTCs *etc.*), whereas the heavier granulocytes will pellet to the bottom of the centrifugal tube along with the RBCs. An additional centrifugation technique is rosetting, where a density medium is combined with a tetrameric antibody complex that binds to the unwanted cells and the surface protein glycophorin A on the RBCs. During the centrifugation step the bound cells will pellet together with the RBCs in a negative

selection process resulting in increased sample purity. Nevertheless, loss of cell viability has been suggested to be the result of cytotoxicity of density mediums [108].

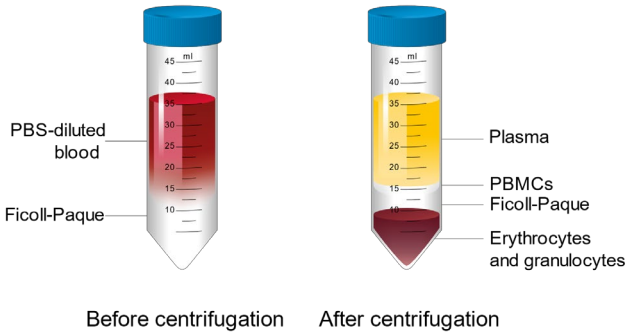

Figure 19. Density medium (Ficoll-Paque) centrifugation of diluted whole blood (left) into well-defined layers (right) containing different cellular and liquid portions of the blood.

Filtration separates cells based on cell size and/or deformability using different kind of filters with micron-sized pores. However, the method has problems with cell loss, often due to clogging of the pores [109, 110]. The method can also be used as a pre-separation step to remove cell aggregates and contaminating particles prior further enrichment of the target cell type.

Additional macroscale methods are magnetic-activated cell sorting (MACS), fluorescence-activated cell sorting (FACS) and the CELLSEARCH system technology, which uses monoclonal antibodies to assist in the capture of specific cell types. These techniques can achieve a higher cell purity compared to label-free bulk approaches, but they are laborious and lengthy. Monoclonal antibodies are specific to a single epitope on an antigen and have low nonspecific cross-reactivity leading to an increased sample purity. They can be commercially acquired for a massive range of targets, and they can also be conjugated with different molecules, such as a reporter protein, a fluorophore, or a magnetic bead. The labeling of cells with fluorophores or magnetic beads can have a negative impact of the cell function and viability, which is another important drawback of the antibody-based techniques [111].

MACS uses antibodies conjugated with magnetic beads to capture cells. The bound cells can be separated from the remaining cells by applying a magnetic field with a permanent magnet (Figure 20). The bound cells will be retained within the magnetic

field whereas the others will flow through, and after a washing step the targeted cells can be eluted. The method has a larger throughput compared to FACS due to its bulk processing properties, but commonly with a much lower purity [112].

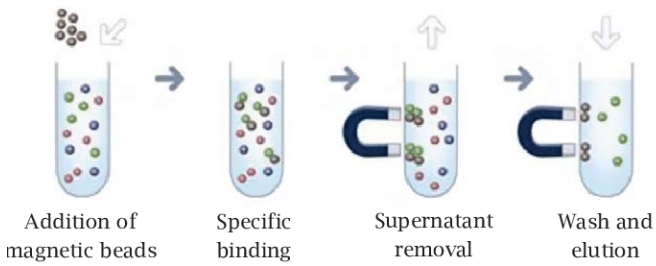

Figure 20. Working principle of magnetic-activated cell sorting (MACS) using specific antibodies conjugated to magnetic beads for positive selection of targeted cells. Reprinted from [113].

FACS is a cell sorting technology based on flow cytometry (as described in section *Fixed cell analysis – Imaging technologies*) where each cell is analyzed, classified, and sorted based on a given criteria (Figure 21). Briefly, the cells are hydrodynamically focused prior an optical interrogation point, where a laser beam generates forward and side scattered light and fluorescence from the illuminated cells that gets detected by photomultiplier tubes (PMTs). The cells are then classified based on the detected signals and finally diverted into separate outlets after being individually encapsulated into electrically charged droplets that passes through two deflection plates (*i.e.,* an electromagnet). As mentioned, FACS offers high purity, but the cell throughput is not sufficient for rare cell sorting. Another significant disadvantage compared to other conventional cell separation and sorting techniques is the high instrumental cost.

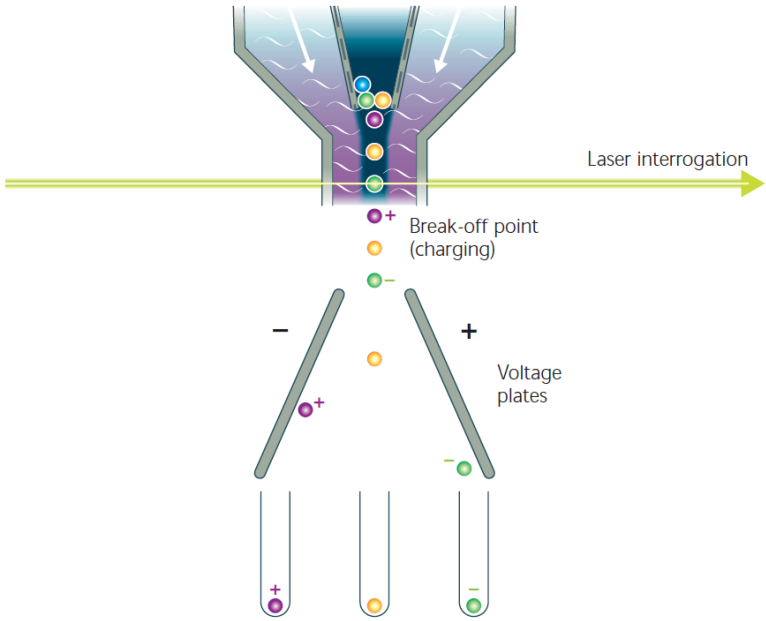

Figure 21. Fluorescence-activated cell sorting (FACS) sorting of charged droplets containing fluorescently labeled cells after an upstream cell analysis and classification. Reprinted with from reference [87].

CELLSEARCH (Menarini Silicon Biosystems, Bologna, Italy) is still today the only technology that has received a clearance by the FDA for enumeration of CTCs as a prognostic biomarker predictive of OS in advanced cancer [114-117]. Therefore, it is considered the "gold-standard" within the field and all other CTC technologies are, so far, only used for research purposes.

Like MACS, CELLSEARCH employs an immunomagnetic capture of the target cells, here by anti-EpCAM-coated magnetic nanoparticles. The magnetically recovered cells are stained with a fluorescent antibody cocktail targeting three different types (8, 9 and 18) of cytokeratin (panCK), WBC marker CD45 and nuclear stain 4', 6-diamidino-2-phenylindole (DAPI) and are thereafter imaged with the built-in CellTracker (Figure 22). The CELLSEARCH definition has become the general description of a CTC as a CK-positive, CD45-negative cell of round or oval shape of at least 4 x 4 μm^2, and with an intact nucleus (DAPI-positive) [118, 119]. Additionally, as the cells have been captured with anti-EpCAM-targeted antibodies, they are also classified as EpCAM-positive, even though the cells are not fluorescently stained for the marker. The CellTracker imaging platform has the capacity to image four fluorophores, so there is an option to use an additional marker

of interest, such as HER2 for metastatic breast cancer [120] or AR for PCa (Figure 22).

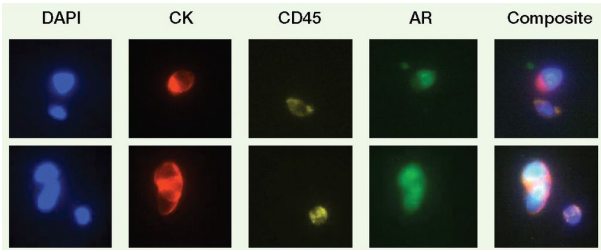

Figure 22. Immunofluorescence images of CTCs (rows) from castration resistant prostate cancer patients enriched with the CELLSEARCH platform and imaged with the CellTracker showing nuclear DAPI and AR staining, and cytoplasmatic CK staining (columns). Both frames also include one DAPI and CD45 positive WBC. Adapted from reference [121] with permission from American Association for Cancer Research.

The advantages of the CELLSEARCH technology are several. It is user friendly, has a fast performance with an ability to process up to eight blood samples in parallel, holds an integrated capacity for in-device staining, imaging, and enumeration, and a possibility to retrieve the captured cells from the sample cartridges. The major disadvantage of the CELLSEARCH method is the antibody-dependent positive selection of EpCAM-positive cells, which limits the detection to only epithelial-like CTCs and it disregards other subtypes, including mesenchymal-like CTCs [122]. This drawback remains for all antibody-based technologies with a positive selection approach. Additionally, several studies have reported a low recovery by the method with a difficulty to detect cells with lower expression levels of EpCAM [118, 123-126]. The studies showed recoveries of control cancer cell lines between 42% to 90% and of clinical samples between 20% to 77.5%. The inability to detect mesenchymal-like CTCs that has undergone EMT and CTCs with reduced EpCAM expression highlights the need for new technologies with a capacity to detect the full range of CTCs from various cancer types.

Increased insight of the cellular diversity and its role in clinical management of cancer patients has motivated for better cell manipulation strategies. Conventional cell separation techniques have, as discussed, many limitations in their performance and are only based on a few sorting principles.

Microfluidics

Microfluidics is a collective term for technologies that control the flow of a fluid and operate within the micrometer scale. The small size scale opens up for separation principles not possible in the macroscale world due to diverse physical effects. Microfluidic cell separations are governed by a phenomenon called laminar flow where the fluid flows in parallel layers with minimal mixing only due to diffusion (Figure 23). This results in predictable fluid trajectories, making cell separation possible when combined with techniques for precise positioning of cells in the fluid stream. The flow velocity varies over the cross-section of the channel with a maximum along the centerline. Laminar flow and the flow velocity profile will be further discussed in the following subsections. Additional advantages for microfluidic separation technologies include low fabrication cost due to microfabrication methods, device portability, and reduced sample, reagent, and solvent consumption.

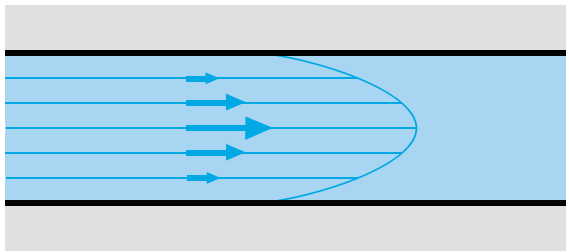

Figure 23. Laminar flow with infinitesimal parallel fluid layers inside a channel. The flow velocity profile has a parabolic nature with the maximum flow velocity in the channel center.

Microfluidic cell separation methods can, just like the conventional techniques, be categorized as label-free or antibody-dependent. The specificity of monoclonal antibodies contributes to high purity of the separated sample fractions and can be used both to capture a target cell type or to remove unwanted cells, through so-called positive or negative selection. Although, most microfluidic cell separation methods are label-free and can be further sub-categorized as *active* or *passive* depending on the exploited separation force. The active methods use an applied force field to attain cell separation, such as a magnetic-, electric-, or acoustic force field. The passive techniques are designed to achieve cell separation based on diverse internal microstructures, such as an obstacle matrix for size separations, or hydrodynamic

drag and wall and shear lift forces. However, cell separation techniques exclusively targeting CTCs commonly combine different approaches and uses both antibody-dependent and label-free methods [127-132].

In the next subsections the basic physics of microfluidics will be described, followed by a chapter describing acoustophoresis and its applications and developments within this thesis. A summary over additional microfluidic methods targeting CTCs will follow in the chapter *Alternative microfluidic technologies for CTC isolation*.

Laminar flow and Reynolds number

The phenomenon of laminar fluid flow can be observed in a channel when the inertial forces acting on the flow are negligible with respect to the viscous forces. As a result, the fluid flows in layers as the viscous forces between the layers prevent turbulence from occurring. The absence of turbulence is essential for microfluidic lab-on-a-chip devices and allows for precise alignment and control of different inlet and outlet flows. The Reynolds number (Re, Eq. 1) can be used as an indicator if the flow remains in the laminar regime or have a turbulent flow profile. The Reynolds number for the channel is given by:

$$Re = \frac{\rho D_h U_{Max}}{\eta} \qquad (1)$$

where ρ is the density of the fluid, D_h is the hydraulic diameter of the channel, U_{Max} is the maximum velocity of the fluid and η is the viscosity of the fluid [133]. Laminar flow typically occurs for a flow system if the Re number is smaller than 2000 [134].

Parabolic flow

The flow velocity profile has a parabolic nature, due to the friction (shear forces) between each fluid level (Figure 23). The no-slip boundary condition gives that there is no relative movement between the wall and the fluid layer in direct contact with the wall, hence there is a zero-flow velocity at the wall. The adjacent fluid layer will have a small movement as the friction there is finite and fluid velocity will increase as layer moves further away from the wall. The maximum flow velocity will thus be in the center of the channel and is called a Poiseuille flow. Thereby, suspended particles or cells flowing in the channel will have different velocities depending on their lateral position within the channel. An illustration of the flow

velocity profile over the cross-section of a microfluidic channel is shown in the subsection *Inertial effects in microfluidics* (Figure 27).

Stokes drag force

If a suspended particle is being manipulated by an applied external force, *e.g.,* an acoustic force, the particle will also experience a counteractive, opposite friction force, called Stokes' drag (F_D). The particle will accelerate to a velocity u, until the forces are of equal magnitudes. If the flow is laminar, the particles are spherical and homogeneous, and the Reynolds number <1, Stokes' drag force (Eq. 2) can be calculated using Stokes' law and can be described as:

$$F_D = 6\pi\eta r\mathrm{u} \qquad (2)$$

where r is the radius of the particle, u is the lateral particle migration velocity, and η the viscosity of the fluid.

Inertial effects in microfluidics

Inertial effects were first observed in the 1960s by Segré and Silberberg who noticed how particles moved across streamlines to form an ordered ring within a cylindrical pipe (Figure 24) [135, 136]. They concluded that this "tubular pinch effect" was due to a second-order effect (*i.e.,* inertial), but it was not until the development of microfluidics and the change to rectangular cross-sections that the real value of inertial focusing was established.

In 2007, Di Carlo *et al.* discovered that dispersed particles that entered an alternating curvature microfluidic channel would eventually both align and be longitudinally ordered after migrating across streamlines to equilibrium positions (Figure 24) [137, 138]. These positions were found to be dependent on the relative particle size, flow properties and the actual channel design. Since then, several different types of microfluidic separation channels have been created to achieve separation between different cells and particles [133].

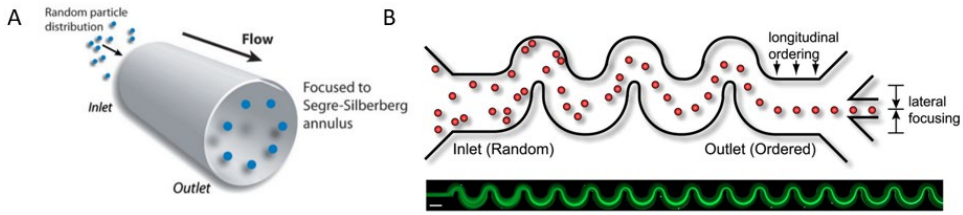

Figure 24. Inertial self-ordering of particles to equilibrium positions. A) Segré and Silberberg discovered how randomly distributed particles focused to an ordered ring within a cylindrical pipe. Adapted from reference [139] with permission from The Royal Society of Chemistry. B) Schematic picture of alignment and longitudinal ordering (upper) and fluorescent image of particle alignment (lower). Reprinted from reference [138]. Copyright (2007) National Academy of Sciences.

The ordered alignment of particles (*i.e.,* inertial focusing) is a result of shear and pressure forces arising in a flow of sufficient high Reynolds number so that the inertial effects are in the same order of magnitude as the viscous effects. The Reynold number equation for the channel (Re_C) and the phenomenon of laminar flow at low Reynolds number are described in the previous subsection *Laminar flow and Reynolds number.* The inertial effects are also described by the Reynolds number of the particle (Re_p, Eq. 3), as only particles of sufficient size in relation to the channel dimensions will be experiencing inertial focusing. Further, for curved channels a third parameter is needed to explain the flow, the Dean number (De, Eq. 4). A perpendicular flow arises at the curve as the high velocity center fluid is being moved to the outer channel wall, which then causes a dual recirculation flow, *i.e.,* Dean flow [139] (Figure 25). The magnitude of such perpendicular flow is given by the Dean number, and it depends on the geometry of the cross-section, the radius of the curvature and the Reynolds number of the channel. The two additional nondimensional parameters Re_p and De are given by:

$$Re_p = Re_C \left(\frac{a}{D_h}\right)^2 = \rho U_{Max} a^2/(\eta D_h) \qquad (3)$$

$$De = Re_C \left(\frac{D_h}{2R}\right)^{1/2} \qquad (4)$$

where a is the particle diameter, U_{max} is the maximum velocity of the fluid, and R is the radius of the channel curvature [133].

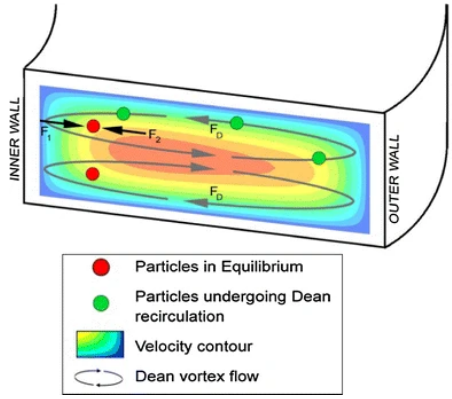

Figure 25. Cross section of a curved microfluidic channel showing dual recirculating perpendicular flow, Dean vortex flow. Reprinted from [140].

The three parameters (Re_C, Re_p, and De) influence the magnitude of the main forces acting on cells and particles during inertial focusing (Figure 26): the wall interaction lift force (F_{WI}, Eq. 5), the shear gradient force (F_{SG}, Eq. 6) and in the case of a curved flow, the Dean flow drag force (F_D, Eq. 7) and are given by:

$$F_{WI} = C_{WI}\rho U_{Max}^2 a^6 / D_h^4 \quad (5)$$

$$F_{SG} = C_{SG}\rho U_{Max}^2 a^3 / D_h \quad (6)$$

$$F_D = 3\pi\eta a U_{SF} \quad (7)$$

where C_{WI} and C_{SG} are lift coefficients, which depend on the Reynolds number and the particles position in the channel [133, 139]. Di Carlo *et al*. showed that the F_{WI} scaled differently near the channel centerline compared to near the channel wall [141]. The F_{WI} equation given above is the lift near the channel wall.

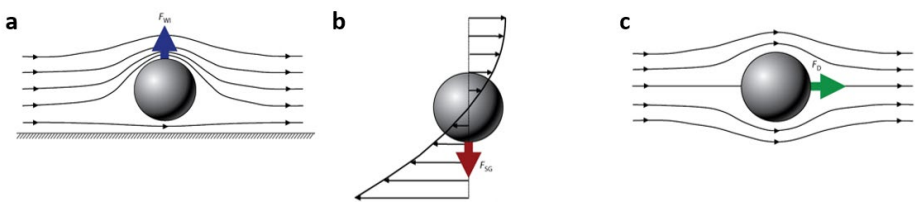

Figure 26. The forces acting on particles and cells during inertial focusing, a) the wall interaction lift force (F_{WI}), b) the shear gradient force (F_{SG}) and in the case of a curved flow, c) the Dean flow drag force (F_D). Reprinted from reference [133] with permission from Annual Reviews.

The wall interaction lift force (F_{WI}) will cause the particles to move away from the wall and is due to an increased pressure on the particles at close proximity to the wall. As the particles move perpendicularly away from the wall, the force on the particles diminishes. The shear gradient force (F_{SG}) is due to the parabolic flow profile and will cause the particles to instead move towards the wall. The final force in curved microchannels, the Dean flow drag force (F_D), is resulting from the secondary flow perpendicular to the main flow direction, as earlier described, and is proportional to the secondary flow velocity (U_{SF}).

For straight channels, the wall interaction lift force and the shear gradient force will create four particle-size-dependent equilibrium positions within the channel cross-section (Figure 27, left insert). Such equilibrium positions are the explanation to the effect seen by Segré and Silberberg back in the 1960s. In the case of curved channels, three out of the four positions (Fig. 27, right insert, light grey particles) will be instable due to the drag force, moving particles to a single particle-size-dependent equilibrium at the inner curvature of the channel [139].

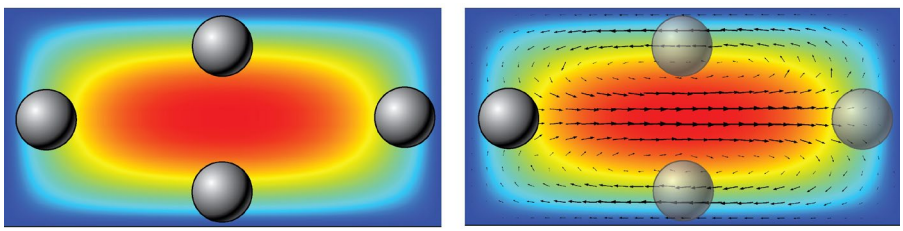

Figure 27. Stable equilibrium positions within the channel cross section for straight (left) and curved (right) channels. The light grey particles in the curved channel represent now instable positions due to the Dean flow (vectors). The background represents the velocity profile from centered high flow velocity (red) to zero velocity (dark blue). Reprinted from reference [133] with permission from Annual Reviews.

The understanding of the complex interplay between viscous and inertial forces is fundamental in the design of microfluidic separation channels. In paper 3, we studied the particle trajectories in a standard λ/2 acoustophoresis separation channel at increased flow rates and discovered an inertia induced phenomenon that may compromise separation performance. We observed a cross-sectional movement of the particle streams towards the center of the separation channel at sufficiently high flow rates, which was independent of particle size and lead to a breakdown of particle separations. We concluded that it was not due to the wall interaction lift force, as such displacement was calculated to be in the order of 10^{-3} times the

particle radius. Instead, the effect was discovered to be due to the formation of a deformed fluid boundary between the sample flow and sheath flow, both at the inlet of the separation channel as well as at the outlet flow splitter, at elevated flow rates. The observed inertia induced phenomenon may be reduced by decreasing the degree of curvatures in the microchip. A greater understanding of the inertial effects in microfluidic systems can help to improve the designs of the separation devices.

Acoustophoresis

Acoustophoresis is a microfluidic technique to manipulate and separate microparticles or cell populations with acoustic waves. When using ultrasound frequencies in the MHz range, the resulting sound waves have a wavelength (λ) smaller than 1 mm, which makes the technique optimal for microfluidic applications. By using a microfluidic chip with channel dimensions corresponding to an integer multiple of λ/2, a standing wave can be created within the microchannel. The established ultrasonic standing wave field gives rise to acoustic forces that will act on suspended particles and cells. The method is thereby inherently label and contact free, and importantly, proven to be gentle on cells [142-144], an essential prerequisite when aiming for live CTC isolation for *in vitro* culturing and functional analysis.

Ultrasonic standing waves

Sound is pressure waves traveling through a medium, such as air, water or even a solid. The alternating pressure will compress and expand the medium, *i.e.*, the constituent molecules of the medium, as the wave propagates (Figure 28).

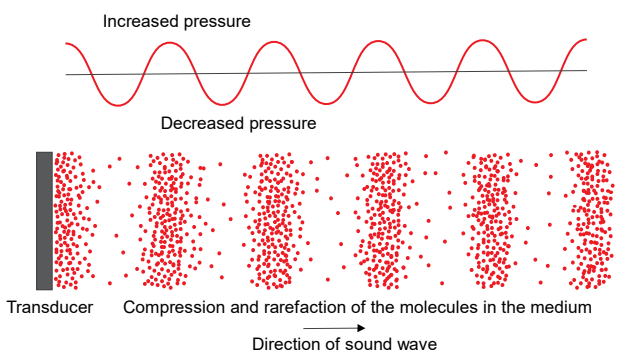

Figure 28. Propagation of transducer altered sound waves as alternating increased and decreased pressure.

If two sound waves with the same frequency and amplitude meet, either formed by two different sound sources (transducers) facing each other or if the propagating wave is reflected upon interaction with a second medium, the waves will experience constructive interference and a standing wave will form. When a soundwave is created inside a microfluidic channel, the wave will propagate through the buffer fluid and get reflected by the channel walls, thereby it can give rise to a standing wave of higher acoustic amplitude than the first, incident wave (Figure 29). By matching the channel dimensions to an integer multiple of half the wavelength, acoustic resonance is created with exact positioning of pressure node(s) (low pressure) and antinodes (high pressure).

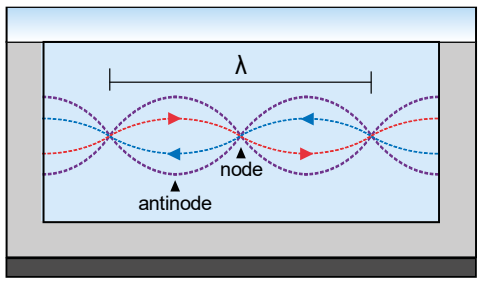

Figure 29. Cross section of a microfluidic channel with an acoustic standing wave field. A transducer generates a pressure wave that gets reflected by the channel walls, which results in acoustic resonance at specific frequencies. The channel dimensions give the number of pressure nodes (low pressure) and antinodes (high pressure).

The human ear can register sounds between approximately 20 Hz to 20 kHz. Sounds with lower or higher frequencies cannot be translated into neuronal signals, and are called infrasound and ultrasound, respectively. For high frequency ultrasonic standing waves, the resulting wavelength is in the micrometer range, and thereby perfectly suited for microfluidic applications.

Primary acoustic radiation force and acoustic contrast factor

The main acoustic force affecting particles in an acoustofluidic channel is the primary acoustic radiation force (ARF, F_R) (Eq.8). Inside a one-dimensional

acoustic standing wave, the ARF can be described according to Yosioka and Kawasima, and Gor'kov [145, 146] by:

$$F_R = 4\pi r^3 \Phi k_y E_{ac} \sin(2k_y y) \quad (8)$$

where r is the particle radius, Φ is the acoustic contrast factor, $k_y = 2\pi/\lambda$ is the wavenumber, E_{ac} is the acoustic energy density and y is the distance from the microchannel wall. Here, the force acts in the direction of the pressure gradient of the standing wave. The force is dependent on acoustophysical properties of suspended particles and surrounding fluid medium, where the force scales with the third power of the particle's radius and therefore is a major determinant to the acoustophoretic velocity.

The acoustic contrast factor (Eq.9) is determined by the particle and fluid density and compressibility differences and is given by:

$$\Phi = \frac{5\rho_p - 2\rho_m}{2\rho_p + \rho_m} - \frac{\kappa_p}{\kappa_m} \quad (9)$$

where κ_m is the isothermal compressibility of the fluid, κ_p is the isothermal compressibility of the particle, ρ_m is the density of the fluid and ρ_p is the density of the particle. The equation gives a dimensionless number, which defines the direction of particle movement in a fluid under the influence of the ARF. If the acoustic contrast factor is positive, the particle will move towards the acoustic pressure node, and if the contrast factor is negative, the particle will move towards the acoustic pressure antinode (Figure 30). Cells exhibit positive contrast when suspended in standard buffer solutions and cell culture media and can therefore be focused to pressure nodes.

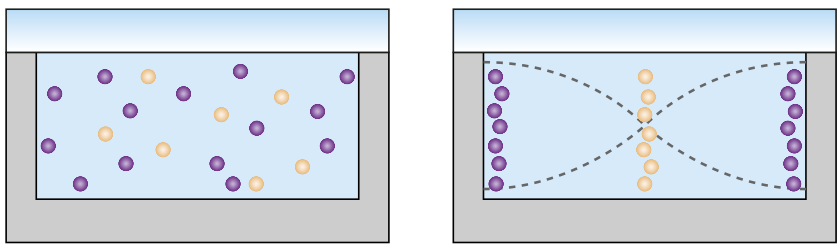

Figure 30. The primary acoustic radiation force (ARF) moves particles from a random distribution (left image) over the channel cross section to pressure node(s) or antinodes depending on the acoustic contrast factor of the particle (right image). Particles with positive acoustic contrast (yellow) focus to the pressure node and particles with negative acoustic contrast (purple) focus to the pressure antinodes.

Elastomeric negative acoustic contrast particles

In contrast to cells, compressible and water insoluble elastomers (*e.g.,* polydimethylsiloxane (PDMS) based elastomeric particles) are typically of negative acoustic contrast [147, 148]. The differences between cells and elastomers in density, compressibility and the resulting acoustic contrast factor can be used in acoustophoresis to bind and separate proteins from a cell suspension [148] and to capture and transport cells to pressure antinodes [149]. In paper 1 and 2, elastomeric negative acoustic contrast particles were used for negative selection acoustophoresis to isolate live tumor cells from WBCs (Figure 31) [150, 151].

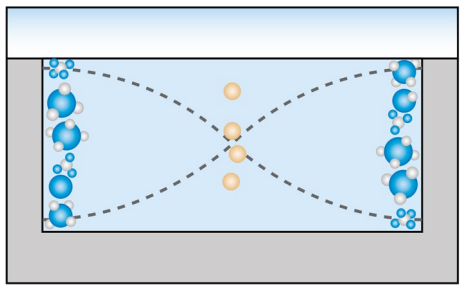

Figure 31. Illustration of negative selection acoustophoresis for the isolation of live tumor cells. Elastomeric negative acoustic contrast particles of variable size (blue) move bound WBCs (white) to pressure antinodes while live tumor cells (yellow) focus to the central pressure node.

To achieve a transportation of bound cells to pressure antinodes by negative acoustic contrast particles, the resulting ARF acting on the contrast particles needs to be greater than the ARF acting on the cells. Thus, the net acoustic contrast factor is negative and therefore the complex will move towards the pressure antinode (Figure 32). This dependance was demonstrated by Shields *et al.* [149], where they showed the required effective elastomeric particle size and the resulting magnitude of the acoustic contrast factor needed to move a typical sized mammalian cell. In practice, the net elastomeric particle bound to a displaced cell can also be a sum of smaller particles. When producing elastomeric particles, it is desired to obtain particles with low density, high compressibility, and a robust ability to bind to cells.

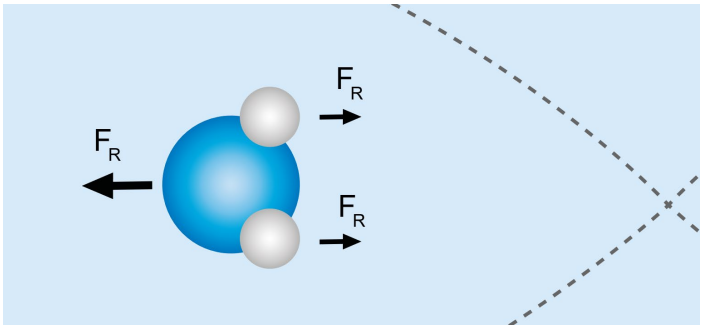

Figure 32. The resulting acoustic contrast factor of a particle-cell complex decides its direction of movement when acted upon by an acoustic standing wave field. The illustrated complex consists of two WBCs (white) bound to a larger elastomeric particle (blue).

Elastomeric particles are cured polymers, made from viscous pre-polymers and a cross-linking agent. The curing procedure is commonly performed with heat or high pressure and causes an unreversible hardening of the pre-polymers due to covalent cross-linking between the long polymer chains. This process gives rise to the characteristic viscoelasticity (*i.e.,* both viscosity and elasticity) of polymers, as the long polymer chains can be reorganized in response to an applied stress and the covalent bonds will bring the polymer back to its original structure once the stress is relaxed.

In paper 1 and 2, PDMS-based elastomers were used as negative acoustic contrast particles, where the compressibility of the particles can be altered based on the amount of added cross-linking agent [152]. In our studies, a PDMS prepolymer to cross-linking agent ratio of 10:2 was used. Modifications of the ratio could explore its influence on the acoustic mobility of the particles in the acoustic field. Other compressible, water insoluble elastomers exist (such as natural rubbers, butyl rubbers and other silicones), all with the potential to be used as negative acoustic contrast particles.

Surfactants and surface modification of elastomeric particles

Silicone-based PDMS is highly hydrophobic, which can cause elastomeric particles to aggregate irreversibly [147]. Therefore, to avoid clogging and enable re-suspension of cured particles, the emulsification of pre-polymer and cross-linking mixtures can be performed in an aqueous solution containing a surfactant. There are several options of buffer surfactant when creating silicone-in-water emulsions, where the block copolymer Pluronic F108 surfactant previously has been shown to

successfully stabilize elastomeric microparticles [147]. Pluronic F108 adsorb well to both hydrophilic and hydrophobic surfaces [153], but through different adsorption mechanisms [154]. Pluronic F108 contains three block copolymer units: two hydrophilic units, separated by a shorter hydrophobic unit. Upon interaction with hydrophobic surfaces, as in the emulsification process of elastomeric particles, the hydrophobic block adsorbs onto the particle surface through hydrophobic interactions, while extending the two hydrophilic block units into the aqueous buffer [153, 154].

Further, due to terminal hydroxyl groups on the hydrophilic block units, Pluronic F108 can also be end-functionalized through covalent-coupling chemistry with N, N'-disuccinimidyl carbonate (DSC) (Figure 33).

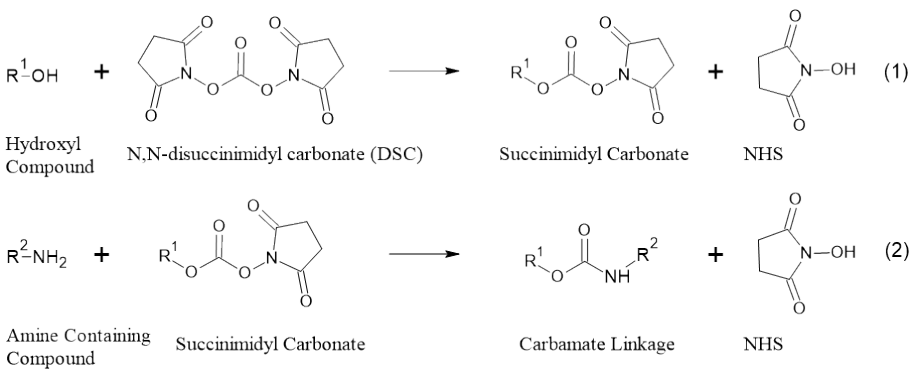

Figure 33. The chemical reaction of disuccinimidyl carbonate (DSC) activating a hydroxyl compound under nonaqueous conditions to form a succinimidyl carbonate derivative, which can conjugate with an amine-containing compound (here, biotin hydrazide) for a stable crosslinked product.

DSC is a strong electrophile and will under nonaqueous conditions react with the hydroxyl group on Pluronic F108 and form a succinimidyl carbonate derivate as an intermediate compound (Fig. 33, 1). Thereafter, the DSC activated hydroxylic compound can conjugate with an amine-containing compound (*e.g.,* biotin hydrazide) to form a stable product (Fig. 33, 2). The second reaction is performed in deionized water and the resulting conjugated surfactant solution can thereafter be used in the emulsification of pre-polymer and cross-linking agent. In paper 1 and 2, biotinylated Pluronic F108 surfactant was manufactured in-house to create surface-activated elastomeric particles through the silicone-in-water emulsification process.

The synthesized biotinylated elastomeric particles can be immuno-functionalized with streptavidin-conjugated antibodies targeting an epitope of interest. The high affinity of streptavidin for biotin (dissociation constant of approximately 1×10^{-14} M), generates robust immuno-functionalized elastomeric particles as potential carriers of target cells or molecules.

In this thesis, the produced elastomeric particles were functionalized with streptavidin conjugated anti-CD45 antibodies (Figure 34). This enabled the binding and transportation of positive contrast WBCs to pressure antinodes in the acoustic field, while focusing tumor cells to the pressure node (Figure 31) [150, 151].

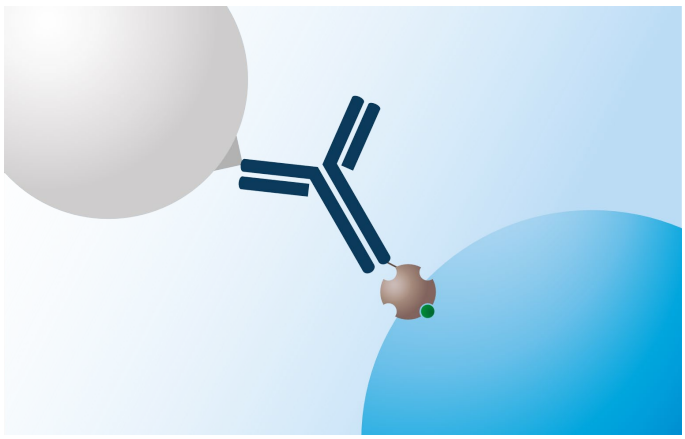

Figure 34. A biotinylated elastomeric particle (blue) can be functionalized with a streptavidin conjugated anti-CD45 antibody to enable binding to WBCs (white). The high affinity of streptavidin for biotin generates a robust particle for transportation of bound target cells.

Acoustic energy density

The primary ARF is proportional to the acoustic energy density (E_{ac}), which has the unit of energy per unit volume at a point in space along the channel. The acoustic energy in a system is a function of the acoustic pressure p, and the acoustic particle velocity u [155].

If the time-average acoustic energy of a system is known, as well as the acoustic contrast factor of a specific cell type, the acoustic compressibility or density of the cell can be obtained by solving the ARF equation. This requires correct assessment of the energy density of the microfluidic system, which can be done through particle

image velocimetry (PIV) measurements. PIV is an optical method for measuring displacement of a reference particle of known size, density, and compressibility. A laser light is being pulsed and the spatial displacement of the particle divided by the time between the laser pulses gives the velocity of the particle and thereby, the acoustic energy density can be calculated. PIV measurements have been used to determine the acoustic compressibility and density for different cell types [156, 157].

Secondary acoustic radiation force

In addition to the primary acoustic radiation force, the acoustic standing wave field gives rise to secondary acoustic radiation forces (SRF, F_{sec}) between particles in close proximity due to sound scattering (Eq. 10) [158, 159]. Gröschl presented an approximation to the SRF, which can be described by:

$$F_{sec} = 4\pi a^6 \frac{(\rho_p - \rho_m)^2 (3\cos^2\theta - 1)}{6\rho_m d^4} v^2(x) - \frac{\omega^2 \rho_m (\kappa_p - \kappa_m)^2}{9d^2} p^2(x) \qquad (10)$$

The resulting SRF between particles of positive acoustic contrast close to a pressure node inside a one-dimensional acoustic standing wave field depends on the particles position within the field. If the particles are aligned in the direction of the incident standing wave (θ = 0), the resulting force will be repulsive, and if the particles are aligned perpendicular to the standing wave direction (θ = 90), the resulting force will be attractive (Figure 35).

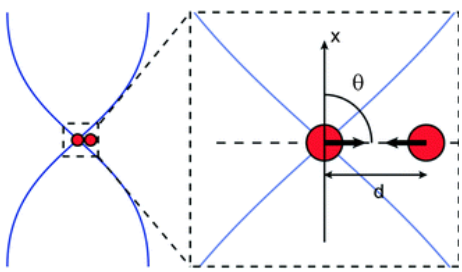

Figure 35. Secondary acoustic radiation force between particles in close proximity being attractive or repulsive depending on the angle between the particles and the axis of the incident wave inside a one-dimensional acoustic standing wave close to a pressure node. The magnitude of the force is a function of particle size, distance, and the velocity and pressure field. Reprinted from reference [160] with permission from The Royal Society of Chemistry.

An attractive interparticle force is thought to be the foundation for acoustofluidic trapping applications, where submicron particles can be acoustically focused (trapped) to larger so-called seed particles. Due to their small size, the submicron particles cannot be focused to acoustic pressure nodes by the ARF. This will be further explained in the following section, *Acoustic streaming*. In addition to a brief summary in the subsection *An alternative acoustofluidic device*, further reading on acoustic trapping and its vast applications can be found in a comprehensive tutorial by Evander and Nilsson [161].

The occurrence of SRF can also lead to deteriorating effects in an acoustofluidic cell or particle separation application. If the cell or particle concentration is too high, the cells or particles can be stuck together and will thus be impossible to separate successfully. Such clumping of elastomeric particles was observed at the pressure antinodes in paper 1. Additionally, a cell or particle concentration that is too high can also impair the separation performance due to hydrodynamically coupled carry over between separation fractions. Consequently, acoustofluidic manipulation of *e.g.*, whole blood components require careful consideration of the sample concentration. In paper 2, the dependency on sample cell concentration in relation to the separation performance is further explored.

Acoustic streaming

An acoustic standing wave field gives rise to a phenomenon of fluidic streaming in the channel, called acoustic streaming. Due to shear stress at the viscous boundary layer by the channel walls, counterclockwise streaming rolls *i.e.*, streaming vortices, appear in the cross-section of the acoustofluidic channel (Figure 36). The fluid movement was observed already in 1884 by Lord Rayleigh and has thus been given the name Rayleigh streaming [162]. Half a century later, in 1932, Hermann Schlichting described how it was inner streaming vortices, within the viscous boundary layer, that were the actual reason for the Rayleigh streaming rolls in the bulk of the fluid [163].

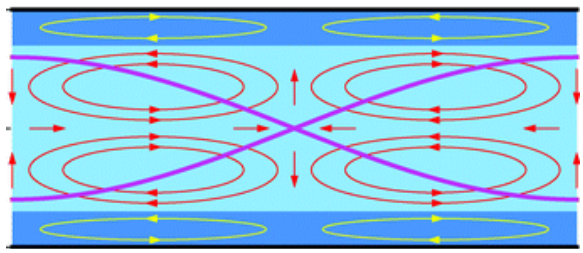

Figure 36. Acoustic streaming. Counterclockwise Rayleigh streaming (red streams) and Schlichting inner streaming vortices (yellow streams) in the cross-section of the microchannel due to shear stresses at the viscous boundary layer. Reprinted from reference [164] with permission from The Royal Society of Chemistry.

The phenomenon of acoustic streaming can be both detrimental and beneficial for acoustofluidic separations. Suspended particles will experience Stokes drag forces in the direction of the fluid vortices and acoustically focused particles might therefore be relocated to the top or bottom of the channel where they can cause aggregates [165]. Additionally, since the drag force scales with the radius of the particle while the ARF is proportional to the particle volume, acoustic translocation to pressure nodes is restricted to specific particle sizes. For half wavelength acoustic systems resonant at 2 MHz, the required polystyrene particle radius is approximately 1.5 µm to overcome acoustic streaming and enable acoustic focusing in water [164]. Thus, acoustic streaming can be overcome for blood cell applications, whereas for example separation of different bacteria or extracellular vesicles require efforts to suppress the streaming or use alternative trapping approaches [165-167]. Such streaming suppressing strategies can be the use of two dimensional (2D) acoustophoresis [166], or an acoustic impedance gradient obtained through density modified buffers [167].

The acoustofluidic device

In the field of acoustofluidics, there are several types of devices. The focus of this dissertation has been on bulk acoustic devices, using bulk acoustic waves (BAW). The design process and additional applications are described below. Other acoustofluidic devices are based on surface acoustic waves or on trapping technology. A short description of the acoustic trapping method will follow.

Bulk acoustic wave devices

In BAW devices of an acoustically hard material, the channel dimensions have been designed to match an integer multiple of half the wavelength (λ) at a selected actuation frequency (*f*) (Eq. 11). For a one-dimensional wave this relation is described by:

$$\lambda = \frac{c}{f} \tag{11}$$

where c is the speed of sound in the wave propagation medium (*i.e.,* 1488 m s^{-1}, the speed of sound in water at room temperature for most acoustofluidic applications). A resonant sound wave can thus be formed within the channel, most frequently in one dimension (width or height of the channel), but also in two dimensions [142, 168, 169], depending on the channel geometry. The design process thereby locates acoustic pressure node(s) and antinodes to defined positions in the cross-section along the channel. If the channel dimensions are matched for 2D focusing, suspended particles will be focused by the ARF to a single point in the cross-section, whereas one dimensional focusing will result in a wall-to-wall line of particles (Figure 37). Due to the non-uniform flow profile in the channel cross section (see subsection *Parabolic flow*), suspended particles will have different velocities depending on their distance from the wall. The one-dimension focused particles will have different particle velocities and retention time within the acoustic field while streaming through the channel, which can influence the final separation result. If two (or more) different types of particles or cells are to be separated by the ARF, their initial position when entering the separation channel will affect the retention time in the channel and thereby the duration of the ARF influence. A 2D focusing reduces such bias and improves the particle separation [142].

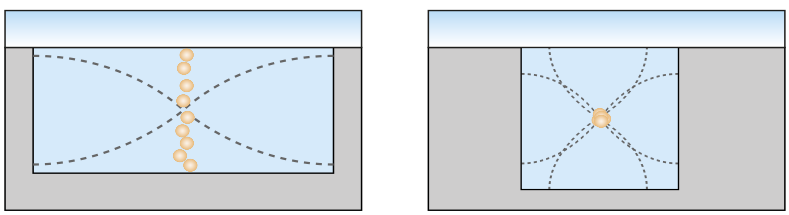

Figure 37. Standing wave formation within a bulk acoustic wave (BAW) device in one (left) and two dimensions (right). One dimensional (1D) focusing has a wall-to-wall pressure minima across the height of the channel, whereas two dimensional (2D) focusing generates a pressure node point in the cross-section of the channel. A 2D focusing reduces inter particle velocity differences resulting from the flow velocity profile in the channel.

Additional blood-based applications of BAW devices

In addition to separating CTCs from large numbers of WBCs [142, 150, 151, 170], the BAW devices can be used for various applications of acoustophoretic cell and particle manipulation. A short summary demonstrating the diversity of acoustophoresis BAW technology for blood-based applications follows below.

Acoustophoresis has been used to separate mononuclear blood cells from diluted whole blood by tuning the buffer conditions with density media and thereby alter the cells relative acoustic mobility and enable separation [171]. Further, multiplexed fractionation of WBC subpopulations has been demonstrated using an acoustofluidic microchip with multiple outlets [172, 173]. Lymphocytes, monocytes, and granulocytes were efficiently separated at high sample throughputs. Furthermore, separation of lymphocyte subgroups from peripheral blood progenitor cells have been done with magnetically labeled monoclonal antibodies, targeting either CD4-positive or CD8-positive lymphocytes [174, 175]. Binding of the magnetic bead antibody complex altered the acoustofluidic mobility of the cells and thereby enabled their isolation.

Acoustophoresis has also been used to develop alternative methods for sepsis diagnosis [167, 176]. In one study, the submicron-sized bacteria were separated from RBCs and WBCs by moving the blood cells from the sample flow into a sheath flow in the acoustic field [176]. The bacteria could then be isolated as they were not affected by the acoustic forces due to their limited size. Additionally, the acoustic impedance of the sheath buffer was matched to the blood cells to avoid buffer relocation and enable a high throughput. Similarly, another study used an acoustic impedance gradient to suppress acoustic streaming and thereby enable separation of bacteria from RBC-lysed blood [167].

Moreover, acoustophoresis have been used to concentrate dilute cell and particle suspensions by different studies. A 2D-acoustic focusing with sequential concentration regions were used to achieve up to 200-fold volumetric concentration of particles or cells in small volume samples [168]. Another study showed over 1,000-fold enrichment of cells using a recirculating acoustophoresis design for sequential processing of samples without reducing the cell viability [177].

An alternative acoustofluidic device

Acoustic trapping devices uses a small transducer attached to a glass capillary, creating a narrow acoustic field in the channel. Due to the strong axial (in the

capillary direction) acoustic gradient over the transducer, cells or particles flowing through the capillary can be trapped in the local acoustic field against the flow (Figure 38). If targeting cells or particles smaller than the critical radius (approximately 1.5 µm, see the previous section *Acoustic streaming*), larger seed particles can be used [160]. The seed particles will be focused and retained at the narrow field over the transducer due to the ARF and can thereafter trap the smaller particles, likely through interparticle forces (SRF, see the earlier section *Secondary acoustic radiation force*). Successful applications have been the enrichment of bacteria from blood for rapid sepsis diagnosis [178] and the isolation of extracellular vesicles from biological fluids [179].

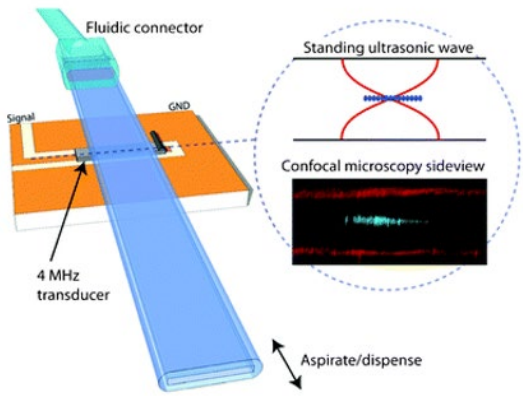

Figure 38. Acoustic trapping of particles (blue) at a narrow acoustic field in the glass capillary. Reprinted from reference [160] with permission from The Royal Society of Chemistry.

Fabrication process

To produce a strong resonant field within a BAW device, the propagating soundwave needs to be well reflected at the channel wall. The reflection of the soundwave will be larger with less energy loss if the difference in acoustic impedance (Z, Eq. 12) between the two materials, *i.e.,* the medium inside the channel and the channel wall, is larger. A larger reflected amplitude coefficient (R, Eq. 13) results in more of the acoustic energy being reflected back into the channel and thereby generating a stronger resonant field. The acoustic impedance describes

the resistance towards an acoustic flow and depends on the medium density (ρ) and speed of sound within the medium (c).

$$Z = \rho c \tag{12}$$

$$R = \frac{Z_1 - Z_2}{Z_2 + Z_1} \tag{13}$$

The BAW devices are therefore often made of silicon or glass to reach a high impedance mismatch between the device and medium and allow for a fabrication process with high precision and reproducibility. Silicon devices have a larger reflected amplitude coefficient (R) than glass when combined with commonly used processing mediums (*e.g.,* water, saline buffer, cell medium or complex bio-fluids). Due to the crystalline structure of silicon, the devices have a rectangular cross-section channel geometry with straight channel walls after an anisotropic etching procedure. As glass is an amorphous solid without a periodic arrangement of its molecules, an isotropic etching will be uniform in all directions and result in curved walls. Despite the less efficient acoustic energy reflection and the disadvantageous geometry of the glass chips, acoustophoretic applications have demonstrated largely equal performance of the glass chip to its silicon counterpart [180]. Glass permits for easy visual inspection of an experiment, but as silicon microchips are bonded with a glass lid after the etching procedure, a top-view visualization is standard.

The acoustofluidic devices used in paper 1, 2 and 4 (Figure 39) were made in-house by anisotropic wet etching in silicon. The microchip used in paper 3 was manufactured by Micronit Microfluidics (Enschede, Netherlands), using deep reactive ion etching, DRIE. The anisotropic wet etching procedure is summarized and illustrated (Figure 40) below.

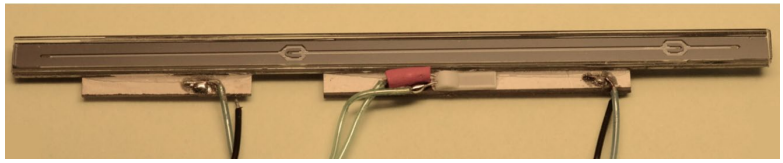

Figure 39. The acoustofluidic silicon microchip used in paper 2 and 4. Two piezoceramic transducers are attached to generate the acoustic standing wave fields. The flow is from left to right with fluid inlet- and outlet holes etched from the backside of the chip.

Wafer oxidation

First, the silicon substrate (a thin circular disk known as a "wafer") **(1)** is placed in an oven and oxidized at 1000°C with a continuous supply of oxygen. The oxidation creates a silicon dioxide (SiO_2) layer on the surface **(2)**, which functions as a protective barrier for the parts of the silicon to be left intact during the etching phase. The final pattern in the silicon wafer is based on the selected mask design.

Mask design

A photolithographic mask is made, which defines the areas of the silicon wafer that need to be etched to produce the desired channel design and dimensions **(3)**. The mask is first drawn in a computer software, before transferred to a mask substrate, *e.g.,* a glass slide with precise gaps in a chromium layer defined by the drawing. The mask is then used to protect the areas which should be left intact upon UV-exposure during the next step, photolithography.

Photolithography

The oxidized wafer is spin coated with a layer of photoresist **(4)** before it gets exposed to UV-light through the chosen mask **(5)**. The unprotected parts of the photoresist become soluble and can be removed with a solvent during a development step **(6)**. The pattern of the mask is now transferred to the resist layer which exposes parts of the SiO_2-layer for silicon dioxide etching.

Silicon dioxide etching and removal of photoresist

The remaining pattern of photoresist preserves selected parts of the silicon dioxide during the silicon dioxide etching. The wafer gets immersed in hydrofluoric acid (HF) to remove the SiO_2-layer and expose the underlaying silicon substrate **(7)**. When the oxide etch is done and the mask pattern has been transferred to the SiO_2, the remaining photoresist is removed with a solvent **(8)**.

Silicon etching and removal of silicon dioxide

Once the silicon substrate is exposed according to the mask design, silicon etching can be done **(9)**. Here, the wafer is immersed in potassium hydroxide (KOH) at 80°C to increase the etching rate. Once the etching has reached the desired channel dimensions and depth, the reaction is terminated, and the residual SiO_2-layer is removed with HF **(10)**.

Dicing and bonding

Generally, several microfluidic chips can be fabricated from one single silicon wafer, depending on the specific chip design. Thus, the wafer is diced into individual channels before finally bonding the microchannels with borosilicate glass lids by heating the chip and the glass at 500°C with a hotplate and applying 1000 V between them **(11)**.

Backside

There are two approaches to create the inlets and outlets for the different fluids. In the more refined method, the holes are etched from the backside of the chip through a second round of wet etching procedure. A much faster approach to create the fluid entries and exits is by straightforward drilling in the silicon. Though, drilling can be problematic as the almost ready-to-use microchip may possibly break during this procedure.

Transducer

Finally, a piezoceramic transducer is glued to the microchip to create acoustic waves within the channel **(11)**. A piezoceramic transducer is a crystalline material, such as quartz or lead zirconate titanate (PZT), which obtains an electric field potential when compressed by a mechanical stress. The deformation is reversible, so an applied AC-voltage forces the transducer to vibrate, which will induce acoustic pressure waves inside the bulk of the chip. A precise cutting of the transducer is fundamental as the thickness specifies its resonance frequency.

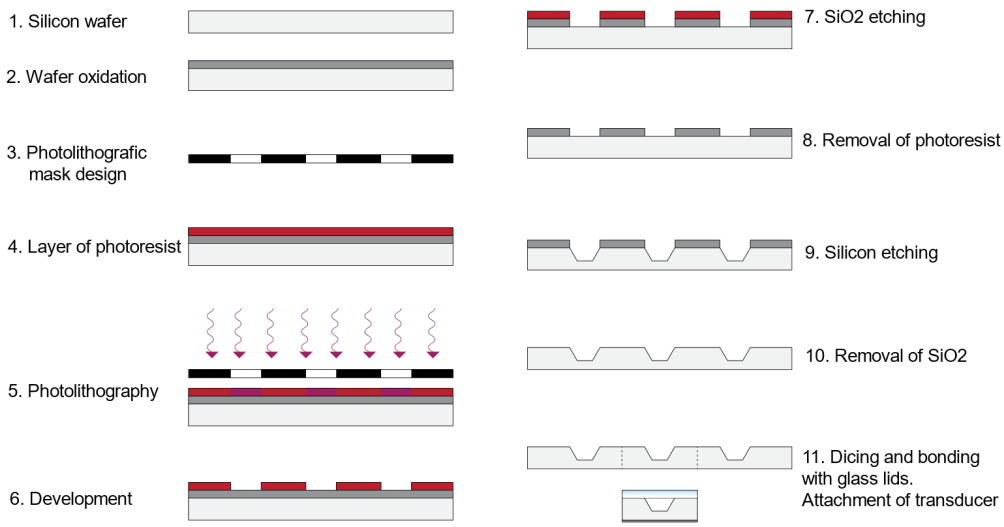

Figure 40. Schematic illustration of the fabrication process of an acoustofluidic microchip by anisotropic wet etching in silicon. Each step is summarized in the main text.

Multiple wavelength designs

By increasing the actuation frequency to match an integer, greater than one, multiple of half the wavelength to the channel width, the number of nodes and antinodes in the channel increases. This reduces the distance between two adjacent nodes if the channel width is constant. Alternatively, a multinode configuration can be obtained by increasing the width of the separation channel while maintaining the original frequency and thereby the distance between two immediate nodes.

Multinode acoustophoresis can be used for several different applications and functions. The introduction of a multinode pre-alignment step dramatically increased the separation performance of WBCs and cancer cells in a single node acoustophoretic separation [142]. Such multinode alignment locates the cells to the same position and flow vector in the channel cross-section prior entering the main separation channel, and thereby minimizing the dispersion induced by the parabolic flow profile [142, 172]. Through a multinode pre-alignment, all cells are separated with the same retention time in the acoustic field.

The multinode configuration can also be used to position cells or particles at a distance from the channel walls to avoid potential aggregation at Gor'kov potential minima [181, 182], which can distort laminar streamlines and reduce separation performance. To avoid this condition, Grenvall *et al.* employed higher harmonics to

separate negative acoustic contrast lipids from raw milk (Figure 41) [183, 184]. By introducing the sample in a sheath flow through the center inlet (Fig. 41, A) and actuating the chip in a 2λ/2 mode, the cells were focused to the pressure nodes at each side of the channel center and the lipid emulsion was focused at the pressure antinode in the channel center (Fig. 41, B). Alternatively, operating a chip at 3λ/2, the cells were focused to the central pressure node and lipids were driven to the first antinode at each side of the center line (Fig. 41, C). In both cases the lipid emulsion never gets the possibility to aggregate at the sidewalls and thus continuous separation could be maintained over time.

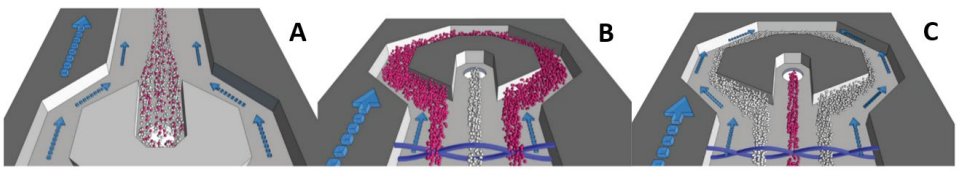

Figure 41. A multinode configuration moved lipids of negative acoustic contrast away from channel walls to avoid aggregation and flow disturbances. A) The sample entered the acoustofluidic device through the center inlet and a sheath buffer was introduced from the side inlet for both multinode configurations (B and C). B) At 2λ/2 the lipids were focused at the center antinode, while the cells were moved to the pressure nodes. C) For 3λ/2 the cells focused at the center node, while the negative acoustic contrast lipids were driven to the antinodes at each side. Both devices (B and C) used a 2 MHz transducer and had a channel width of 750 µm and 1125 µm, respectively. Adapted from reference [184]. Copyright © 2009, American Chemical Society.

In this dissertation, the 3λ/2 multinode approach was employed in paper 2 to prevent negative acoustic contrast particles from accumulating at the channel walls, and thereby maintain a uniform flow profile without perturbations. A prerequisite to use multinode acoustophoresis for sorting cells and particles of positive or negative acoustic contrast is having the sample entrance through the center inlet, instead of from the side inlet. As the nodes and antinodes functions as attraction points or impassable walls, depending on the acoustic contrast factor of the cells or particles, there can be no crossover to adjacent attracting nodes or antinodes, and the sample entrance must therefore be through the center inlet of the chip.

Alternative microfluidic technologies for CTC isolation

Over the last two decades, several microfluidic CTC isolation technologies have been developed with diverse strategies for cell separation and isolation. In the following sections, an overview will be given for alternative microfluidic technologies targeting CTCs, classified as either *passive* or *active* separations. However, CTC targeting platforms frequently have a combined approach with two or more separation strategies, often including the use of monoclonal antibodies.

Active methods

Magnetophoresis uses high specificity monoclonal antibodies coupled to magnetic nanobeads to separate cell populations by positive or negative selection approaches (Figure 42, A) [185]. As cells have low magnetic permeability (with the exception of RBCs [186]), an applied magnetic field will act exclusively on cells that are tagged with magnetic particles and with no interference from unlabeled cells or the buffer medium [187]. The velocity of the cell-magnetic label complex and hence their separation efficiency is determined by the interplay of magnetic body forces and viscous forces in the solution. The magnetic particles can also be fluorescently labeled to analyze separated cell fractions with FLOW cytometry.

Due to the vast repertoire of monoclonal antibodies and the availability of affordable permanent magnets capable of generating high magnetic field gradients, magnetophoresis has become a fast-growing field of cell separations including isolation of CTCs [185, 188]. In contrast to macroscale MACS with bulk sample processing, magnetophoresis allows for a continuous flow separation of cells and can be combined with alternative microfluidic cell separation approaches (Figure 47).

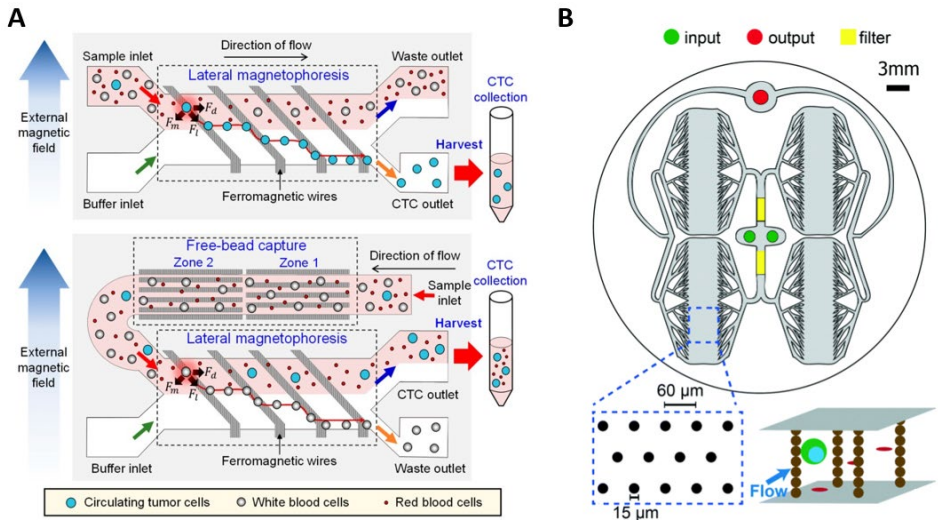

Figure 42. Active microfluidic technologies for CTC isolation that use a magnetic force field. A) Lateral magnetophoresis uses monoclonal antibodies coupled to magnetic beads for the positive selection of CTCs (top image) or depletion of WBCs (bottom image). B) Ephesia cell capture device with capturing zones (top image) where the sample is flown through a dense array of self-arranged magnetic columns labeled with antibodies (bottom image). Reprinted from (A) reference [185] and (B) reference [189] with permission from Royal Society of Chemistry.

An alternate microfluidic CTC isolation method based on an applied magnetic field is the Ephesia cell capture technology (Figure 42, B) [189]. The method uses anti-EpCAM coated magnetic beads that self-assemble into magnetic columns in the CTC capture zones under the influence of the magnetic field. The columns are precisely positioned in a periodic dense array perpendicular to the flow by magnetic "anchors" in the bottom of the PDMS device. The captured cells can be easily released for further analysis by simply switching off the magnetic field and rinsing the device. Validation studies using various epithelial cell lines showed a high sensitivity and specificity of the method, where the capture efficiency was correlated to the EpCAM expression of the cells [189]. Additionally, a comparison to the CELLSEARCH system using clinical samples showed that similar or higher numbers of CTCs were obtained with the Ephesia technology for the majority of the processed samples.

A drawback of the methods is the dependance of the expression of a predetermined surface epitope on the target cells, as discussed earlier in the section *Macroscale techniques and current "gold-standard" for CTC isolation*. The disadvantage is true for all antibody-based enrichment methods with a positive selection approach, macroscale techniques as well as microfluidic methods. Additionally, studies have shown that the capture ability is dependent on the expression level of the selected

surface epitope [118, 123-126, 189]. Due to the constant selection pressure for advantageous genotypes and phenotypes, an epitope-agnostic enrichment approach is preferable for targeting the heterogenous CTC population. However, an antibody-based negative selection approach enriches the target cells in an unbiased matter. Although, in order to minimize expensive reagent consumption, a pre-separation step to reduce the number of contaminating cells is desired.

Dielectrophoresis (DEP) achieves a separation of cells using an applied electric field gradient (Figure 43), analogous to magnetophoresis. The method separates cells based on differences in dielectric properties, which are dependent on the morphology and electric conductivity of the cell [190]. Cells typically have a negatively charged surface and can therefore be moved in an electric field due to Coulomb force (F_{DEP}), which is dependent on the total charge and the surface charge density of the cell. DEP is thereby a label-free and noncontact way to manipulate cells. Due to the microscale dimensions of a DEP device, a high electric field strength is generated, which allows for a relatively low-voltage separation of cells.

A disadvantage of the method is the need to use specific buffer mediums with low conductivity to avoid detrimental heating effects. DEP-based methods have been used for the isolation of CTCs and other rare cells in blood [191] and to trap pre-enriched cells for downstream single-cell analysis [192-194]. Two of these technologies targeting CTCs are ApoStream (ApoCell) and DEPArray (Menarini Silicon Biosystems).

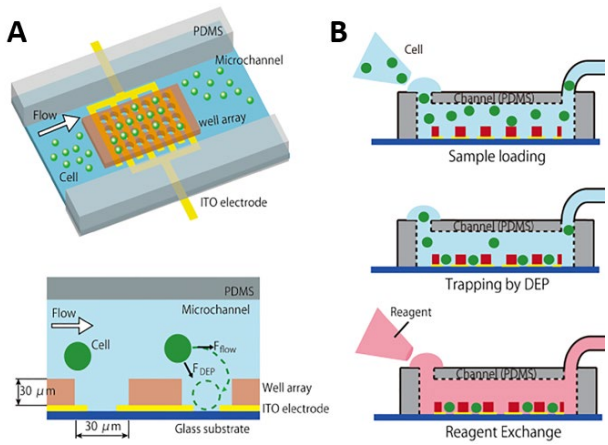

Figure 43. Dielectrophoresis (DEP) technology. A) CTCs are captured in a well array by an electric field gradient as the suspended cells experience different Coulomb forces depending on their dielectric properties. B) A sample is loaded and trapped by positive DEP, followed by an exchange of reagents for cell analysis. Reprinted from reference [192].

ApoStream operates in a continuous flow-based mode and captures CTCs as they pass the electric field and get pulled down, whereas the WBCs flow by [190]. Although, the microfluidic device requires a pre-separation step to remove both the RBCs and the large population of granulocytes prior DEP separation of the mononuclear blood cell fraction and the CTCs [195, 196].

DEPArray is a microfluidic CTC sorter, using a low volume of pre-enriched input sample (12 μL) to isolate individual CTCs in a so-called DEP cage [194]. The chip integrates an array of microelectrodes to create up to 30.000 cages for CTC capture. The DEPArray technology can be used downstream of basically any pre-separation and enrichment method as a way to retrieve single cells (live and fixed) for further analysis [197, 198].

Passive methods

Inertial focusing uses passively generated forces to separate cells within microfluidic devices. An overview of the fundamental physics governing inertial focusing and cell separations is given in the subsection *Inertial effects in microfluidics*, above. As described, inertial focusing moves cells based on the cell size, properties of the flow, and the microchannel design. Even though less exploited, cell separations are also possible based upon other cell properties, such as shape and deformability, and utilize how the cells are positioned at equilibrium in relation to those parameters.

In inertial focusing the inertial forces move the cells to equilibrium positions within the microfluidic channel. For a straight channel, the equilibrium positions are determined balancing the shear gradient and the wall lift forces, and for various cell sizes these are in close proximity due to the fast-declining wall lift force and thus pure cell separations are hard to obtain. To achieve more efficient cell separations, curved or spiral channel designs have shown to be advantageous. As earlier described, in curved channels an additional force, the Dean flow drag force, is balancing the wall lift and shear gradient lift forces and it creates an increased separation distance between the different sized cells. The curved channels also have an improved throughput due to a larger channel cross-section.

One such inertial focusing method is Dean flow fractionation (DFF), also called spiral microfluidics, which uses two inlet streams (one for sheath buffer and one for the sample) and a curved channel designed to complete one Dean flow cycle of the

sample before collecting the separated fractions (Figure 44). Larger cells will focus to an equilibrium position due to the lift forces and the Dean drag force, whereas the smaller cells will be moved by the Dean flow in a full cycle back to the initial position. DFF has been validated to separate WBCs and cancer cells differing approximately 5 µm in diameter and can separate cells with a relatively high throughput with an ability to perform multiplexed separation by stacking individual microchips together [199, 200].

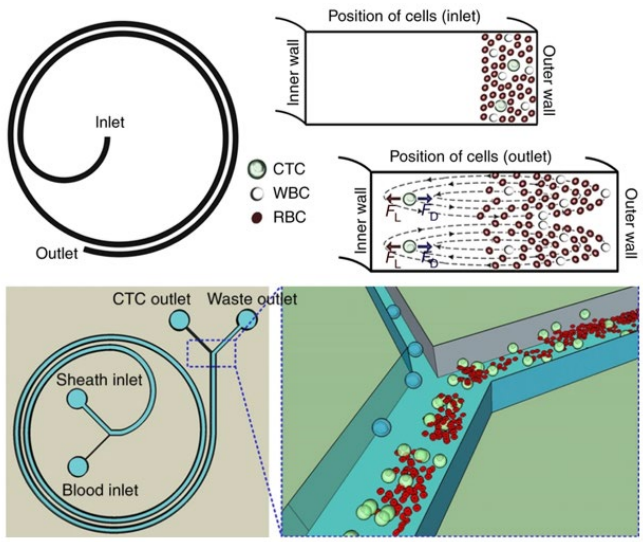

Figure 44. Inertial focusing separation of CTCs and WBCs by Dean flow fractionation (DFF), also called spiral microfluidics. Top image illustrates the spiral channel with a rectangular cross-section, in which the blood sample enters the inlet by the outer wall. At the outlet, the blood cells (RBCs and WBCs) have completed one full Dean flow cycle and are therefore back by the outer wall, whereas the larger CTCs are focused near the inner wall due to the balancing lift forces and the transversal Dean flow drag force. Bottom image shows a schematic overview of the two inlets for blood and sheath buffer respectively, and the two outlets for the separated cell fractions. Adapted from reference [199] with permission from Springer Nature.

Another type of inertial focusing is vortex trapping [201-203]. The technology is based on microfluidic channels with serial expansions along the channel. At high flow velocities, microfluidic vortices will develop in the expansions due to the sudden disappearance of the wall lift force while the shear gradient is still retained (Figure 45). As the shear gradient lift force is cell size dependent (diameter^3), the larger CTCs will migrate laterally across streamlines into the reservoir and get trapped, whereas smaller blood cells will continue in the central flow. The captured CTCs can be released from the vortices by simply reducing the flow velocity.

Although, the inertial cell separation methods have demonstrated an efficient sample throughput and an effective separation of tumor cells and smaller-sized blood cells, they have an inherent difficulty to detect smaller or same-sized CTCs. Studies have shown a large variability in CTC size, both between patients and within a single patient sample [204, 205]. This signifies that separation approaches entirely based on cell size might miss a considerable number of CTCs.

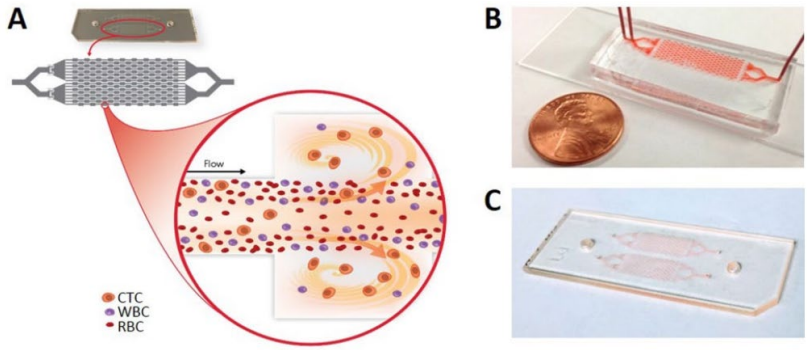

Figure 45. Vortex trapping technology. A) Schematic image of microfluidic vortices developing at expansions along the microchip trapping the larger CTCs. B) and C) Photo of the Vortex HT microchip with a parallelized array of microfluidic channels with serial expansions. Reprinted from reference [201] with permission from SAGE publications.

Deterministic lateral displacement (DLD) is a size and deformability-based separation method, similar to the macroscale filtration methods (as described in the section *Macroscale techniques and current "gold-standard" for CTC isolation*). While macroscale filtration methods are straightforward and easy to use, they are prone to clogging due to the high cell density in blood. Here, DLD uses an array of pillars to separate cells in a laminar fluid flow [206]. If a cell encounters an obstacle along its center-of-mass streamline, the cell will be shifted onto a new streamline when it moves around the obstacle and the magnitude of such movement is size dependent (Figure 46). By designing the DLD array to ensure a continuous size-based diagonal movement of larger cells (Fig. 46, B), as smaller cells will follow the fluid streamline downwards (Fig. 46, A), an efficient separation can be achieved. DLD can also separate cells based on deformability due to shear stress at the fluid flow closest to a pillar (the boundary) [207]. Such shear stress can compress and deform nearby cells, which give them smaller effective size and center-of-mass streamline and hence separation can be accomplished based on the cell stiffness.

The mechanical deformability is particularly relevant for blood cells as it determines their migratory capacity within the blood vessels.

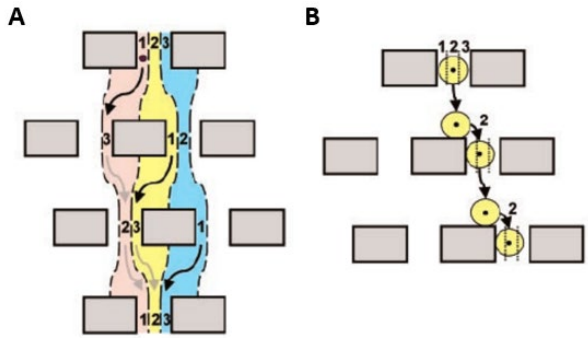

Figure 46. DLD array for size-based separations. A) Illustration of vertical pathways for three fluid streamlines (red, yellow, and blue) passing through a DLD array. Smaller particles will follow its current streamline. B) Larger particles will be moved to new streamlines at which its center of mass is located. Reprinted from reference [206] with permission from American Association for the Advancement of Science.

Thus, DLD is an efficient method for size-based cell separations and has been used as a pre-separation step to remove RBCs and debris from a whole blood sample, prior further cell separation strategies, including inertial focusing followed by magnetophoresis (Figure 47) [129, 132].

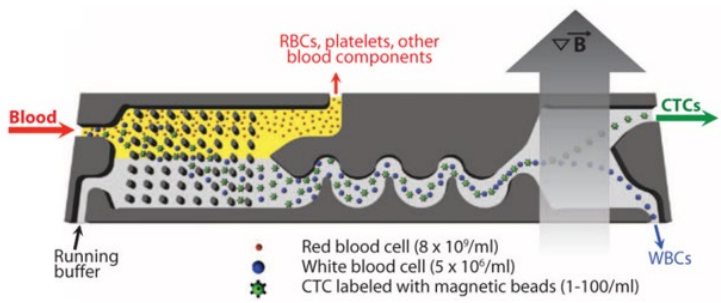

Figure 47. Combinational approach of three microfluidic methods for the separation of CTCs from whole blood. First, a DLD array ensures a diagonal movement of larger cells, while smaller-sized RBCs and platelets are removed. The separated WBCs and CTCs are then aligned through inertial focusing, prior a magnetic separation of CTCs from WBCs through positive selection magnetophoresis. Reprinted from reference [129] with permission from American Association for the Advancement of Science.

Mechanical microstructures, such as micropost geometries and surface ridges (*e.g.,* herringbone structure), labeled with monoclonal antibodies have been used to disrupt the streamlines in laminar flow to enable fluid mixing and facilitate interactions between target CTCs and the antibody-coated surfaces (Figure 48) [130, 131]. Under laminar flow conditions the spontaneous variation in velocity is absent and the molecule diffusion is minimal, which prevents mixing and critical cell-surface contacts to capture the target cells. Mechanical distortions within the channel induces secondary flow fields (*i.e.,* fluidic microvortices), which moves cells into different transversal positions and enhances fluid mixing [208].

The herringbone wall design (Fig. 48, A and B) is considered superior to micropost structures (Fig. 48, C) to target CTCs due to an increased number of interactions between the cells and coated surfaces, leading to an increased CTC capture efficiency [131]. The herringbone wall design also allows for a higher blood volume throughput. Using micropost geometries, the flow velocity is an essential parameter for the capture efficiency as it influences the duration of the cell-surface interaction. In comparison, the herringbone chip showed a two-fold increase in blood volume throughput. However, the methods are surface epitope dependent by using monoclonal antibodies for a positive selection of the target cells, which limits the capacity to detect a phenotypic diverse population of CTCs.

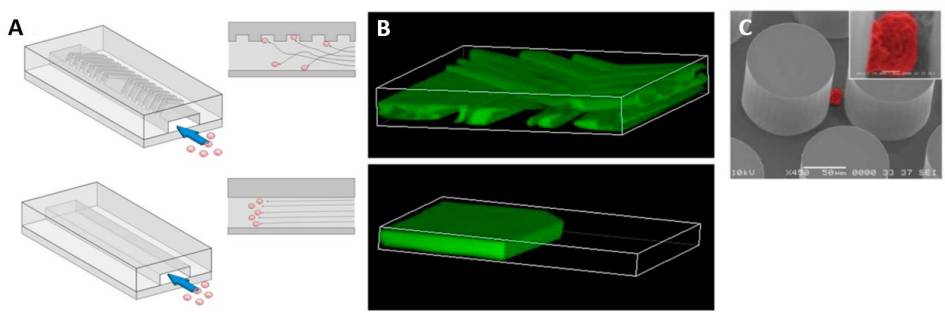

Figure 48. Mechanical microstructures to disrupt laminar flow streamlines and enhance cell-surface interactions. A) Illustration of the cell-surface interactions in a herringbone microfluidic chip (top) compared to a traditional microfluidic chip with straight walls and laminar flow condition (bottom). B) Flow visualization using two streams (green and clear) of same viscosity showing the fluid mixing in the chip with herringbone structures (top) and the laminar flow in traditional microfluidic devices (bottom). C) Scanning electron microscopy image of a microfluidic chip with antibody-coated micropost structures etched in silicon and a captured lung cancer cell. Color added for visualization. Reprinted from references [131] (A and B) and [130] (C) with permission from National Academy of Sciences and Springer Nature.

Outlining CTC biomarkers

Personalized cancer care is in urgent need of novel biomarkers to aid clinicians in the decision process throughout the various clinical states of the disease. In addition to its current use as a prognostic marker for overall survival, CTCs hold promise to be used as a predictive biomarker and as an indicator of post-treatment response. In other words, CTCs could help with a dynamic assessment of the real-time response to a selected treatment and further, as a surrogate endpoint measure to substitute lengthy clinical endpoints, such as OS. Most promising might be the use of CTCs as pre-treatment predictive biomarkers to guide physicians in the selection of targeted therapies based on the current profile of the cancer. Therefore, CTCs as a biomarker, must be validated in the context of its intended clinical use.

In tissue biopsies, the tumor heterogeneity can cause a sampling bias and important subset of cells can be missed, cells that might resist treatment and evolve into a dominant type of malignant cells at a later state of the disease [209, 210]. CTCs have shown to be a representative tumor source for various subclones present in a cancer patient [53, 54] and as a liquid biopsy is quick and minimally invasive, it can be repeated throughout the patient care. Further, as cancer cells inherently have an instable genome, new mutations toward advantageous genotypes and phenotypes will likely be acquired during the natural history of the disease and from the selective pressure of chosen treatment strategies. Consequently, the need to profile the malignant cells during the progression of the disease will likely be as important as profiling of diagnostic biopsies.

The multifaceted complexity of CTCs makes their isolation and profiling a challenging task for the existing and emerging technologies. The technologies have diverse approaches and as a result different subgroups of cells are targeted for enrichment and analysis. The subsequent molecular characterization of the tumor cells can focus on DNA, RNA, or proteins, as well as cell size, nuclear-cytoplasmic ratio *etc*. Therefore, different technological approaches to CTC isolation and profiling have different advantages and disadvantages (as for example time, cost, complexness, and accuracy of the assays). However, to qualify as a translational

technology, the biomarker assay needs to prove not only that the measurement is robust, but also that it has clinical validity in a given context of use (COU).

Analytical and clinical validation

The FDA is the regulatory body that oversees the qualifications and approvals of drug development tools and devices to measure specific biomarkers. To acquire an FDA approval, the technology needs to demonstrate both the consistent and accurate measure of the biomarker, and its clinical validity in thorough analytical and clinical validation processes (Figure 49). During the analytical validation, the technical quality is assessed, in which the assay needs to show reproducibility (intra-assay and inter-assay) of the biomarker measurements and demonstrate its precision for such measurements. The precision can be addressed by using internal controls, reference standards, or positive and negative controls, depending on the biomarker assay. Additionally, the diverse preanalytical conditions needs to be addressed, including standardization of sample acquisition, processing, and storage conditions. Various analytical concepts are used to describe the performance of the technology, as discussed in the section *Performance terminology*.

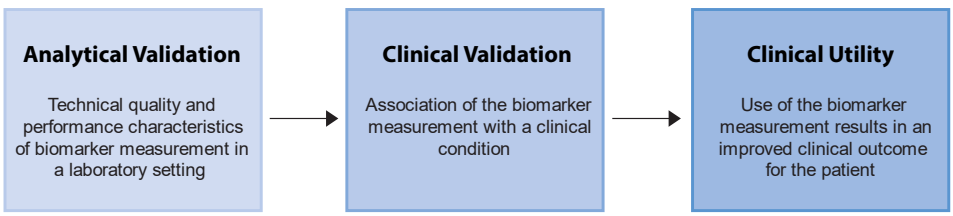

Figure 49. Development steps of a biomarker assay, from the laboratory to clinical practice.

After rigorous analytical validation, a clinical validation is performed to evaluate if the measured biomarker can be linked to specific points in the disease progression and to clinical endpoints in a given COU, a requirement for an FDA clearance or approval of the biomarker. Although, to prove a clinical utility, the biomarker assay needs to provide clinicians with additional information to help in a medical decision making and demonstrate that such decision results in an improvement of the clinical outcome for patients [211, 212]. The clinical utility is usually demonstrated after a longer period of clinical use of the biomarker assay.

Concluding remarks

The presented thesis broadens the applications of acoustophoresis technology in the field of CTC separation and isolation, including both fixed and live cell samples. The approach using an acoustic standing wavefield for the enrichment of CTCs may result in an efficient methodology to access clinically relevant information from a non-invasive sample source to guide the management of metastatic cancer patients.

The work also made discoveries in fluid mechanics relevant to acoustophoresis and possibly other microfluidic cell and particle separation technologies operating at high flow velocities for a fast sample processing.

Summary of included papers

In the following chapter, a brief presentation of the included papers will be given. The four papers are described in a chronological order, whereof the first three studies are published or submitted for publication and the last one is a draft manuscript for an ongoing validation study.

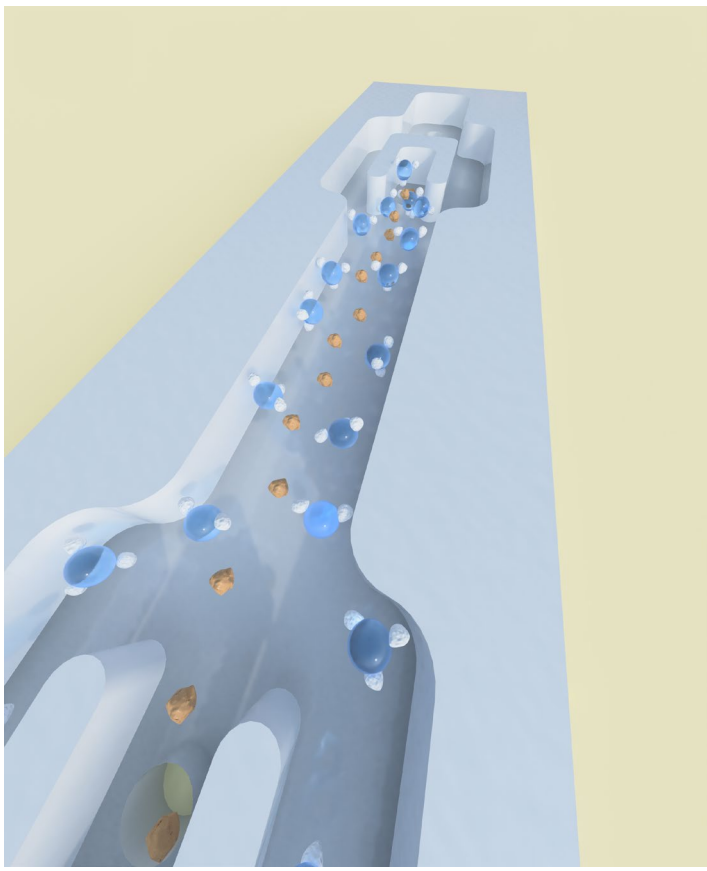

Figure 50. Illustration of the working principle of negative selection acoustophoresis used in paper 1 and 2. Close-up of the separation of tumor cells (orange) and WBCs (white) bound to elastomeric negative contrast particles (blue) at the outlet junction.

Paper 1 - Reducing WBC background in cancer cell separation products by negative acoustic contrast particle immuno-acoustophoresis

There is a strong interest in developing efficient cell separation technologies with an epitope-agnostic approach for the isolation of heterogenous circulating tumor cells (CTCs), aimed to validate novel biomarkers for effective treatment management of cancer patients. Tumor cells display acoustic properties that enables an acoustophoretic separation from white blood cells (WBCs). However, a subset of WBCs has overlapping acoustic properties with tumor cells, especially when doing live cell separation, which was the motivation behind this study.

Paper 1 presents a proof-of-principle study for negative selection acoustophoresis using negative acoustic contrast elastomeric particles to deplete WBCs, while enriching for live prostate and breast cancer cells from *in vitro* cultures (Figure 50 and 51). The elastomeric particles were functionalized with anti-CD45 antibodies that bind specific to WBCs (Fig. 51, left), and which enabled the acoustic transportation of WBCs to pressure antinodes along the channel walls, while tumor cells focused to the pressure node in the center of the channel (Fig. 51, right). A frequency modulation was used to prevent aggregation of negative complexes at the pressure antinodes along the side walls and thus avoid flow disturbances.

The results showed a WBC depletion efficacy of >98% and cancer cell recoveries of >85%. We envisioned that the technology should be used as an elegant part in combination with an initial step of label-free acoustophoresis to further reduce the WBC background in CTC separation products.

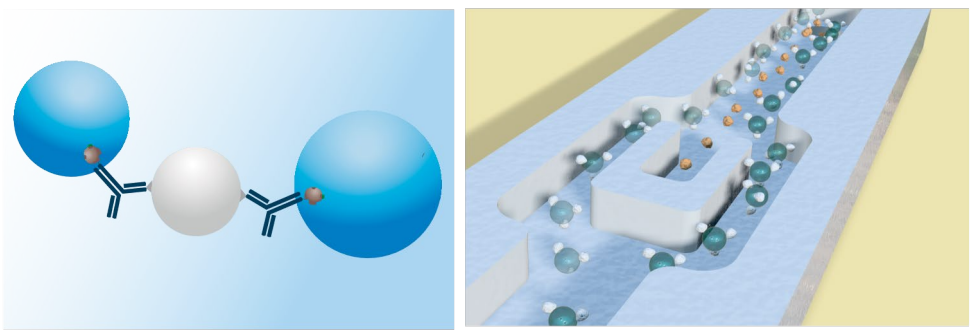

Figure 51. Immunofunctionalized negative acoustic contrast particles (blue) binding to WBCs (white) enabled negative selection acoustophoresis with an enrichment of tumor cells (orange) from prostate and breast cancer cell lines in a proof-of-concept study.

Paper 2 - Two-step acoustophoresis separation of live tumor cells from whole blood

In the second paper, the proof-of-concept study was extended to carry out processing of red blood cell (RBC) lysed whole blood samples for the isolation of viable cancer cells. A two-step acoustophoresis method was presented with an acoustofluidic pre-separation step, followed by negative selection acoustophoresis (Figure 52). The initial step enriched the cancer cells in a central outlet, although a significant number of WBCs remained. The secondary purging step removed the contaminating WBCs by using anti-CD45-functionalized negative acoustic contrast particles, analogously to paper 1. A combination of frequency modulation and an acoustic multinode resonance configuration were employed to avoid negative acoustic contrast complexes from accumulating at the channel walls, and thereby promote a uniform flow profile without disturbances.

A WBC depletion efficacy of ≥99.5% was achieved with the sequential processing and up to 42% of the viable cancer cells were recovered. The dependency on the sample cell concentration in relation to the separation performance was explored and showed that a dilution of the RBC lysed whole blood was necessary to avoid hydrodynamic interactions between cells. Finally, we demonstrated the biocompatibility of the method through viability and proliferation studies of the recovered cancer cells. The novel method provided an extensive removal of WBCs combined with a gentle recovery of viable cancer cells, suitable for downstream functional analyses and *in vitro* culture.

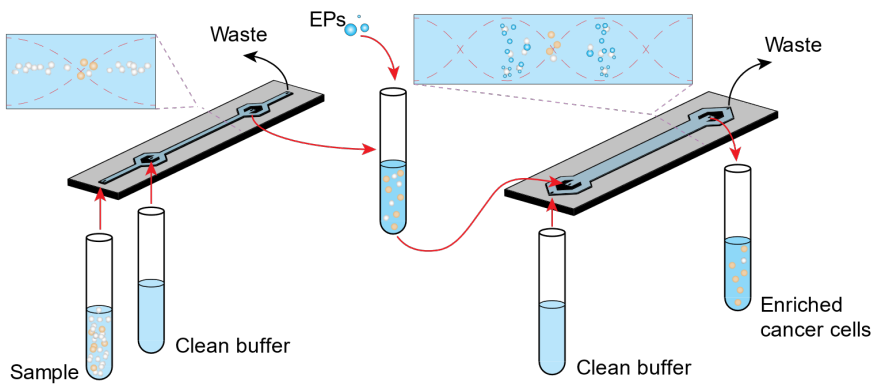

Figure 52. Illustration of two-step acoustophoresis. Step I: A pre-separation step enriched the cancer cells by single node acoustophoretic separation from WBCs. Step II: Contaminating WBCs were removed by negative acoustic contrast particles (EPs) in a secondary multinode acoustophoretic step.

Paper 3 - Inertia induced breakdown of acoustic sorting efficiency at high flow rates

The sample throughput is an important parameter for microfluidic processing of clinical samples, especially for rare cell applications where a larger volume might be required for the detection of target cells. In paper 3, the effect of inertial forces on acoustofluidic particle sorting at high sample throughputs was investigated experimentally and theoretically.

We observed an inertia induced phenomenon that may compromise separation performance at higher flow velocities. The effect illustrates the complex interplay of viscous and inertial forces. At increased flow rates a lateral relocation of the particle trajectories was seen and above specific flow settings the particles spilled over into the adjacent outlet, independent of acoustic actuation (Figure 53, bottom). The impact of the spillover effect on the separation of two different-sized particles was subsequently studied. At specific flow settings the inertia induced effect caused all particles, independent of size, to exit via the center outlet, leading to a breakdown of the separation. The effect was discovered to be due to a distorted fluid boundary between the sample and sheath flow at the inlet of the separation channel (Fig. 53, top), as well as at the outlet flow splitter (middle), at elevated flow rates. Theoretical calculations of critical flow settings for the particle separations were found to agree with the experimental outcome, providing means of future in-silico chip design optimization.

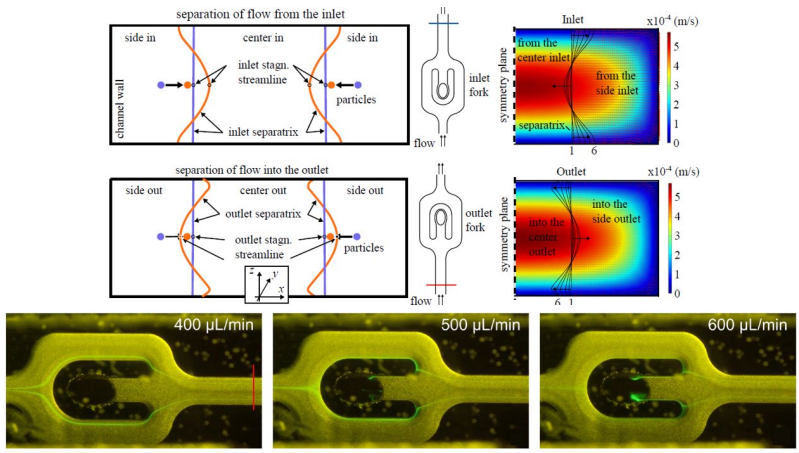

Figure 53. Inertia induced phenomenon caused spilling of particles (bottom) into the center outlet at increased flow velocities due to the formation of curved fluid boundaries. The inlet curvature (top) shifted the particle trajectories toward the channel center and the deformation of the outlet fluid boundary (middle) moved the outlet stagnation streamline closer to the channel wall.

Paper 4 - Outline for the benchmarking of CTC-acoustophoresis to the current state-of-the-art technology

Paper 4 presents the framework for a comparative analytical validation of CTC-acoustophoresis technology to the US Food and Drug Administration (FDA) cleared CELLSEARCH CTC enumeration system.

Blood samples from metastatic prostate cancer patients were obtained and processed with either acoustophoresis (Figure 54) or the CELLSEARCH system. The separated fractions were immunofluorescently labeled and analyzed by image flow cytometry. The preliminary results showed an increased detection of plausible CTCs of an epithelial phenotype using CTC-acoustophoresis compared to the reference modality. Heterogenous CTC clusters were also detected after CTC-acoustophoresis, which were not reported by the CELLSEARCH system. The initial results of the benchmarking study indicate an improved recovery of patient-derived CTCs. Further, the epitope-agnostic approach of acoustophoresis enables the isolation of heterogenous CTCs, including cells undergoing a genotypic and phenotypic transition. Ongoing studies will conclude the performance characteristics of the novel CTC assay in the laboratory setting.

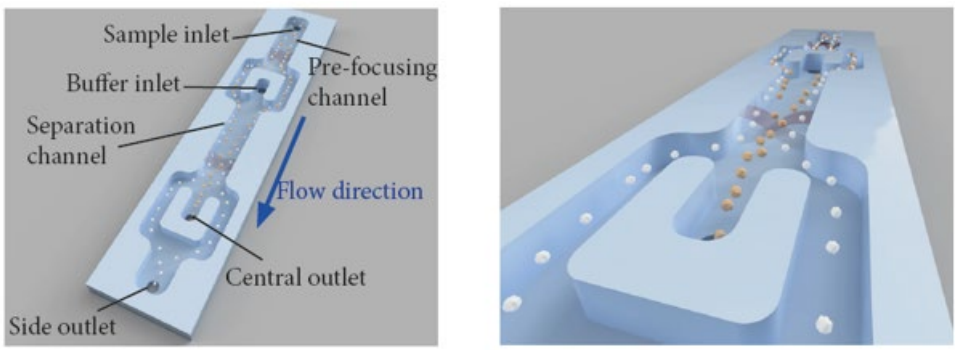

Figure 54. Illustration of the CTC-acoustophoresis chip. Overview (left) of the fundamental parts of the separation device, including the sample inlet, 2D-alignment channel, sheath buffer inlet followed by the acoustic separation channel and finally the outlet junction for the separated cell fractions. A close-up (right) of the outlet junction where CTCs (orange particles) exit through the central outlet and the WBCs (white particles) pass by on the sides.

Popular Science Summary

What if a doctor could know how a patient with metastatic cancer would respond to the various treatments available? What if there was a way to access the patient's malignant cells without the need for an invasive and painful tissue biopsy? A strategy that would allow access to clinically relevant information but is not causing any increased risk for the patient, and is a feasible, low-cost option available to standard of care. Such measures would act as informative biomarkers, aiding physicians in the patient stratification through the various states of disease progression.

One promising biomarker to address such unmet clinical needs is circulating tumor cells (CTCs). CTCs are malignant cells that have shed from the primary tumor or any metastatic site into the blood stream, where they can be found at an extremely low concentration, approximately 1 to 10 CTCs per milliliter of whole blood. A milliliter of blood contains billions of blood cells and cell fragments of various types (red blood cells (RBCs), different white blood cells (WBCs) and platelets), therefore, it is a tremendous technical challenge to identify and single-out the rare tumor cells. Many isolation methods have been developed over the last decade, all aiming for an efficient assay with high sensitivity and specificity for the target tumor cells. Their approaches vary and are based on both macroscale methods, like cell density-based centrifugation and cell size-based filters, and different types of microscale technologies (*i.e.,* microfluidics) using external forces or passive methods.

In this thesis, a microfluidic technology called acoustophoresis have been explored and optimized for the isolation of CTCs. Acoustophoresis uses ultrasound to manipulate cells and particles in microfluidic channels, *i.e.,* cylindrical, or square channels with micrometer-scaled cross-sections and of centimeter-sized lengths. The applied ultrasound give rise to acoustic forces acting transversely in the channel on suspended cells and particles flowing through. The acoustic force is dependent on the objects size, density, and compressibility, as well as the properties of the suspension fluid. Thereby, the cells and particles can be separated based on their individual acoustic properties.

In paper 1 and 2, live cancer cells from a model system with a prostate cancer cell line added into diluted WBCs were isolated with acoustophoresis. To enhance the separation of cancer cells and blood cells, micrometer-sized elastomeric particles were used to remove the contaminating WBCs. The rubber-like particles behave in the opposite way to cells when impacted by an acoustic wave field. Instead of moving to a pressure-minima, they move to a pressure maximum, here, that is to the sidewalls of the channel. By modifying the particles surface and attaching antibodies that binds specific to WBCs, the particles can act like transporters with the blood cells as cargo. In paper 1, the method was demonstrated in a proof-of-principle study. Paper 2 extended the concept to carry our processing of whole blood. It was done by two-step acoustophoresis, with negative selection acoustophoresis with the modified elastomeric particles as a second step. Future studies contain the processing of patient samples with the objective to isolate and grow patient-derived prostate cancer cells.

Paper 3 studied the cell separation performance of acoustophoresis at increased sample throughputs. The throughput is an important consideration with rare cell separations for clinical use, as a sufficiently large volume of blood needs to be processed to find the target cells, and also be completed within a reasonable time frame. A phenomenon was discovered at the higher sample throughputs investigated, in which separations failed due to a fluid inertia effect. The gained knowledge can assist in the development of novel acoustofluidic chip designs for high throughput assays.

In paper 4, acoustophoresis was compared to the current state-of-the-art technology for CTC isolation. Two blood samples were drawn from each prostate cancer patient included in the study. The samples were chemically preserved and processed with the two CTC isolation platforms. Image analysis showed that acoustophoresis was able to detect more CTCs with the commonly described CTC characteristics compared to the standard modality. Further, several cells with an alternative CTC feature were also discovered, which would be missed with the current standard due to its isolation approach. Future studies will continue the comparison of CTC-acoustophoresis to the clinical standard technology, including prospective validation of the technology.

The presented work extends the applications of cutting edge acoustophoresis technology in the field of rare cell isolation. The novel approach for CTC isolation may result in a non-invasive methodology to access clinically relevant information to guide management of metastatic cancer patients.

Acknowledgements

And so, in the end, it strikes me how much luck or maybe fate has played a role in me writing this thesis. All the people that I have met, and the surprising turns life has taken.

This thesis would not have been written without the support of my family and friends, and the influence of so many brilliant people. There is so many that I would like to thank, so I will take it from where it began:

Hans Lilja, thank you for meeting with me all those years ago and for letting me join your research group at Memorial Sloan Kettering Cancer Center to do my master thesis. It was a great time and I learnt so much from all the fantastic people in your team (Dipti, Annie, Christian and David). Thank you for introducing me to the distinguished Dr. Howard Scher and Dr. Martin Fleisher, who recruited me to the circulating tumor cell research group after my graduation from KTH. The years at MSKCC were inspiring and truly life-defining (as I also met my future husband in the CTC group). Thank you for being my mentor during my years in New York and for encouraging me to pursue a PhD, without your influence (and phone call to Thomas), I probably would not have written this thesis.

Thomas Laurell, thank you for giving me the opportunity to join your research group in Lund. Your expertise and supervision have been invaluable to my dissertation. Thank you for all the support and encouragement throughout the years, your positive attitude has been inspirational, especially at times of setbacks. It has been amazing years and I am forever grateful.

Yvonne Ceder, thank you for your guidance and valuable inputs over the years. Your enthusiastic support and motivation have been vital throughout this journey.

Andreas Lenshof, thank you for all the help in the lab, for being the chip doctor that can fix every issue, and for great inputs on the research. Not least, thank you for the fun times at BMC.

Cecilia Magnusson, thank you for all your help, for great teamwork and for staying positive when things did not want to work. Thank you for your friendship and for the good times over the years.

Kevin Cushing, thank you for teaching me about elastomeric particles and for being such a positive spirit.

Thierry Baasch, thank you for teaching me about fluid mechanics and for all your time and help.

Thank you to all my other present and former colleagues of the Acoustofluidics group. It has been a true pleasure to work in such a supportive and brainy environment. Thank you Per, Pelle, Wei, Fabio, Klara, Anke, Franzi, Ola, Mikael, Mattias, Axel, Megan, and everyone else.

Thank you to all my BME colleagues for being the friendliest and best department at the university. And thank you Johan Nilsson, for making that happen by being the best head of department possible. Special thanks also to Ulrika for all the help and positive energy throughout the years, and to Axel, who could solve any computer problem that I came across.

To conclude, I want to thank my family and friends. My mom for her constant support and my late dad who always knew everything, but never said a word. Thank you for inspiring me to also be a KTH alumni.

Thank you, Christine, for a lifetime of friendship and for all your time and help teaching me some graphic design.

And finally, thank you to my own little family, Aseem, Elsa and Lovisa. There is no one I admire more than you Aseem, your grit and talent is truly inspiring. Thank you for all your support and for always believing in me. Thank you, Elsa and Lovisa for giving our life another dimension. I love you to the end of the universe and back.

References

1. Welfare, T.N.B.o.H.a. *Statistics on newly discovered cancer 2019*. 2020; Available from: https://www.socialstyrelsen.se/globalassets/sharepoint-dokument/artikelkatalog/statistik/2020-12-7132.pdf.
2. Jahn, J.L., E.L. Giovannucci, and M.J. Stampfer, *The high prevalence of undiagnosed prostate cancer at autopsy: implications for epidemiology and treatment of prostate cancer in the Prostate-specific Antigen-era.* International Journal of Cancer, 2015. **137**(12): p. 2795-2802.
3. Bell, K.J.L., et al., *Prevalence of incidental prostate cancer: A systematic review of autopsy studies.* International Journal of Cancer, 2015. **137**(7): p. 1749-1757.
4. Murphy, G.P., et al., *The National Survey of Prostate-Cancer in the United-States by the American-College-of-Surgeons.* Journal of Urology, 1982. **127**(5): p. 928-934.
5. Mcneal, J.E., et al., *Zonal Distribution of Prostatic Adenocarcinoma - Correlation with Histologic Pattern and Direction of Spread.* American Journal of Surgical Pathology, 1988. **12**(12): p. 897-906.
6. Stamey, T.A., et al., *Prostate-Specific Antigen as a Serum Marker for Adenocarcinoma of the Prostate.* New England Journal of Medicine, 1987. **317**(15): p. 909-916.
7. Sathianathen, N.J., et al., *Landmarks in prostate cancer.* Nature Reviews Urology, 2018. **15**(10): p. 627-642.
8. Bratt, O., et al., *Upper limit of cancer extent on biopsy defining very low-risk prostate cancer.* Bju International, 2015. **116**(2): p. 213-219.
9. D'Amico, A.V., et al., *Biochemical outcome after radical prostatectomy, external beam radiation therapy, or interstitial radiation therapy for clinically localized prostate cancer.* Jama-Journal of the American Medical Association, 1998. **280**(11): p. 969-974.
10. Gleason, D.F., *Classification of prostatic carcinomas.* Cancer Chemother Rep, 1966. **50**(3): p. 125-8.
11. Partin, A.W., et al., *Combination of prostate-specific antigen, clinical stage, and gleason score to predict pathological stage of localized prostate cancer - A multi-institutional update.* Jama-Journal of the American Medical Association, 1997. **277**(18): p. 1445-1451.
12. Akre, O., et al., *Mortality among Men with Locally Advanced Prostate Cancer Managed with Non-Curative Intent; a Nationwide Study in Pcbase Sweden.* European Urology Supplements, 2011. **10**(2): p. 239-240.
13. Romero-Otero, J., et al., *Active surveillance for prostate cancer.* International Journal of Urology, 2016. **23**(3): p. 211-218.

14. Han, M., et al., *Biochemical (prostate specific antigen) recurrence probability following radical prostatectomy for clinically localized prostate cancer.* Journal of Urology, 2003. **169**(2): p. 517-523.
15. van der Toom, E.E., et al., *Prostate-specific markers to identify rare prostate cancer cells in liquid biopsies.* Nat Rev Urol, 2019. **16**(1): p. 7-22.
16. Bubendorf, L., et al., *Survey of gene amplifications during prostate cancer progression by high-throughout fluorescence in situ hybridization on tissue microarrays.* Cancer Res, 1999. **59**(4): p. 803-6.
17. Ruizeveld de Winter, J.A., et al., *Androgen receptor status in localized and locally progressive hormone refractory human prostate cancer.* Am J Pathol, 1994. **144**(4): p. 735-46.
18. Sadi, M.V., P.C. Walsh, and E.R. Barrack, *Immunohistochemical study of androgen receptors in metastatic prostate cancer. Comparison of receptor content and response to hormonal therapy.* Cancer, 1991. **67**(12): p. 3057-64.
19. Wang, W. and J.I. Epstein, *Small cell carcinoma of the prostate. A morphologic and immunohistochemical study of 95 cases.* Am J Surg Pathol, 2008. **32**(1): p. 65-71.
20. Aggarwal, R., et al., *Neuroendocrine prostate cancer: subtypes, biology, and clinical outcomes.* J Natl Compr Canc Netw, 2014. **12**(5): p. 719-26.
21. Velho, P.I., D.A. Bastos, and E.S. Antonarakis, *New Approaches to Targeting the Androgen Receptor Pathway in Prostate Cancer.* Clinical Advances in Hematology & Oncology, 2021. **19**(4): p. 228-240.
22. Hu, R., et al., *Ligand-Independent Androgen Receptor Variants Derived from Splicing of Cryptic Exons Signify Hormone-Refractory Prostate Cancer.* Cancer Research, 2009. **69**(1): p. 16-22.
23. Qu, Y.Y., et al., *Constitutively Active AR-V7 Plays an Essential Role in the Development and Progression of Castration-Resistant Prostate Cancer.* Scientific Reports, 2015. **5**.
24. Welti, J., et al., *Analytical Validation and Clinical Qualification of a New Immunohistochemical Assay for Androgen Receptor Splice Variant-7 Protein Expression in Metastatic Castration-resistant Prostate Cancer.* European Urology, 2016. **70**(4): p. 599-608.
25. Sharp, A., et al., *Androgen receptor splice variant-7 expression emerges with castration resistance in prostate cancer.* Journal of Clinical Investigation, 2019. **129**(1): p. 192-208.
26. Antonarakis, E.S., et al., *Androgen receptor splice variant, AR-V7, and resistance to enzalutamide and abiraterone in men with metastatic castration-resistant prostate cancer (mCRPC).* Journal of Clinical Oncology, 2014. **32**(15).
27. Luo, J., et al., *Role of Androgen Receptor Variants in Prostate Cancer: Report from the 2017 Mission Androgen Receptor Variants Meeting.* European Urology, 2018. **73**(5): p. 715-723.
28. Antonarakis, E.S., et al., *Clinical Significance of Androgen Receptor Splice Variant-7 mRNA Detection in Circulating Tumor Cells of Men With Metastatic Castration- Resistant Prostate Cancer Treated With First- and Second-Line Abiraterone and Enzalutamide.* Journal of Clinical Oncology, 2017. **35**(19): p. 2149-+.

29. Scher, H.I., et al., *Assessment of the Validity of Nuclear-Localized Androgen Receptor Splice Variant 7 in Circulating Tumor Cells as a Predictive Biomarker for Castration-Resistant Prostate Cancer.* Jama Oncology, 2018. **4**(9): p. 1179-1186.
30. Antonarakis, E.S., et al., *Androgen Receptor Splice Variant 7 and Efficacy of Taxane Chemotherapy in Patients With Metastatic Castration-Resistant Prostate Cancer.* Jama Oncology, 2015. **1**(5): p. 582-591.
31. Bernemann, C., et al., *Expression of AR-V7 in Circulating Tumour Cells Does Not Preclude Response to Next Generation Androgen Deprivation Therapy in Patients with Castration Resistant Prostate Cancer.* Eur Urol, 2017. **71**(1): p. 1-3.
32. Nakazawa, M., et al., *Serial blood-based analysis of AR-V7 in men with advanced prostate cancer.* Ann Oncol, 2015. **26**(9): p. 1859-1865.
33. Todenhofer, T., et al., *AR-V7 Transcripts in Whole Blood RNA of Patients with Metastatic Castration Resistant Prostate Cancer Correlate with Response to Abiraterone Acetate.* Journal of Urology, 2017. **197**(1): p. 135-142.
34. Josefsson, A., J.E. Damber, and K. Welen, *AR-V7 expression in circulating tumor cells as a potential prognostic marker in metastatic hormone-sensitive prostate cancer.* Acta Oncologica, 2019. **58**(11): p. 1660-1664.
35. Zhang, T., et al., *Androgen Receptor Splice Variant, AR-V7, as a Biomarker of Resistance to Androgen Axis-Targeted Therapies in Advanced Prostate Cancer.* Clinical Genitourinary Cancer, 2020. **18**(1): p. 1-10.
36. Lesko, L.J. and A.J. Atkinson, Jr., *Use of biomarkers and surrogate endpoints in drug development and regulatory decision making: criteria, validation, strategies.* Annu Rev Pharmacol Toxicol, 2001. **41**: p. 347-66.
37. Amur, S., et al., *Biomarker Qualification: Toward a Multiple Stakeholder Framework for Biomarker Development, Regulatory Acceptance, and Utilization.* Clin Pharmacol Ther, 2015. **98**(1): p. 34-46.
38. Casavant, B.P., D. Kosoff, and J.M. Lang, *Directing Circulating Tumor Cell Technologies Into Clinical Practice*, in *Circulating Tumor Cells*. 2016. p. 351-364.
39. Newling, D.W.W., *Issues with the Use of Prostate-Specific Antigen as a Surrogate End Point in Hormone-Resistant Prostate Cancer.* European Urology Supplements, 2009. **8**(1): p. 13-19.
40. Nilsson, S., et al., *Patient-reported quality-of-life analysis of radium-223 dichloride from the phase III ALSYMPCA study.* Ann Oncol, 2016. **27**(5): p. 868-74.
41. Small, E.J., et al., *Placebo-controlled phase III trial of immunologic therapy with sipuleucel-T (APC8015) in patients with metastatic, asymptomatic hormone refractory prostate cancer.* J Clin Oncol, 2006. **24**(19): p. 3089-94.
42. Halabi, S., et al., *Prostate-Specific Antigen Changes As Surrogate for Overall Survival in Men With Metastatic Castration-Resistant Prostate Cancer Treated With Second-Line Chemotherapy.* Journal of Clinical Oncology, 2013. **31**(31): p. 3944-+.
43. Kim, M.Y., et al., *Tumor self-seeding by circulating cancer cells.* Cell, 2009. **139**(7): p. 1315-26.
44. Muller, V., et al., *Circulating tumor cells in breast cancer: correlation to bone marrow micrometastases, heterogeneous response to systemic therapy and low proliferative activity.* Clin Cancer Res, 2005. **11**(10): p. 3678-85.

45. Bednarz-Knoll, N., C. Alix-Panabieres, and K. Pantel, *Plasticity of disseminating cancer cells in patients with epithelial malignancies.* Cancer Metastasis Rev, 2012. **31**(3-4): p. 673-87.
46. Baccelli, I., et al., *Identification of a population of blood circulating tumor cells from breast cancer patients that initiates metastasis in a xenograft assay.* Nat Biotechnol, 2013. **31**(6): p. 539-44.
47. Gribko, A., et al. *Is small smarter? Nanomaterial-based detection and elimination of circulating tumor cells: current knowledge and perspectives*. International journal of nanomedicine, 2019. **14**, 4187-4209 DOI: 10.2147/ijn.s198319.
48. Burrell, R.A., et al., *The causes and consequences of genetic heterogeneity in cancer evolution.* Nature, 2013. **501**(7467): p. 338-45.
49. Nowell, P.C., *The clonal evolution of tumor cell populations.* Science, 1976. **194**(4260): p. 23-8.
50. Greaves, M. and C.C. Maley, *Clonal evolution in cancer.* Nature, 2012. **481**(7381): p. 306-13.
51. Gerlinger, M., *Intratumor Heterogeneity and Branched Evolution Revealed by Multiregion Sequencing (vol 366, pg 883, 2012).* New England Journal of Medicine, 2012. **367**(10): p. 976-976.
52. Gerlinger, M., et al., *Intratumor heterogeneity and branched evolution revealed by multiregion sequencing.* N Engl J Med, 2012. **366**(10): p. 883-892.
53. Keller, L. and K. Pantel, *Unravelling tumour heterogeneity by single-cell profiling of circulating tumour cells.* Nature Reviews Cancer, 2019. **19**(10): p. 553-567.
54. Powell, A.A., et al., *Single cell profiling of circulating tumor cells: transcriptional heterogeneity and diversity from breast cancer cell lines.* PLoS One, 2012. **7**(5): p. e33788.
55. Pantel, K. and C. Alix-Panabieres, *Real-time liquid biopsy in cancer patients: fact or fiction?* Cancer Res, 2013. **73**(21): p. 6384-8.
56. Danila, D.C., et al., *Circulating Tumors Cells as Biomarkers Progress Toward Biomarker Qualification.* Cancer Journal, 2011. **17**(6): p. 438-450.
57. Gorges, T.M., et al., *Circulating tumour cells escape from EpCAM-based detection due to epithelial-to-mesenchymal transition.* BMC Cancer, 2012. **12**: p. 178.
58. Lecharpentier, A., et al., *Detection of circulating tumour cells with a hybrid (epithelial/mesenchymal) phenotype in patients with metastatic non-small cell lung cancer.* Br J Cancer, 2011. **105**(9): p. 1338-41.
59. Guarino, M., *Epithelial-mesenchymal transition and tumour invasion.* Int J Biochem Cell Biol, 2007. **39**(12): p. 2153-60.
60. Christiansen, J.J. and A.K. Rajasekaran, *Reassessing epithelial to mesenchymal transition as a prerequisite for carcinoma invasion and metastasis.* Cancer Res, 2006. **66**(17): p. 8319-26.
61. Ocana, O.H., et al., *Metastatic colonization requires the repression of the epithelial-mesenchymal transition inducer Prrx1.* Cancer Cell, 2012. **22**(6): p. 709-24.
62. Zhang, N., et al., *Novel therapeutic strategies: targeting epithelial–mesenchymal transition in colorectal cancer.* The Lancet Oncology, 2021. **22**(8): p. e358-e368.

63. Fischer, K.R., et al., *Epithelial-to-mesenchymal transition is not required for lung metastasis but contributes to chemoresistance.* Nature, 2015. **527**(7579): p. 472-476.
64. Zheng, X., et al., *Epithelial-to-mesenchymal transition is dispensable for metastasis but induces chemoresistance in pancreatic cancer.* Nature, 2015. **527**(7579): p. 525-530.
65. Papadaki, M.A., et al., *Circulating Tumor Cells with Stemness and Epithelial-to-Mesenchymal Transition Features Are Chemoresistant and Predictive of Poor Outcome in Metastatic Breast Cancer.* Mol Cancer Ther, 2019. **18**(2): p. 437-447.
66. Liu, H., et al., *Cancer stem cells from human breast tumors are involved in spontaneous metastases in orthotopic mouse models.* Proc Natl Acad Sci U S A, 2010. **107**(42): p. 18115-20.
67. Nieto, M.A., et al., *Emt: 2016.* Cell, 2016. **166**(1): p. 21-45.
68. Aceto, N., et al., *Circulating tumor cell clusters are oligoclonal precursors of breast cancer metastasis.* Cell, 2014. **158**(5): p. 1110-1122.
69. Hou, J.M., et al., *Clinical significance and molecular characteristics of circulating tumor cells and circulating tumor microemboli in patients with small-cell lung cancer.* J Clin Oncol, 2012. **30**(5): p. 525-32.
70. Giuliano, M., et al., *Perspective on Circulating Tumor Cell Clusters: Why It Takes a Village to Metastasize.* Cancer Res, 2018. **78**(4): p. 845-852.
71. Sarioglu, A.F., et al., *A microfluidic device for label-free, physical capture of circulating tumor cell clusters.* Nat Methods, 2015. **12**(7): p. 685-91.
72. Zeinali, M., et al., *High-Throughput Label-Free Isolation of Heterogeneous Circulating Tumor Cells and CTC Clusters from Non-Small-Cell Lung Cancer Patients.* Cancers (Basel), 2020. **12**(1).
73. Au, S.H., et al., *Microfluidic Isolation of Circulating Tumor Cell Clusters by Size and Asymmetry.* Scientific Reports, 2017. **7**(1): p. 2433.
74. Bakir, B., et al., *EMT, MET, Plasticity, and Tumor Metastasis.* Trends Cell Biol, 2020. **30**(10): p. 764-776.
75. Kollermann, J., et al., *Prognostic Significance of Disseminated Tumor Cells in the Bone Marrow of Prostate Cancer Patients Treated With Neoadjuvant Hormone Treatment.* Journal of Clinical Oncology, 2008. **26**(30): p. 4928-4933.
76. Weckermann, D., et al., *Perioperative Activation of Disseminated Tumor Cells in Bone Marrow of Patients With Prostate Cancer.* Journal of Clinical Oncology, 2009. **27**(10): p. 1549-1556.
77. Braun, S., et al., *A pooled analysis of bone marrow micrometastasis in breast cancer.* New England Journal of Medicine, 2005. **353**(8): p. 793-802.
78. Mahalingam, D., et al., *Single-Cell Molecular Profiles and Biophysical Assessment of Circulating Tumor Cells*, in *Circulating Tumor Cells*. 2016. p. 329-350.
79. Pantel, K. and C. Alix-Panabieres, *Functional Studies on Viable Circulating Tumor Cells.* Clin Chem, 2016. **62**(2): p. 328-34.
80. Gao, D., et al., *Organoid cultures derived from patients with advanced prostate cancer.* Cell, 2014. **159**(1): p. 176-187.
81. Ratan, Z.A., et al., *Application of Fluorescence In Situ Hybridization (FISH) Technique for the Detection of Genetic Aberration in Medical Science.* Cureus, 2017. **9**(6): p. e1325.

82. Leversha, M.A., et al., *Fluorescence in situ hybridization analysis of circulating tumor cells in metastatic prostate cancer.* Clin Cancer Res, 2009. **15**(6): p. 2091-7.
83. Tomlins, S.A., et al., *Recurrent fusion of TMPRSS2 and ETS transcription factor genes in prostate cancer.* Science, 2005. **310**(5748): p. 644-648.
84. Danila, D.C., et al., *TMPRSS2-ERG Status in Circulating Tumor Cells as a Predictive Biomarker of Sensitivity in Castration-Resistant Prostate Cancer Patients Treated With Abiraterone Acetate.* European Urology, 2011. **60**(5): p. 897-904.
85. Chenlo, M., et al., *Sequential Colocalization of ERa, PR, and AR Hormone Receptors Using Confocal Microscopy Enables New Insights into Normal Breast and Prostate Tissue and Cancers.* Cancers, 2020. **12**(12).
86. Barteneva, N.S., E. Fasler-Kan, and I.A. Vorobjev, *Imaging Flow Cytometry: Coping with Heterogeneity in Biological Systems.* Journal of Histochemistry & Cytochemistry, 2012. **60**(10): p. 723-733.
87. Rahman, M., *Introduction to Flow Cytometry*. 2006: Serotec Ltd. 36.
88. Zuba-Surma, E.K., et al., *The ImageStream system: a key step to a new era in imaging.* Folia Histochemica Et Cytobiologica, 2007. **45**(4): p. 279-290.
89. Holzner, G., et al., *High-throughput multiparametric imaging flow cytometry: toward diffraction-limited sub-cellular detection and monitoring of sub-cellular processes.* Cell Reports, 2021. **34**(10).
90. Sollier-Christen, E., et al., *VTX-1 Liquid Biopsy System for Fully-Automated and Label-Free Isolation of Circulating Tumor Cells with Automated Enumeration by BioView Platform.* Cytometry Part A, 2018. **93a**(12): p. 1240-1245.
91. Yu, M., et al., *Circulating Breast Tumor Cells Exhibit Dynamic Changes in Epithelial and Mesenchymal Composition.* Science, 2013. **339**(6119): p. 580-584.
92. Krebs, M.G., et al., *Molecular analysis of circulating tumour cells-biology and biomarkers.* Nat Rev Clin Oncol, 2014. **11**(3): p. 129-44.
93. Lohr, J.G., et al., *Whole-exome sequencing of circulating tumor cells provides a window into metastatic prostate cancer.* Nat Biotechnol, 2014. **32**(5): p. 479-84.
94. Josefsson, A., et al., *Circulating tumor cells mirror bone metastatic phenotype in prostate cancer.* Oncotarget, 2018. **9**(50): p. 29403-29413.
95. Grun, D., L. Kester, and A. van Oudenaarden, *Validation of noise models for single-cell transcriptomics.* Nat Methods, 2014. **11**(6): p. 637-40.
96. Baker, S.C., et al., *The External RNA Controls Consortium: a progress report.* Nat Methods, 2005. **2**(10): p. 731-4.
97. Thorp, H.H., *The importance of being r: greater oxidative stability of RNA compared with DNA.* Chemistry & Biology, 2000. **7**(2): p. R33-R36.
98. Visvikis, S., A. Schlenck, and M. Maurice, *DNA extraction and stability for epidemiological studies.* Clinical Chemistry and Laboratory Medicine, 1998. **36**(8): p. 551-555.
99. Ni, X.H., et al., *Reproducible copy number variation patterns among single circulating tumor cells of lung cancer patients.* Proceedings of the National Academy of Sciences of the United States of America, 2013. **110**(52): p. 21083-21088.
100. Czyz, Z.T., et al., *Reliable Single Cell Array CGH for Clinical Samples.* Plos One, 2014. **9**(1).

101. Heitzer, E., et al., *Complex Tumor Genomes Inferred from Single Circulating Tumor Cells by Array-CGH and Next-Generation Sequencing.* Cancer Research, 2013. **73**(10): p. 2965-2975.
102. Zhang, F., et al., *Copy number variation in human health, disease, and evolution.* Annu Rev Genomics Hum Genet, 2009. **10**: p. 451-81.
103. Wang, X., et al., *Copy number alterations are associated with metastatic-lethal progression in prostate cancer.* Prostate Cancer and Prostatic Diseases, 2020. **23**(3): p. 494-506.
104. Colaianni, V., R. Mazzei, and S. Cavallaro, *Copy number variations and stroke.* Neurological Sciences, 2016. **37**(12): p. 1895-1904.
105. Behjati, S. and P.S. Tarpey, *What is next generation sequencing?* Archives of Disease in Childhood-Education and Practice Edition, 2013. **98**(6): p. 236-238.
106. Gasch, C., et al., *Heterogeneity of Epidermal Growth Factor Receptor Status and Mutations of KRAS/PIK3CA in Circulating Tumor Cells of Patients with Colorectal Cancer.* Clinical Chemistry, 2013. **59**(1): p. 252-260.
107. Bednarz-Knoll, N., C. Alix-Panabières, and K. Pantel, *Clinical relevance and biology of circulating tumor cells.* Breast Cancer Res, 2011. **13**(6): p. 228.
108. Posel, C., et al., *Density gradient centrifugation compromises bone marrow mononuclear cell yield.* PLoS One, 2012. **7**(12): p. e50293.
109. Harouaka, R.A., et al., *Flexible Micro Spring Array Device for High-Throughput Enrichment of Viable Circulating Tumor Cells.* Clinical Chemistry, 2014. **60**(2): p. 323-333.
110. Zhou, M.D., et al., *Separable Bilayer Microfiltration Device for Viable Label-free Enrichment of Circulating Tumour Cells.* Scientific Reports, 2014. **4**.
111. Gossett, D.R., et al., *Label-free cell separation and sorting in microfluidic systems.* Analytical and Bioanalytical Chemistry, 2010. **397**(8): p. 3249-3267.
112. Miltenyi, S., et al., *High-Gradient Magnetic Cell-Separation with Macs.* Cytometry, 1990. **11**(2): p. 231-238.
113. Albertoni, G.A., et al., *Magnetic bead technology for viral RNA extraction from serum in blood bank screening.* Brazilian Journal of Infectious Diseases, 2011. **15**(6): p. 547-552.
114. de Bono, J.S., et al., *Circulating Tumor Cells Predict Survival Benefit from Treatment in Metastatic Castration-Resistant Prostate Cancer.* Clinical Cancer Research, 2008. **14**(19): p. 6302-6309.
115. Cohen, S.J., et al., *Relationship of circulating tumor cells to tumor response, progression-free survival, and overall survival in patients with metastatic colorectal cancer.* Journal of Clinical Oncology, 2008. **26**(19): p. 3213-3221.
116. Danila, D.C., et al., *Circulating tumor cell number and prognosis in progressive castration-resistant prostate cancer.* Clinical Cancer Research, 2007. **13**(23): p. 7053-7058.
117. Cristofanilli, M., et al., *Circulating tumor cells, disease progression, and survival in metastatic breast cancer.* New England Journal of Medicine, 2004. **351**(8): p. 781-791.
118. Allard, W.J., et al., *Tumor cells circulate in the peripheral blood of all major carcinomas but not in healthy subjects or patients with nonmalignant diseases.* Clin Cancer Res, 2004. **10**(20): p. 6897-904.

119. Andree, K.C., G. van Dalum, and L.W. Terstappen, *Challenges in circulating tumor cell detection by the CellSearch system.* Mol Oncol, 2016. **10**(3): p. 395-407.
120. Nanou, A., et al., *HER2 expression on tumor-derived extracellular vesicles and circulating tumor cells in metastatic breast cancer.* Breast Cancer Research, 2020. **22**(1).
121. Yap, T.A., et al., *Circulating tumor cells: a multifunctional biomarker.* Clin Cancer Res, 2014. **20**(10): p. 2553-68.
122. Rhim, A.D., et al., *EMT and dissemination precede pancreatic tumor formation.* Cell, 2012. **148**(1-2): p. 349-61.
123. Miller, M.C., G.V. Doyle, and L.W. Terstappen, *Significance of Circulating Tumor Cells Detected by the CellSearch System in Patients with Metastatic Breast Colorectal and Prostate Cancer.* J Oncol, 2010. **2010**: p. 617421.
124. Riethdorf, S., et al., *Detection of circulating tumor cells in peripheral blood of patients with metastatic breast cancer: a validation study of the CellSearch system.* Clin Cancer Res, 2007. **13**(3): p. 920-8.
125. Punnoose, E.A., et al., *Molecular biomarker analyses using circulating tumor cells.* PLoS One, 2010. **5**(9): p. e12517.
126. Harb, W., et al., *Mutational Analysis of Circulating Tumor Cells Using a Novel Microfluidic Collection Device and qPCR Assay.* Translational Oncology, 2013. **6**(5): p. 528-+.
127. Lee, A.C., et al., *OPENchip: an on-chip in situ molecular profiling platform for gene expression analysis and oncogenic mutation detection in single circulating tumour cells.* Lab Chip, 2020. **20**(5): p. 912-922.
128. Mishra, A., et al., *Ultrahigh-throughput magnetic sorting of large blood volumes for epitope-agnostic isolation of circulating tumor cells.* Proc Natl Acad Sci U S A, 2020. **117**(29): p. 16839-16847.
129. Ozkumur, E., et al., *Inertial focusing for tumor antigen-dependent and -independent sorting of rare circulating tumor cells.* Sci Transl Med, 2013. **5**(179): p. 179ra47.
130. Nagrath, S., et al., *Isolation of rare circulating tumour cells in cancer patients by microchip technology.* Nature, 2007. **450**(7173): p. 1235-9.
131. Stott, S.L., et al., *Isolation of circulating tumor cells using a microvortex-generating herringbone-chip.* Proceedings of the National Academy of Sciences of the United States of America, 2010. **107**(43): p. 18392-18397.
132. Karabacak, N.M., et al., *Microfluidic, marker-free isolation of circulating tumor cells from blood samples.* Nat Protoc, 2014. **9**(3): p. 694-710.
133. Martel, J.M. and M. Toner, *Inertial focusing in microfluidics.* Annu Rev Biomed Eng, 2014. **16**: p. 371-96.
134. Squires, T.M. and S.R. Quake, *Microfluidics: Fluid physics at the nanoliter scale.* Reviews of Modern Physics, 2005. **77**(3): p. 977-1026.
135. SegrÉ, G. and A. Silberberg, *Radial Particle Displacements in Poiseuille Flow of Suspensions.* Nature, 1961. **189**(4760): p. 209-210.
136. Segre, G. and A. Silberberg, *Behaviour of Macroscopic Rigid Spheres in Poiseuille Flow .2. Experimental Results and Interpretation.* Journal of Fluid Mechanics, 1962. **14**(1): p. 136-157.
137. Humphry, K.J., et al., *Axial and lateral particle ordering in finite Reynolds number channel flows.* Physics of Fluids, 2010. **22**(8).

138. Di Carlo, D., et al., *Continuous inertial focusing, ordering, and separation of particles in microchannels.* Proceedings of the National Academy of Sciences of the United States of America, 2007. **104**(48): p. 18892-18897.
139. Di Carlo, D., *Inertial microfluidics.* Lab on a Chip, 2009. **9**(21): p. 3038-3046.
140. Johnston, I.D., et al., *Dean flow focusing and separation of small microspheres within a narrow size range.* Microfluidics and Nanofluidics, 2014. **17**(3): p. 509-518.
141. Di Carlo, D., et al., *Particle Segregation and Dynamics in Confined Flows.* Physical Review Letters, 2009. **102**(9).
142. Augustsson, P., et al., *Microfluidic, label-free enrichment of prostate cancer cells in blood based on acoustophoresis.* Anal Chem, 2012. **84**(18): p. 7954-62.
143. Burguillos, M.A., et al., *Microchannel Acoustophoresis does not Impact Survival or Function of Microglia, Leukocytes or Tumor Cells.* Plos One, 2013. **8**(5).
144. Wiklund, M., *Acoustofluidics 12: Biocompatibility and cell viability in microfluidic acoustic resonators.* Lab on a Chip, 2012. **12**(11): p. 2018-2028.
145. Yosioka, K. and Y. Kawasima, *Acoustic radiation pressure on a compressible sphere.* Acta Acustica united with Acustica, 1955. **5**(3): p. 167-173.
146. Gor'kov, L.P., *On the Forces Acting on a Small Particle in an Acoustical Field in an Ideal Fluid.* Soviet Physics Doklady, 1962. **6**: p. 773.
147. Johnson, L.M., et al., *Elastomeric microparticles for acoustic mediated bioseparations.* J Nanobiotechnology, 2013. **11**: p. 22.
148. Cushing, K.W., et al., *Elastomeric negative acoustic contrast particles for affinity capture assays.* Anal Chem, 2013. **85**(4): p. 2208-15.
149. Shields, C.W.t., et al., *Elastomeric negative acoustic contrast particles for capture, acoustophoretic transport, and confinement of cells in microfluidic systems.* Langmuir, 2014. **30**(14): p. 3923-7.
150. Cushing, K., et al., *Reducing WBC background in cancer cell separation products by negative acoustic contrast particle immuno-acoustophoresis.* Anal Chim Acta, 2018. **1000**: p. 256-264.
151. Undvall Anand, E., et al., *Two-Step Acoustophoresis Separation of Live Tumor Cells from Whole Blood.* Analytical Chemistry, 2021. **93**(51): p. 17076-17085.
152. Wilder, E.A., et al., *Measuring the modulus of soft polymer networks via a buckling-based metrology (vol 39, pg 4138, 2006).* Macromolecules, 2006. **39**(17): p. 5956-5956.
153. Barnes, T.J. and C.A. Prestidge, *PEO-PPO-PEO block copolymers at the emulsion droplet-water interface.* Langmuir, 2000. **16**(9): p. 4116-4121.
154. Hellmich, W., et al., *Poly(oxyethylene) based surface coatings for poly(dimethylsiloxane) microchannels.* Langmuir, 2005. **21**(16): p. 7551-7557.
155. Xu, B., S.D. Sommerfeldt, and T.W. Leishman, *Generalized acoustic energy density.* J Acoust Soc Am, 2011. **130**(3): p. 1370-80.
156. Barnkob, R., et al., *Measuring density and compressibility of white blood cells and prostate cancer cells by microchannel acoustophoresis.* 15th International Conference on Miniaturized Systems for Chemistry and Life Sciences 2011, MicroTAS 2011, 2011. **1**.
157. Hartono, D., et al., *On-chip measurements of cell compressibility via acoustic radiation.* Lab on a Chip, 2011. **11**(23): p. 4072-4080.

158. Bjerknes, V., *On the absolute measurement of electromagnetic quantities.* Physical Review (Series I), 1909. **29**(3): p. 310.
159. Groschl, M., *Ultrasonic separation of suspended particles - Part I: Fundamentals.* Acustica, 1998. **84**(3): p. 432-447.
160. Hammarstrom, B., T. Laurell, and J. Nilsson, *Seed particle-enabled acoustic trapping of bacteria and nanoparticles in continuous flow systems.* Lab Chip, 2012. **12**(21): p. 4296-304.
161. Evander, M. and J. Nilsson, *Acoustofluidics 20: applications in acoustic trapping.* Lab Chip, 2012. **12**(22): p. 4667-76.
162. Rayleigh, L., *On the Circulation of Air Observed in Kundt's Tubes, and on Some Allied Acoustical Problems.* Philosophical Transactions of the Royal Society of London, 1884. **175**: p. 1-21.
163. Schlichting, H., *Berechnung ebener periodischer grenzschichtstromungen.* Physikalische Zeit., 1932. **33**: p. 327-335.
164. Muller, P.B., et al., *A numerical study of microparticle acoustophoresis driven by acoustic radiation forces and streaming-induced drag forces.* Lab Chip, 2012. **12**(22): p. 4617-27.
165. Wiklund, M., R. Green, and M. Ohlin, *Acoustofluidics 14: Applications of acoustic streaming in microfluidic devices.* Lab Chip, 2012. **12**(14): p. 2438-51.
166. Antfolk, M., et al., *Focusing of sub-micrometer particles and bacteria enabled by two-dimensional acoustophoresis.* Lab Chip, 2014. **14**(15): p. 2791-9.
167. Van Assche, D., et al., *Gradient acoustic focusing of sub-micron particles for separation of bacteria from blood lysate.* Scientific Reports, 2020. **10**(1).
168. Nordin, M. and T. Laurell, *Two-hundredfold volume concentration of dilute cell and particle suspensions using chip integrated multistage acoustophoresis.* Lab on a Chip, 2012. **12**(22): p. 4610-4616.
169. Oberti, S., A. Neild, and J. Dual, *Manipulation of micrometer sized particles within a micromachined fluidic device to form two-dimensional patterns using ultrasound.* Journal of the Acoustical Society of America, 2007. **121**(2): p. 778-785.
170. Magnusson, C., et al., *Clinical-Scale Cell-Surface-Marker Independent Acoustic Microfluidic Enrichment of Tumor Cells from Blood.* Analytical Chemistry, 2017. **89**(22): p. 11954-11961.
171. Urbansky, A., et al., *Rapid and effective enrichment of mononuclear cells from blood using acoustophoresis.* Sci Rep, 2017. **7**(1): p. 17161.
172. Urbansky, A., et al., *Label-free separation of leukocyte subpopulations using high throughput multiplex acoustophoresis.* Lab Chip, 2019. **19**(8): p. 1406-1416.
173. Grenvall, C., et al., *Concurrent Isolation of Lymphocytes and Granulocytes Using Prefocused Free Flow Acoustophoresis.* Analytical Chemistry, 2015. **87**(11): p. 5596-5604.
174. Urbansky, A., et al., *Affinity-Bead-Mediated Enrichment of CD8+Lymphocytes from Peripheral Blood Progenitor Cell Products Using Acoustophoresis.* Micromachines, 2016. **7**(6).
175. Lenshof, A., et al., *Efficient purification of CD4+ lymphocytes from peripheral blood progenitor cell products using affinity bead acoustophoresis.* Cytometry A, 2014. **85**(11): p. 933-41.
176. Ohlsson, P., et al., *Acoustic impedance matched buffers enable separation of bacteria from blood cells at high cell concentrations.* Scientific Reports, 2018. **8**.

177. Jakobsson, O., et al., *Thousand-Fold Volumetric Concentration of Live Cells with a Recirculating Acoustofluidic Device.* Analytical Chemistry, 2015. **87**(16): p. 8497-8502.
178. Ohlsson, P., et al., *Integrated Acoustic Separation, Enrichment, and Microchip Polymerase Chain Reaction Detection of Bacteria from Blood for Rapid Sepsis Diagnostics.* Analytical Chemistry, 2016. **88**(19): p. 9403-9411.
179. Ku, A., et al., *Acoustic Enrichment of Extracellular Vesicles from Biological Fluids.* Anal Chem, 2018. **90**(13): p. 8011-8019.
180. Evander, M., et al., *Acoustophoresis in wet-etched glass chips.* Anal Chem, 2008. **80**(13): p. 5178-85.
181. Gorkov, L.P. and L.P. Pitaevskii, *The Transition of Liquid He-3 into the Superfluid State.* Soviet Physics Jetp-Ussr, 1962. **15**(2): p. 417-421.
182. Gerlt, M.S., et al., *Acoustofluidic medium exchange for preparation of electrocompetent bacteria using channel wall trapping.* Lab on a Chip, 2021. **21**(22): p. 4487-4497.
183. Grenvall, C., et al., *Label-free somatic cell cytometry in raw milk using acoustophoresis.* Cytometry A, 2012. **81**(12): p. 1076-83.
184. Grenvall, C., et al., *Harmonic microchip acoustophoresis: a route to online raw milk sample precondition in protein and lipid content quality control.* Anal Chem, 2009. **81**(15): p. 6195-200.
185. Kang, H., et al., *Evaluation of Positive and Negative Methods for Isolation of Circulating Tumor Cells by Lateral Magnetophoresis.* Micromachines (Basel), 2019. **10**(6).
186. Zborowski, M., et al., *Red blood cell magnetophoresis.* Biophys J, 2003. **84**(4): p. 2638-45.
187. Zborowski, M., J.J. Chalmers, and W.G. Lowrie, *Magnetic Cell Manipulation and Sorting*, in *Microtechnology for Cell Manipulation and Sorting*, W. Lee, P. Tseng, and D. Di Carlo, Editors. 2017, Springer International Publishing: Cham. p. 15-55.
188. Luo, L. and Y. He, *Magnetically driven microfluidics for isolation of circulating tumor cells.* Cancer Medicine, 2020. **9**(12): p. 4207-4231.
189. Autebert, J., et al., *High purity microfluidic sorting and analysis of circulating tumor cells: towards routine mutation detection.* Lab on a Chip, 2015. **15**(9): p. 2090-2101.
190. Gupta, V., et al., *ApoStream (TM), a new dielectrophoretic device for antibody independent isolation and recovery of viable cancer cells from blood.* Biomicrofluidics, 2012. **6**(2).
191. Maidin, N.N.M., et al., *Dielectrophoresis applications in biomedical field and future perspectives in biomedical technology.* Electrophoresis, 2021.
192. Kobayashi, M., et al., *Cancer Cell Analyses at the Single Cell-Level Using Electroactive Microwell Array Device.* PLOS ONE, 2015. **10**(11): p. e0139980.
193. Park, J., et al., *Sequential Cell-Processing System by Integrating Hydrodynamic Purification and Dielectrophoretic Trapping for Analyses of Suspended Cancer Cells.* Micromachines, 2020. **11**(1): p. 47.
194. Di Trapani, M., N. Manaresi, and G. Medoro, *DEPArray (TM) system: An automatic image-based sorter for isolation of pure circulating tumor cells.* Cytometry Part A, 2018. **93a**(12): p. 1260-1266.

195. Balasubramanian, P., et al., *Antibody-independent capture of circulating tumor cells of non-epithelial origin with the ApoStream (R) system.* Plos One, 2017. **12**(4).
196. Le Du, F., et al., *EpCAM-independent isolation of circulating tumor cells with epithelial-to-mesenchymal transition and cancer stem cell phenotypes using ApoStream (R) in patients with breast cancer treated with primary systemic therapy.* Plos One, 2020. **15**(3).
197. Carter, L., et al., *Molecular analysis of circulating tumor cells identifies distinct copy-number profiles in patients with chemosensitive and chemorefractory small-cell lung cancer.* Nature Medicine, 2017. **23**(1): p. 114-119.
198. Polzer, B., et al., *Molecular profiling of single circulating tumor cells with diagnostic intention.* Embo Molecular Medicine, 2014. **6**(11): p. 1371-1386.
199. Warkiani, M.E., et al., *Ultra-fast, label-free isolation of circulating tumor cells from blood using spiral microfluidics.* Nat Protoc, 2016. **11**(1): p. 134-48.
200. Khoo, B.L., et al., *Clinical validation of an ultra high-throughput spiral microfluidics for the detection and enrichment of viable circulating tumor cells.* PLoS One, 2014. **9**(7): p. e99409.
201. Lemaire, C.A., et al., *Fast and Label-Free Isolation of Circulating Tumor Cells from Blood: From a Research Microfluidic Platform to an Automated Fluidic Instrument, VTX-1 Liquid Biopsy System.* SLAS Technol, 2018. **23**(1): p. 16-29.
202. Sollier-Christen, E., et al., *VTX-1 Liquid Biopsy System for Fully-Automated and Label-Free Isolation of Circulating Tumor Cells with Automated Enumeration by BioView Platform.* Cytometry A, 2018. **93**(12): p. 1240-1245.
203. Hur, S.C., A.J. Mach, and D. Di Carlo, *High-throughput size-based rare cell enrichment using microscale vortices.* Biomicrofluidics, 2011. **5**(2): p. 22206.
204. Fachin, F., et al., *Monolithic Chip for High-throughput Blood Cell Depletion to Sort Rare Circulating Tumor Cells.* Scientific Reports, 2017. **7**.
205. Mendelaar, P.A.J., et al., *Defining the dimensions of circulating tumor cells in a large series of breast, prostate, colon, and bladder cancer patients.* Molecular Oncology, 2021. **15**(1): p. 116-125.
206. Huang, L.R., et al., *Continuous particle separation through deterministic lateral displacement.* Science, 2004. **304**(5673): p. 987-90.
207. Beech, J.P., et al., *Sorting cells by size, shape and deformability.* Lab on a Chip, 2012. **12**(6): p. 1048-1051.
208. Stroock, A.D., et al., *Chaotic mixer for microchannels.* Science, 2002. **295**(5555): p. 647-51.
209. Fisher, R., L. Pusztai, and C. Swanton, *Cancer heterogeneity: implications for targeted therapeutics.* British Journal of Cancer, 2013. **108**(3): p. 479-485.
210. Marusyk, A. and K. Polyak, *Tumor heterogeneity: Causes and consequences.* Biochimica Et Biophysica Acta-Reviews on Cancer, 2010. **1805**(1): p. 105-117.
211. Pletcher, M.J. and M. Pignone, *Evaluating the Clinical Utility of a Biomarker A Review of Methods for Estimating Health Impact.* Circulation, 2011. **123**(10): p. 1116-U261.
212. Parkinson, D.R., et al., *Evidence of Clinical Utility: An Unmet Need in Molecular Diagnostics for Patients with Cancer.* Clinical Cancer Research, 2014. **20**(6): p. 1428-1444.

LUND UNIVERSITY

ISBN: ISBN 978-91-8039-136-8 (print)
ISBN: 978-91-8039-135-1 (pdf)
ISRN: LUTEDX/TEEM – 1128 – SE
Report-nr: 1/22